RSC Advances

REVIEW

View Article Online
View Journal | View Issue

Cite this: *RSC Adv.*, 2025, **15**, 36534

Valorization of citrus processing waste into high-performance bionanomaterials: green synthesis, biomedicine, and environmental remediation

Sham AlZahabi and Wael Mamdouh *

Received 17th June 2025
Accepted 9th September 2025

DOI: 10.1039/d5ra04307g

rsc.li/rsc-advances

The global citrus industry generates millions of tons of citrus processing waste (CPW), composed primarily of peel, pulp, and seeds. This agro-industrial byproduct represents both an environmental challenge and a valuable feedstock for sustainable nanotechnology. This review explores green synthesis approaches for transforming CPW, rich in bioactive compounds such as flavonoids, essential oils, and pectin, into high-performance bionanomaterials. Emphasis is placed on their biomedical applications, including antimicrobial formulations, wound healing agents, and nanocarriers for drug delivery, as well as their use in environmental remediation and catalysis. In contrast to earlier reviews, this work highlights recent progress in eco-friendly synthesis techniques (*e.g.*, microwave-assisted, biological, and hydrothermal methods) while addressing challenges related to scalability, reproducibility, and bioavailability. The review also frames CPW valorization within the broader context of circular economy models and the UN Sustainable Development Goals. By offering a critical synthesis of current knowledge and identification of key knowledge gaps, this work aims to support future research and industrial translation in green nanotechnology.

1. Introduction

The food and agriculture (F&A) industry is experiencing rapid growth, driven by a burgeoning population and improving economic conditions. This growth has attracted substantial investments, reaching USD 75 billion in 2017. However, the industrialization of agriculture has led to significant waste generation, posing environmental and economic challenges.[1] Globally, over five million metric tons of agricultural biomass are produced annually, including fruit peel, rice bran, sugarcane bagasse, and vegetable residues.[2]

According to the Food and Agriculture Organization (FAO), global fruit and vegetable production in 2023 reached approximately 2.1 billion tons, marking a 1 percent increase from 2022 (Agricultural production statistics 2010–2023, Food and Agriculture Organization of the United Nations). A significant portion of this ends up as waste, particularly during food processing operations. Among the most prevalent residues is citrus processing waste (CPW), a mixture of peel, pulp, and seeds, generated during juice extraction and other industrial applications (FAO, 2023).

CPW represents up to 50–60% of the total citrus fruit mass, making it one of the largest sources of agro-industrial waste.[3–8] In many cases, the volume of this waste exceeds the actual product yield, especially during large-scale citrus juice production. According to FAO, approximately 1 billion tons of food waste are annually produced, which roughly corresponds to one-third of the food produced for human consumption (FAO, 2023). Improper management of such waste contributes to greenhouse gas emissions, soil and water contamination, and microbial hazards.

In 2023, global trade in food-processing byproducts, including "residues and waste from the food industries", surpassed USD 102 billion, indicating both the scale of the challenge and potential value (TrendEconomy, 2023). Agro-industrial waste is rich in nutrients and, if left inadequately treated or untreated, can serve as a breeding ground for pathogenic microorganisms.[9–11] Traditionally, this waste, including citrus residues, has been incinerated or dumped into landfills, releasing harmful compounds such as SO_2, CH_4, and N_2O, and increasing environmental burdens.[10,12,13] The lack of efficient recycling exacerbates these effects.

To address these concerns, valorization of CPW into high-value bioproducts has emerged as a sustainable strategy to effectively and economically convert these wastes into valuable products with industrial and commercial potential, thereby reducing their detrimental environmental impact.[14] CPW is rich in bioactive compounds, including pectin, cellulose, flavonoids, and essential oils (EOs), making it a promising feedstock for nanomaterial synthesis *via* green chemistry routes.[15–18]

Citrus is the largest genus in the Rutaceae family, encompassing approximately 70 species, including various edible

Department of Chemistry, School of Sciences and Engineering, The American University in Cairo (AUC), AUC Avenue, P. O. Box 74, New Cairo 11835, Egypt. E-mail: wael_mamdouh@aucegypt.edu

Table 1 Chemical classes of the most predominant compounds extracted from peels of different citrus species, with representative molecular weights and structures. This table provides a reference framework that supports subsequent discussions on their roles in nanoparticles synthesis, biomedical activity, and environmental applications

Category	Subgroup	Components	Formula	Mol-Wt. (g mol^{-1})	IUPAC name	Chemical structure
Phenolic compounds	Phenolic acids	*p*-Hydroxybenzoic acid	$C_7H_6O_3$	138.12	4-Hydroxybenzoic acid	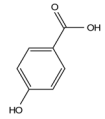
		Ferulic acid	$C_{10}H_{10}O_4$	194.18	(4-Hydroxy-3-methoxyphenyl) prop-2-enoic acid	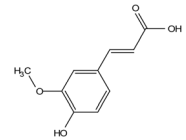
		Gallic acid	$C_7H_6O_5$	170.12	3,4,5-Trihydroxybenzoic acid	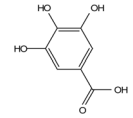
		Caffeic acid	$C_9H_8O_4$	180.16	3-(3,4-Dihydroxyphenyl)-2-propenoic acid	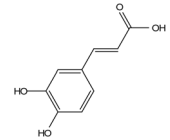
		Protocatechuic acid	$C_7H_6O_4$	154.12	3,4-Dihydroxybenzoic acid	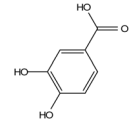
	Polymethoxyflavones	Nobiletin	$C_{21}H_{22}O_8$	402.39	5,6,7,8,3′,4′-hexamethoxyflavone	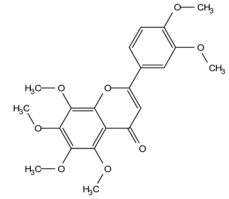
		5-Demethylnobiletin	$C_{20}H_{20}O_8$	388.37	5-Hydroxy-6,7,8,3′,4′-pentamethoxyflavone	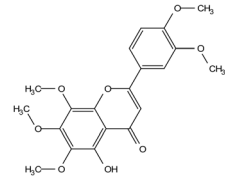
		Tangeretin	$C_{20}H_{20}O_7$	372.37		

Table 1 (*Contd.*)

Category	Subgroup	Components	Formula	Mol-Wt. (g mol^{-1})	IUPAC name	Chemical structure
					5,6,7,8,4′-Pentamethoxyflavone	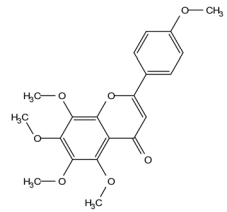
		Sudachitin	$C_{18}H_{16}O_8$	360.31	4′,5,7-Trihydroxy-3′,6,8-trimethoxyflavone	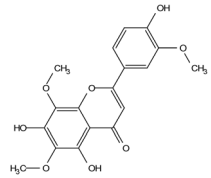
		Sinensetin	$C_{20}H_{20}O_7$	372.36	5,6,7,3′,4′-Pentamethoxyflavone	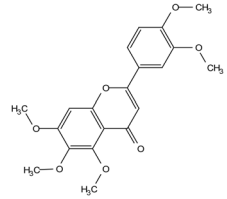
		Naringenin	$C_{15}H_{12}O_5$	475	(2*S*)-5,7-Dihydroxy-2-(4-hydroxyphenyl)-2,3-dihydro-4*H*-1-benzopyran-4-one	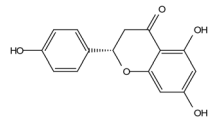
	Flavonoid aglycones	Hesperetin	$C_{16}H_{14}O_6$	302.27	(2*S*)-3′,5,7-Trihydroxy-4′-methoxyflavan-4-one	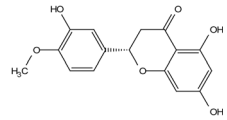
		Quercetin	$C_{15}H_{10}O_7$	302.23	3,3′,4′,5,7-Pentahydroxyflavone	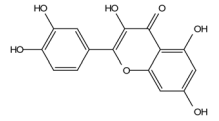
	Flavone O-glycosides	Hesperidin	$C_{28}H_{34}O_{15}$	610.56	(2*S*)-3′,5-Dihydroxy-4′-methoxy-7-[α-L-rhamnopyranosyl-(1 → 6)-β-D-glucopyranosyloxy] flavan-4-one	

Table 1 (*Contd.*)

Category	Subgroup	Components	Formula	Mol-Wt. (g mol^{-1})	IUPAC name	Chemical structure
		Naringin	$C_{27}H_{32}O_{14}$	580.54	(2*S*)-4′,5-Dihydroxy-7-[α-L-rhamnopyranosyl-(1 → 2)-β-D-glucopyranosyloxy] flavan-4-one	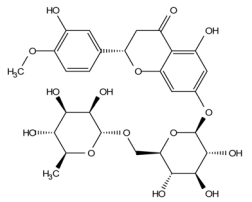
		Narirutin	$C_{27}H_{32}O_{14}$	580.53	(2*S*)-5-Hydroxy-2-(4-hydroxyphenyl)-7-[(2*S*,3*R*,4*S*,5*S*,6*R*)-3,4,5-trihydroxy-6-[[(2*R*,3*R*,4*R*,5*R*,6*S*)-3,4,5-trihydroxy-6-methyloxan-2-yl] oxymethyl]oxan-2-yl] oxy-2,3-dihydrochromen-4-one	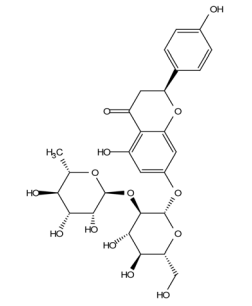
		Eriocitrin	$C_{27}H_{32}O_{15}$	596.53	(2*S*)-3′,4′,5-Trihydroxy-7-[α-L-rhamnopyranosyl-(1 → 6)-β-D-glucopyranosyloxy] flavan-4-one	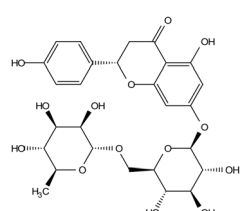
	Flavone C-glycosides	Lucenin-2	$C_{27}H_{30}O_{16}$	610.52	3′,4′,5,7-Tetrahydroxyflavone	

Table 1 (*Contd.*)

Category	Subgroup	Components	Formula	Mol-Wt. (g mol^{-1})	IUPAC name	Chemical structure
						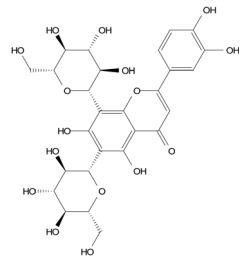
		Diosmetin-6,8-di-C glucoside	$C_{28}H_{32}O_{16}$	610.52	5,7-Dihydroxy-2-(3-hydroxy-4-methoxyphenyl)-6,8-bis[3,4,5-trihydroxy-6-(hydroxymethyl)oxan-2-yl]-4*H*-chromen-4-one	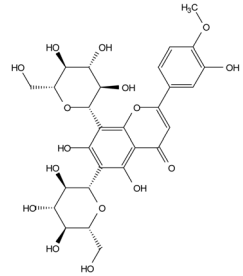
		Vicenin-2	$C_{27}H_{30}O_{15}$	594.52	5,7-Dihydroxy-2-(4-hydroxyphenyl)-6,8-bis[(2*S*,3*R*,4*R*,5*S*,6*R*)-3,4,5-trihydroxy-6-(hydroxymethyl)oxan-2-yl]chromen-4-one	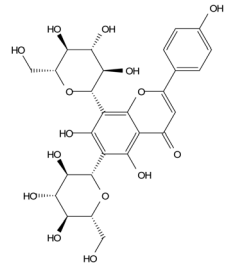
		Limonene	$C_{10}H_{16}$	136.24	1-Methyl-4-(prop-1-en-2-yl)cyclohex-1-ene	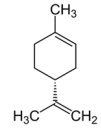
EOs	Monoterpenes	α-Pinene	$C_{10}H_{16}$	136.24	2,6,6-Trimethylbicyclo[3.1.1]hept-2-ene	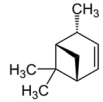
		β-Pinene	$C_{10}H_{16}$	136.24	6,6-Dimethyl-2-methylidenebicyclo[3.1.1]heptane Pin-2(10)-ene	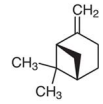
		α-Phellandrene	$C_{10}H_{16}$	136.24		

Table 1 (*Contd.*)

Category	Subgroup	Components	Formula	Mol-Wt. (g mol^{-1})	IUPAC name	Chemical structure
					2-Methyl-5-propan-2-ylcyclohexa-1,3-diene	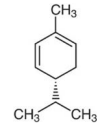
		(*E*)/(*Z*)-ocimene	$C_{10}H_{16}$	136.23	(4*E*,6*Z*)-2,6-Dimethylocta-2,4,6-triene	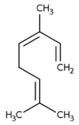
	Monoterpene aldehyde	*Cis*-citral (Neral)	$C_{10}H_{16}O$	152.24	(2*Z*)-3,7-Dimethylocta-2,6-dienal	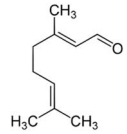
	Monoterpene alcohol	Linalool	$C_{10}H_{18}O$	154.25	3,7-Dimethylocta-1,6-dien-3-ol	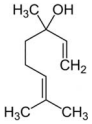
		α-Humulene	$C_{15}H_{24}$	204.35	[1(11)*E*,4*E*,8*E*]-Humula-1(11),4,8-triene	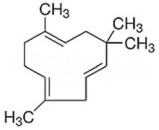
	Sesquiterpenes	α-/β-Copaene	$C_{15}H_{24}$	204.35	(1*R*,2*S*,6*S*,7*S*,8*S*)-8-Isopropyl-1,3-dimethyltricyclo[4.4.0.02,7]dec-3-ene	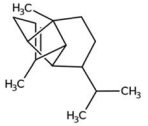
		(*E*)-/β-Caryophyllene	$C_{15}H_{24}$	204.35	(1*R*,4*E*,9*S*)-4,11,11-Trimethyl-8-methylidenebicyclo[7.2.0]undec-4-ene	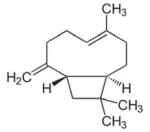
		Valencene	$C_{15}H_{24}$	204.35	4α,5α-Eremophila-1(10),11-diene	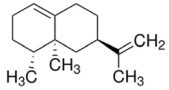

Table 1 (*Contd.*)

Category	Subgroup	Components	Formula	Mol-Wt. (g mol^{-1})	IUPAC name	Chemical structure
Dietary fiber	Insoluble fibers	Cellulose	$(C_{12}H_{20}O_{10})_n$		(6*S*)-2-(Hydroxymethyl)-6-[(3*S*)-4,5,6-trihydroxy-2-(hydroxymethyl)oxan-3-yl]oxyoxane-3,4,5-triol	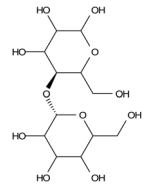
		Hemicellulose	$(C_5H_8O_4)_n$			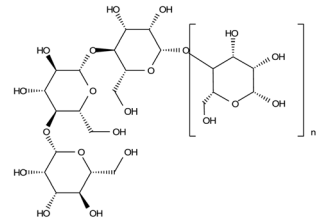
		Lignin	$(C_{31}H_{34}O_{11})$ n			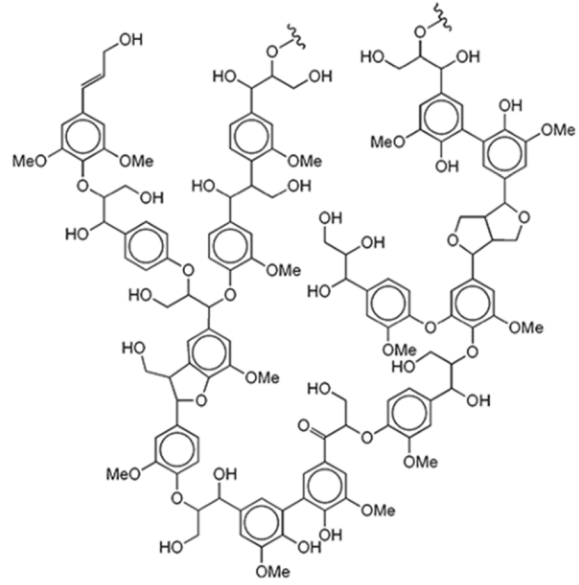
	Soluble fibers	Pectin				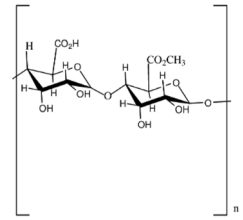

varieties such as *Citrus limon* (lemon), *C. medica* (citron), *C. aurantium* (sour orange), *C. paradisi* (grapefruit), *C. reticulata* (mandarin, tangerine), *C. clementina* (clementine), *C. bergamia* (Bergamot), *C. junos* (Yuzu), *C. japonica* (Kumquat), and *C. sinensis* (sweet orange).[19–22] Citrus species are native to Asiatic crops growing in the Himalayan foothills of Northern India, Northern Myanmar, Southern China, and Southeast Asia, from where they have spread to over 140 worldwide.[22,23] Global production of citrus fruits reached 158 million tons in 2020, with oranges being the most widely cultivated (FAOSTAT, 2020). Approximately 30 million tons of citrus fruits are used annually for juice production, generating vast quantities of CPW.[24–27]

These residues are rich in functional compounds and biopolymers that offer antioxidant, antimicrobial, anti-inflammatory, and potential anticancer properties.[20,28–32] For example, external ionotropic gelation has been used to encapsulate *C. aurantifolia* peel extract in alginate–gelatin microbeads with antibacterial activity against *S. aureus* and *E. coli*.[33] In another study, *C. unshiu* peel extract demonstrated inhibitory effects on melanoma in animal models.[34]

Nanotechnology is a rapidly evolving field with significant interactions with other scientific disciplines, leading to innovative applications. It involves the synthesis and application of nanomaterials with sizes ranging from 1 to 100 nm.[35] In general, nanomaterials are produced through physical and chemical methods, which often require substantial energy inputs and utilize toxic chemicals.[36]

Green synthesis refers to the production of nanomaterials using natural substances or plant extracts and their metabolites. The natural compounds, such as alkaloids, flavonoids, terpenoids, aldehydes, and amides, act as capping, stabilizing, and reducing agents. Nanomaterials biosynthesized through green chemistry approaches are less toxic, more eco-friendly, reliable, sustainable, and have significant potential for pharmaceutical and other applications.[37]

The green synthesis of nanoparticles (NPs) *via* the nanobiotechnology approach has an important role in boosting production compared to chemical and physical methods.[38] In the field of materials science, biogenic synthesis of NPs from plant derivatives has become a prominent area of research. Greenly synthesized nanomaterials exhibit various biological properties, including antimicrobial, anticancer, and antioxidants activities.

For example, *C. sinensis* peel extract has been used to produce silver NPs (AgNPs) and cellulose nanofibers that effectively remove cadmium and chromium from wastewater. Transmission electron microscopy images revealed that the average diameters of AgNPs and cellulose nanofibers were 32

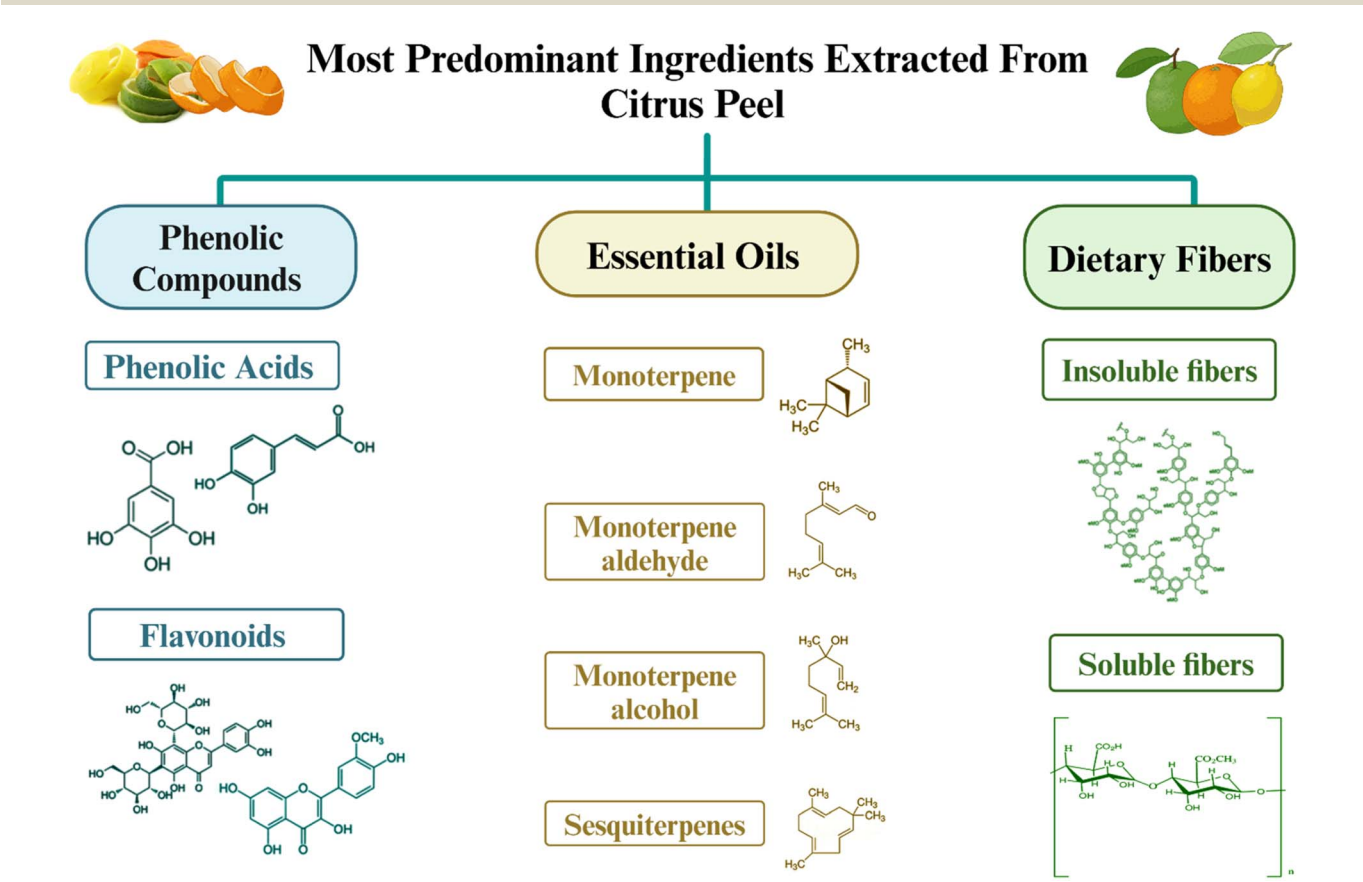

Fig. 1 Examples of the most predominant ingredients extracted from Citrus peel with their respective chemical structures. Figure created in Biorender.

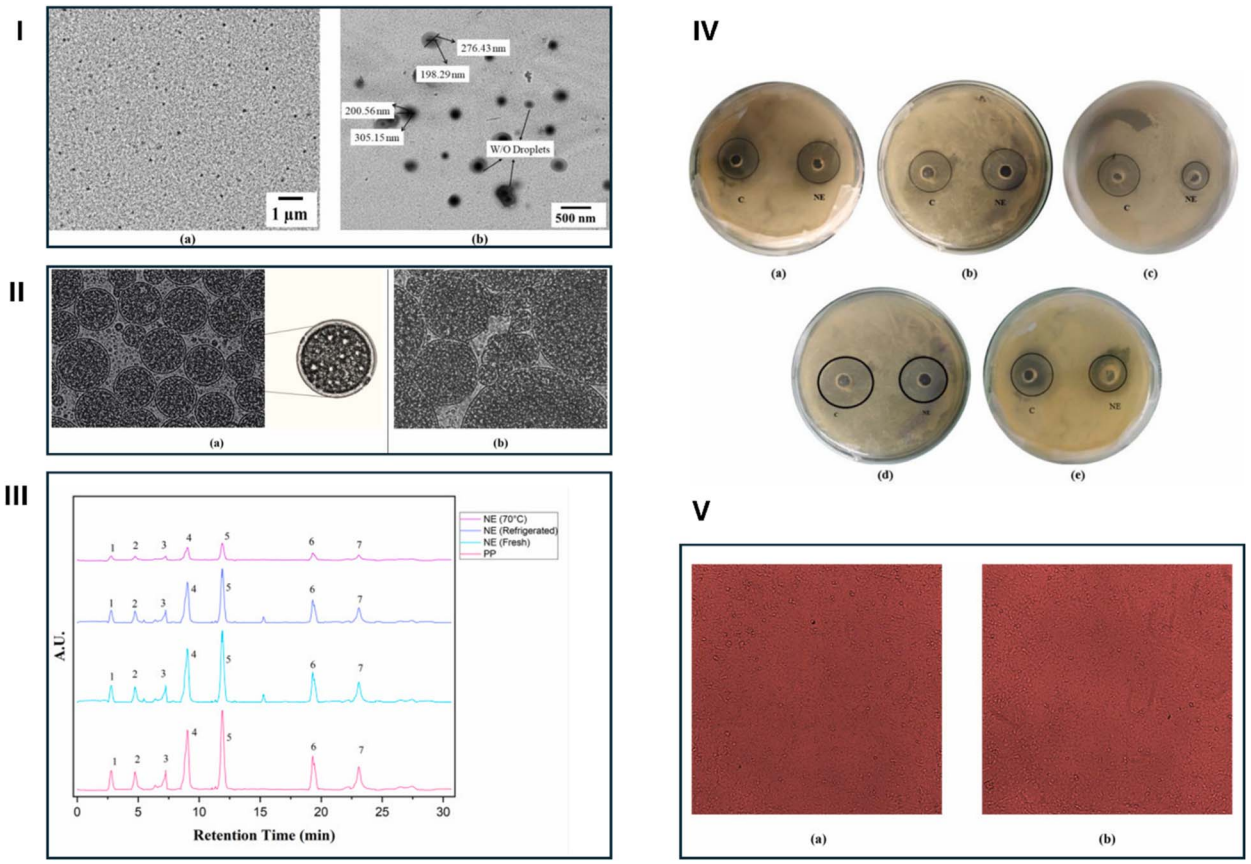

Fig. 2 Characterization and evaluation of nano-emulsions. (I) Transmission electron microscopy (TEM) images of freshly prepared nano-emulsions. (II) Microscopic comparison of fresh nano-emulsion and nano-emulsion stored at ambient temperature for 45 days. (III) High-performance liquid chromatography (HPLC) analysis of kinnow peel extract and nano-emulsion before and after storage. Peaks: gallic acid (1); chlorogenic acid (2); *p*-coumaric acid (3); ferulic acid (4); hesperidin (5); naringenin (6); quercetin (7). (IV) Antimicrobial properties of obtained nano-emulsions against *S. paucimobilis* (a), *B. subtilis* (b), *A. niger* (c), *S. aureus* (d), and *E. coli* (e) (NE: nanoemulsion; C: control). (V) Morphological changes in Vero-cell lines treated by encapsulated nanoemulsions (12.5 μg mL^{-1}) (a), compared to the control (b). Reproduced with permission from ref. 46, copyright 2024 Elsevier.

and 47 nm, respectively. The composite material, composed of AgNPs and cellulose nanofibers, demonstrated a preference for eliminating chromium ions over cadmium ions. The efficiency of chromium removal was measured at 83.5%, while cadmium removal was 32.2%.[39]

Another study demonstrated the use of *C. sinensis* peel extract to produce superparamagnetic iron oxide NPs (SPIONs). TEM examination revealed that the greenly produced SPIONs were spherical with particle sizes ranging from 20 to 24 nm. Magnetization measurements confirmed the superparamagnetic properties of the produced SPIONs at normal temperatures. This study investigated the antibacterial activity, minimum inhibitory concentration (MIC), antioxidant potential, anti-inflammatory effect, and catalytic degradation of methylene blue by the SPIONs.[40]

Given the multifaceted value of CPW, this review critically examines its role in the green synthesis of nanomaterials and their applications in biomedicine and environmental remediation. Two core valorisation strategies are discussed:

(1) Utilizing CPW-derived extracts as active components encapsulated in nanocarriers for therapeutic and functional applications (*e.g.*, drug delivery, wound healing, food packaging).

(2) Employing green synthesis methods to convert CPW directly into carbon-based, metallic, metal-oxide, and polymeric nanomaterials.

This review integrates recent findings, compares synthesis approaches, highlights current limitations, and outlines future directions to support sustainable nanotechnology rooted in circular economy principles. Unlike conventional reviews that focus narrowly on either synthesis methods or biomedical outcomes, this work offers a holistic perspective from the extraction of CPW-derived bioactives (*e.g.*, flavonoids, pectin) to their use in fabricating carbon-based, metallic, polymeric, and other nanomaterials. By consolidating recent advances and highlighting emerging strategies such as nano-encapsulation and magnetic hyperthermia, this review emphasizes sustainability, industrial relevance, and alignment with the UN Sustainable Development Goals, particularly SDG 12.

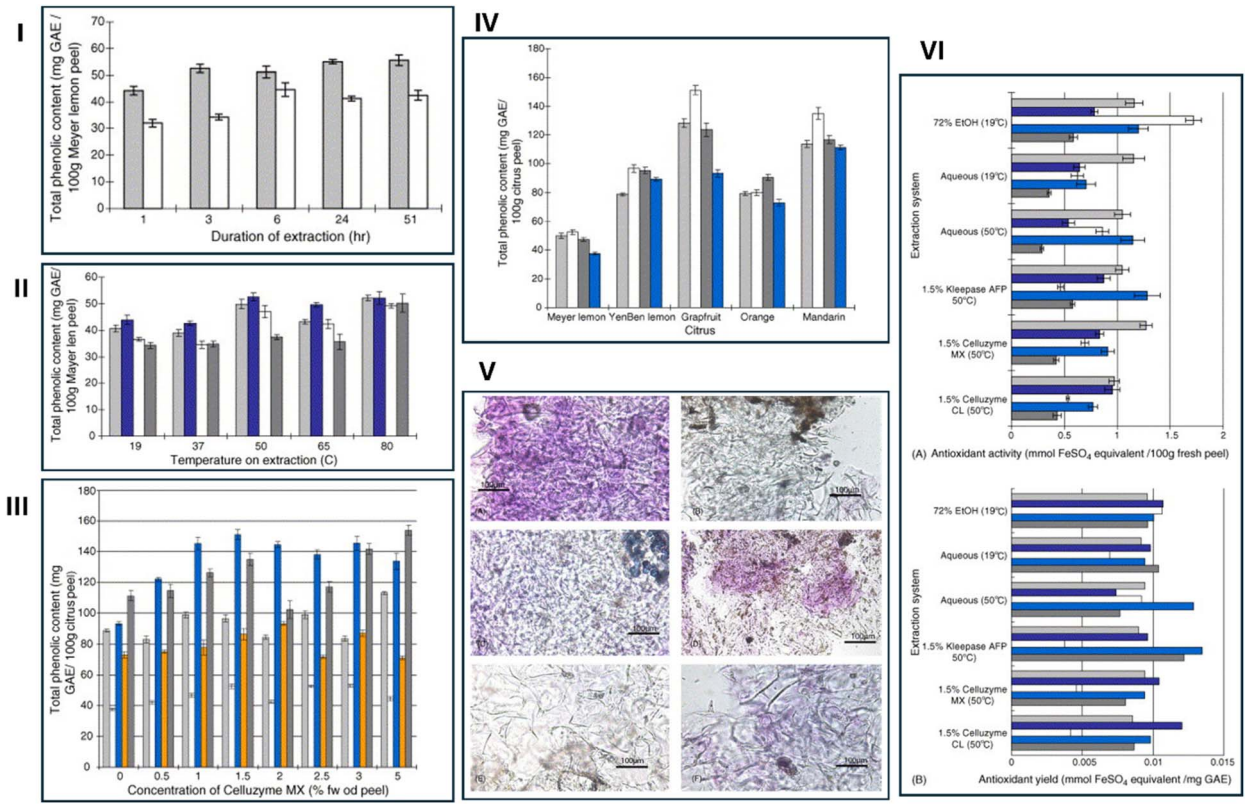

Fig. 3 Optimization and characterization of enzyme-assisted extraction of phenolic compounds from citrus peels. (I) Contact time impact on phenolic yield using enzyme-assisted (▩) and conventional aqueous (☐) extraction. (II) Temperature influence on phenolic yield using different enzyme preparations (Kleepase AFP 106L (☐), celluzyme MX (■), celluzyme CL (▩)) compared to a control (■). (III) Impact of celluzyme MX concentration on phenolic total content extracted from various citrus peels (mandarin (■), orange (■), grapefruit (■), Meyer lemon peel (☐), Yen Ben lemon (▩)). (IV) Comparison of phenolic yield obtained using different enzymes (Kleepase AFP 106L (■), celluzyme MX (☐), celluzyme CL (▩)) and conventional aqueous (■) extraction from various citrus peels. (V) Visual comparison of Meyer lemon peel before and after different extraction methods (aqueous, ethanolic (72%; 19 °C), enzyme-assisted (50 °C) with celluzyme MX, celluzyme CL, and kleepase AFP 106L). (VI) Antioxidant activity of extracts from different citrus peels determined by (A) $FeSO_4$ equivalent per 100 g fresh peel and (B) $FeSO_4$ equivalent per mg gallic acid equivalent (GAE) using various extraction methods. (Meyer lemon (■), Yen Ben lemon (■), grapefruit (☐), orange (■), mandarin (▩)). Reproduced with permission from ref. 53, copyright 2006 Elsevier.

2. Citrus peel constituents: basis for valorization

While extensive research has focused on the nutritional and medicinal properties of citrus fruits, relatively less attention has been given to their byproducts, particularly CPW, despite a long history of use in food preservation and traditional medicine. Phytochemical and nutritional assessments have demonstrated that CPW is a rich source of bioactive molecules, including a variety of functional compounds such as flavonoids, limonoids, EOs, and pectin, which possess diverse medicinal purposes.[41]

To date, approximately 140 compounds have been identified in CPW, including dietary fibers, polyphenols, and volatile components. For example, M'hiri *et al.* (2016) reported that citrus residues contain fiber (6.30–42.13 g/100 g dry basis), vitamin C (0.109–1.150 g/100 g), phenolic compounds (0.67–19.62 g/100 g), and EOs (0.6–1%). Key phenolics include flavanones such as narirutin (0.03–26.90 mg g^{-1}), hesperidin (up to 80.90 mg g^{-1}), naringin (0.08–14.40 mg g^{-1}), and neohesperidin (0.05–11.70 mg g^{-1}), along with polymethoxylated flavones like tangeretin (0.16–7.99 mg g^{-1}), sinensetin (0.08–0.29 mg g^{-1}), and nobiletin (0.20–14.05 mg g^{-1}).[42]

The predominant bioactive groups in CPW are phenolic compounds, EOs, and dietary fiber, each contributing to antioxidant, antimicrobial, and anti-inflammatory activities.[43] Phenolic compounds, in particular, are subclassified into phenolic acids and flavonoids, as outlined in Table 1 and Fig. 1. Flavonoids could be further subdivided into four sub-groups: polymethoxyflavones, flavonoid aglycones, flavone O-glycosides, and flavone C-glycosides. EOs are mainly composed of monoterpenes, monoterpenes aldehydes, monoterpenes alcohols, and sesquiterpenes, while dietary fiber is categorized as insoluble fibers (IDF) and soluble fibers (SDF),

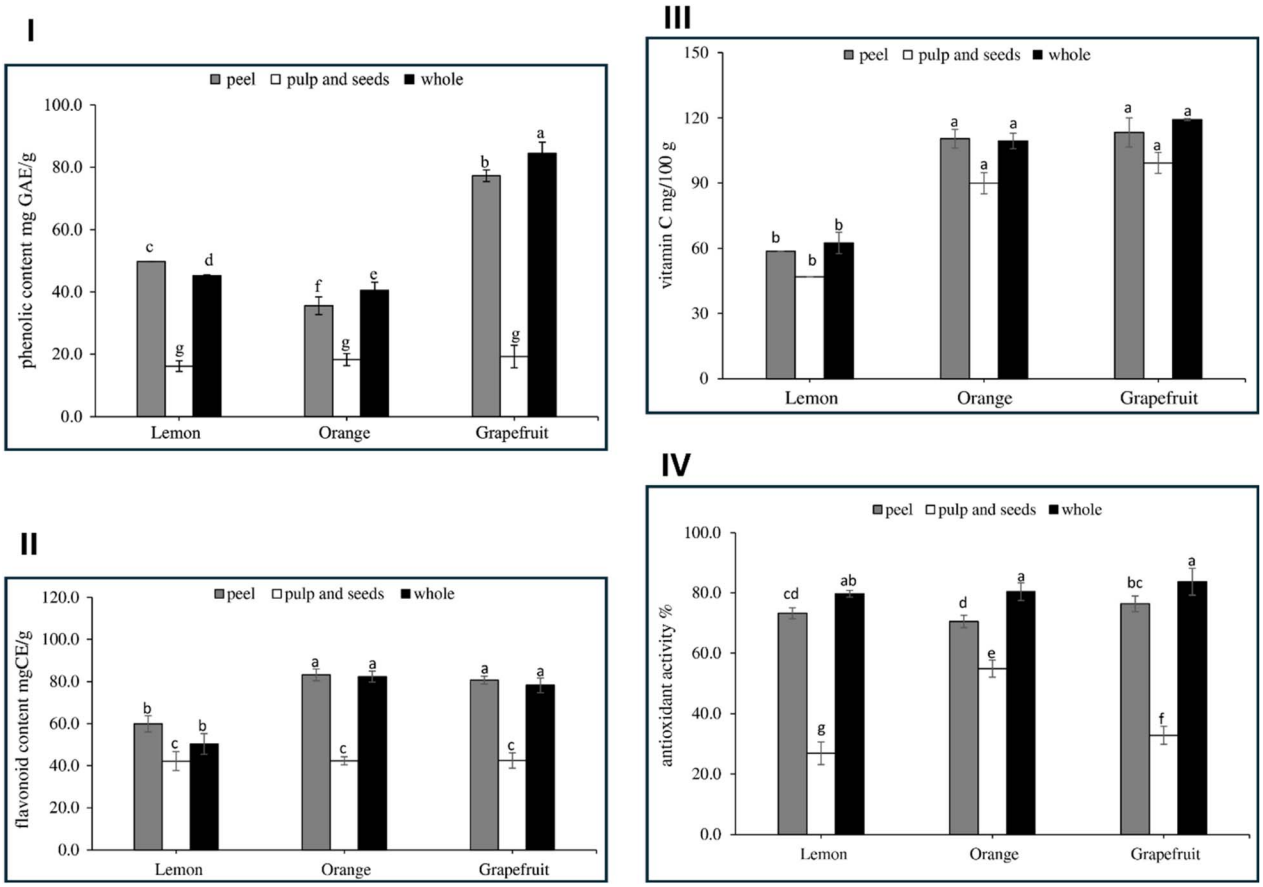

Fig. 4 Biochemical characterization of extracts from wasted parts of lemon, orange, and grapefruit. (I) Total phenolic content. (II) Total flavonoid content. (III) Vitamin C content. (IV) Antioxidant activity. Reproduced from ref. 54, copyright 2018 John Wiley & Sons.

based on water solubility. Table 1 serves as a reference framework by summarizing these classes with their representative compounds, molecular weights, and chemical structures, which are later linked to their biomedical and environmental applications.

2.1. Phenolic compounds

Phenolic compounds are a diverse class of plant-derived secondary metabolites known for their antioxidant, antimicrobial, and anti-inflammatory activities. They are considered one of the most valuable groups of bioactive molecules in CPW, particularly in the peel fraction. Their health benefits have been linked to reducing the risk of chronic diseases, including cancer, cardiovascular, and neurodegenerative disorders.[44,45]

Studies have demonstrated that citrus peels possess higher phenolic content compared to the pulp or juice. For example, M'hiri *et al.* (2016) quantified total phenolics in various citrus peels and found values ranging from 0.67 to 19.62 g/100 g dry weight, with hesperidin, narirutin, naringin, and neohesperidin being dominant.[42] These compounds exhibit multiple mechanisms of action, including free radical scavenging, metal chelation, and enzyme inhibition.

However, despite their bioactivity, phenolic compounds are susceptible to degradation due to exposure to light, temperature, and oxygen. To overcome these limitations, several encapsulation approaches have been applied. For instance, Kaur *et al.* (2024) developed nanoemulsions containing *p*-coumaric acid (201.43 ± 0.81), gallic acid (356.5 ± 1.41), chlorogenic acid (373.93 ± 4.38), quercetin (419.75 ± 4.47) μg g^{-1}, ferulic acid (1278.8 ± 9.09), naringenin (570.63 ± 0.88), and hesperidin (1192.56 ± 8.61), extracted from kinnow (*C. reticulata*) peels, enhancing their stability, antibacterial activity, and bioavailability. The nanoemulsions showed significant antibacterial action against both Gram-positive and Gram-negative bacteria, as well as pathogenic molds, indicating a strong preservation potential (Fig. 2). These formulations were also shown to be biocompatible with normal cell lines (Vero cells), with cell viability greater than 85%.[46]

In terms of extraction, both traditional and advanced techniques have been used to improve phenolic recovery. These include solvent extraction, enzyme-assisted extraction (EAE), microwave-assisted extraction (MAE), and supercritical

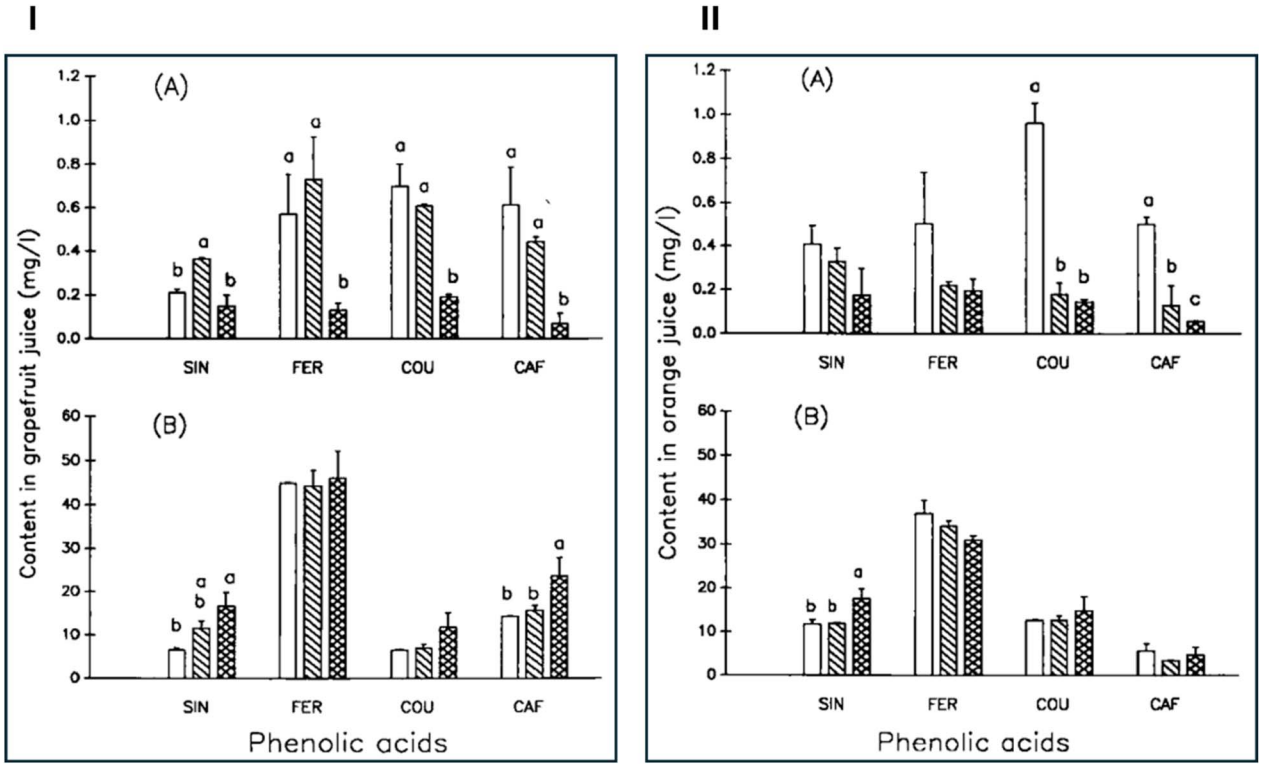

Fig. 5 Content of free and bound phenolic acids in (I) grapefruit (*var. Marsh*) and (II) orange (*var. Shamuti*) juice extracted from fruit harvested early (blank bars), mid-season (hatched bars), and late-season (crosshatched bars). (A) Free phenolic acids. (B) Bound phenolic acids. Caffeic (CAF), coumaric (COU), ferulic (FER), and sinapic (SIN) acids. Reproduced with permission from ref. 57, copyright 1991 John Wiley & Sons.

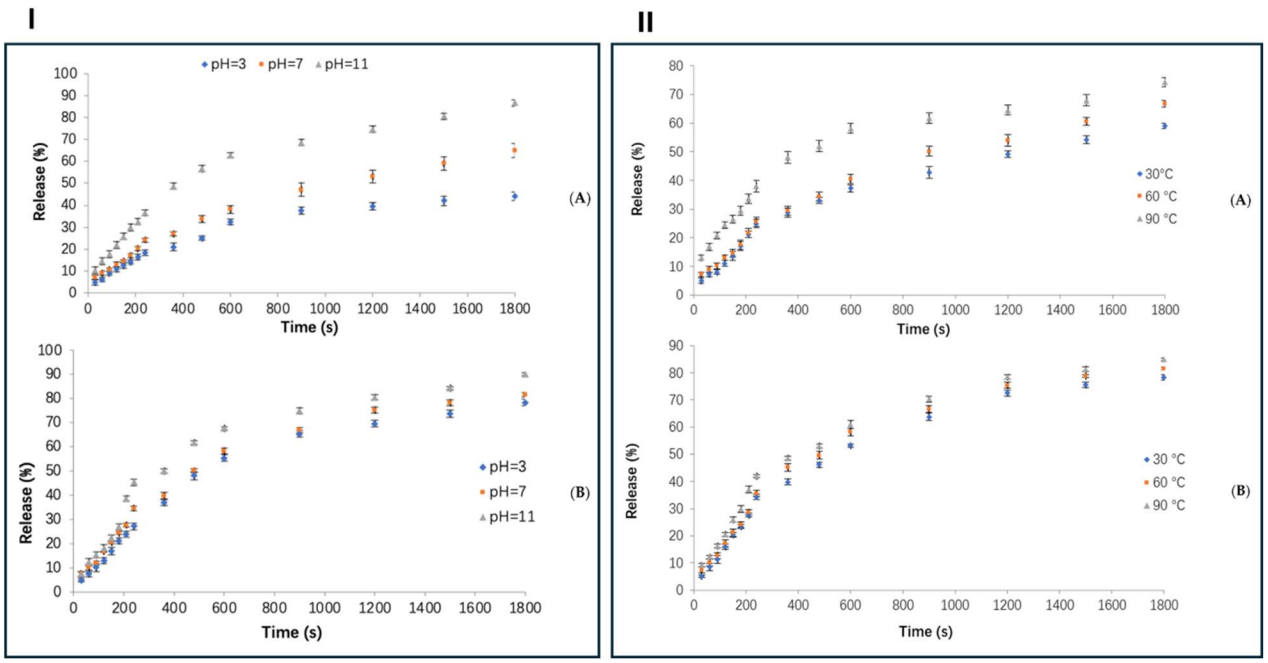

Fig. 6 Orange peel oil release from nanocomposite powders. (I) Effect of pH (3, 7, 11) on oil release at 60 °C for nanocomposite powders. (II) Effect of temperature (30, 60, 90 °C) on oil release at pH 7 for nanocomposite powders. Reproduced from ref. 85, copyright 2023 MDPI.

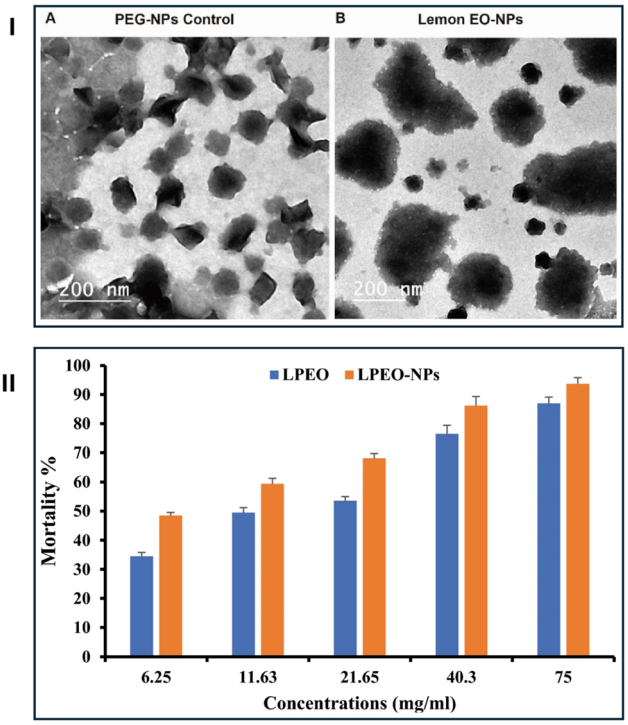

Fig. 7 Characterization and toxicity of LPEO-NPs. (I): (A) Transmission electron microscopy (TEM) image of PEGNPs (control); (B) TEM image of LPEO-NPs. (II) Percentage accumulated mortality of Agrotis ipsilon larvae treated with different concentrations of LPEO and LPEO-NPs. Reproduced from ref. 86, copyright 2023 Scientific Reports – Nature.

fluid extraction (SFE).[47–51] Extraction efficiency varies based on solvent type (*e.g.*, methanol, ethanol, acetone), polarity, pH, temperature, and time.[52] In this regard, Li *et al.* (2006) investigated the primary characteristics that influenced phenolic yield, such as peel condition, extraction temperature, solvent concentration, citrus species, and types of enzymes and their corresponding concentrations (Fig. 3). Folin–Ciocalteu assay was used to analyze and compare the total phenolic contents of five citrus peels (grapefruit, Yen Ben lemon, orange, Meyer lemon, and mandarin) extracted using simple water extraction or ethanol. Overall, grapefruit peel had the highest total phenolic content, followed by mandarin, Yen Ben lemon, orange, and Meyer lemon peel. Using ethanol as a solvent resulted in a high extraction rate (about 74%), which could be enhanced further by heating to 80 °C. Furthermore, the total antioxidant activity of phenolic contents isolated from various citrus peels was evaluated using FRAP assay. Grapefruit peels have the highest overall antioxidant activity, followed by Yen Ben lemon, mandarin, orange, and Meyer lemon.[53]

Furthermore, different varieties of citrus fruit peel have varying total phenolic contents. For example, Sir Elkhatim *et al.* (2018) studied the antioxidant activity, phenolic compounds, and vitamin C contents of wastes derived from citrus fruits of grapefruit, lemon, and orange. Each citrus type's whole fruit, peel, and pulp with seeds were used to make ethanolic extracts. Within each variety of citrus, peels included more phenolic compounds, flavonoids, vitamin C, and antioxidant activity than the inner discarded sections (pulp and seeds). Grapefruit peels exhibited the highest total phenolic content, followed by lemon and orange peels, with 77.3, 49.8, and 35.6 mg of gallic acid equivalent per gram of peel, respectively. On the other hand, orange peels contain the most flavonoids (83.3 mg of catechin equivalent per g) and vitamin C (110.4 mg/100 g) compared to the peels of the other citrus fruits studied in this study (Fig. 4). In general, the high antioxidant capacity and activity of citrus waste, particularly the peels, suggested that they could provide health and nutritional benefits when used in the food sector as a natural antioxidant.[54]

2.1.1. Phenolic acids. Phenolic acids are aromatic compounds possessing one or more hydroxyl groups attached to a benzene ring. They are primarily synthesized *via* the shikimic acid and phenylpropanoid pathways in plants and exist in both free and bound forms in citrus peel.[55] They are structurally categorized into: hydroxybenzoic acids (HBAs), including gallic acid, syringic acid, protocatechuic acid, *p*-hydroxybenzoic acid, and vanillic acid, and hydroxycinnamic acids (HCAs), including caffeic acid, ferulic acid, *p*-coumaric acid, and sinapic acid.[45,56] Peleg *et al.* (1999) discovered that free phenolic acids could be the precursors for vinyl phenols and off-flavors generated in citrus products during storage. The free and bound phenolic acids in grapefruit (*C. paradisi*) and oranges (*C. sinensis*) were quantified using ethyl acetate extraction, silica gel column chromatography, and HPLC analyses of samples before and after alkaline hydrolysis. The concentration of free and bound phenolic acids was also evaluated in juice made from fruit picked early, mid, and late in the season. Consequently, the bound forms of phenolic acids were found to be more abundant in *C. sinensis* and *C. paradisi* than free forms. Flavedo tissues (outer peel) typically contained higher concentrations than albedo (inner white part). Among these, ferulic acid had been consistently identified as the most abundant cinnamic acid derivative in citrus peel (Fig. 5). The results also showed that the content of bound cinnamic acids remained stable or slightly increased from early to late season. However, the concentration of free acids decreased throughout that time.[57]

Phenolic acids possess strong antioxidant activity, attributed to their ability to donate hydrogen atoms or electrons, neutralize free radicals, and chelate metal ions. These properties also make them suitable reducing and stabilizing agents in the biosynthesis of NPs, such as silver, gold, iron oxide, and zinc oxide NPs.[58] In a study by Fejzić *et al.* (2014), five citrus juice and peel extracts (pink grapefruit, tangerine, white grapefruit, lemon, and orange) were evaluated for antioxidant activity and total phenolic content. The spectrophotometric Folin–Ciocalteu technique was used to assess total phenolic content. Values ranged from 0.192 ± 0.015 mg GAE per mL for white grapefruit peel to 0.747 ± 0.098 mg GAE per mL for white grapefruit juice. The antioxidant activity of the samples was determined using the total antioxidant technique, which involves the reduction of molybdenum ions and is represented as IC50. The IC50 values varied between 6.00 ± 0.50 mg mL^{-1} for orange juice and 78.11

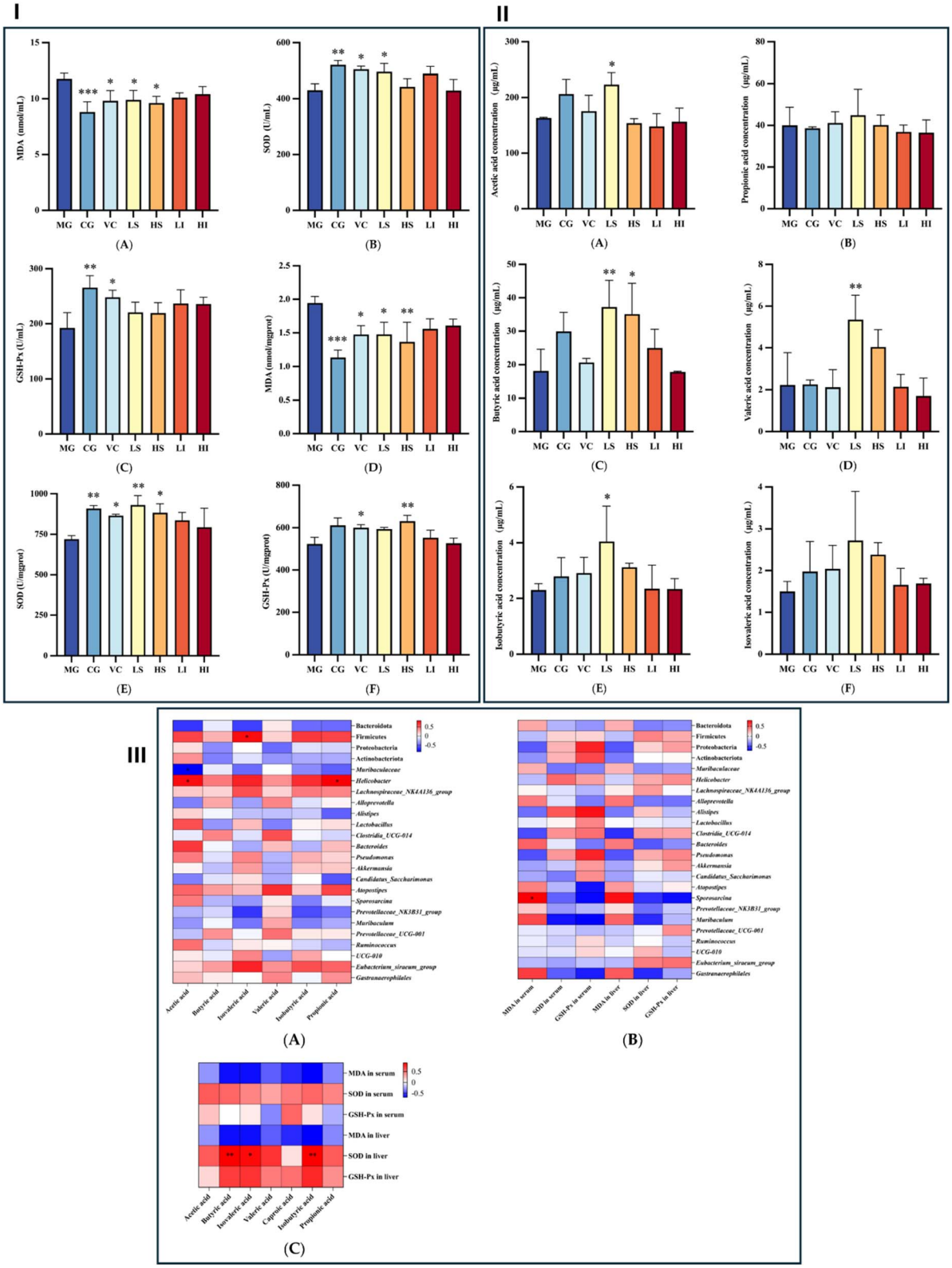

Fig. 8 Effects of dietary fiber supplementation (PSDF and PIDF) on oxidative stress (I), intestinal SCFA production (II), and gut microbiota (III) in D-galactose-induced aging mice. (I) Serum and liver oxidative stress markers in response to PSDF and PIDF supplementation: (A) serum malondialdehyde (MDA), (B) serum superoxide dismutase (SOD), (C) serum glutathione peroxidase (GSH-Px), (D) liver MDA, (E) liver SOD, (F) liver GSH-Px. (II) Intestinal short-chain fatty acid (SCFA) production in mice supplemented with PSDF and PIDF: (A) acetic acid, (B) propionic acid, (C) butyric acid, (D) valeric acid, (E) isobutyric acid, (F) isovaleric acid. (III) Correlations between intestinal microbiota, SCFAs, and antioxidant indexes: (A) correlation between intestinal microbiota (top 20 genus level and top 4 phylum level) and SCFAs, (B) correlation between antioxidant indexes and intestinal microbiota, (C) correlation between antioxidant indexes and SCFAs. Red indicates a positive correlation, and blue indicates a negative correlation. Reproduced from ref. 95, copyright 2024 MDPI.

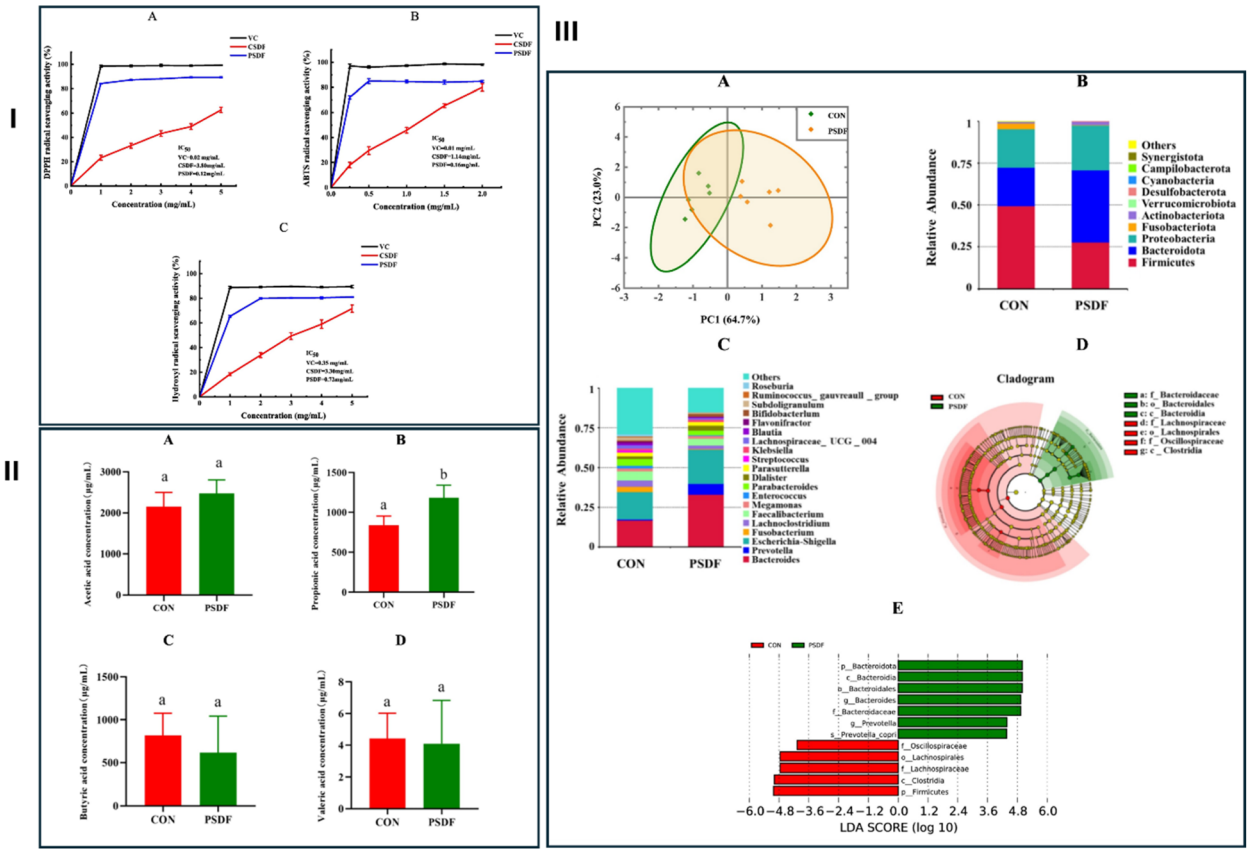

Fig. 9 Effects of SDF on antioxidant activity and gut microbiota. (I) Radical scavenging capacity of CSDF and PSDF: (A) DPPH radical scavenging assay, (B) ABTS+ radical scavenging assay, (C) hydroxyl radical scavenging assay. (II) Concentrations of short-chain fatty acids (SCFAs) during *in vitro* fermentation: (A) acetic acid, (B) propionic acid, (C) butyric acid, (C) valeric acid; CON: fermentation without SDF; PSDF: fermentation with 8 g L^{-1} SDF. (III) Comparison of gut microbiota composition. (A) Principal co-ordinates analysis (PCoA) of gut microbiota at the genus level. (B) Relative abundance of gut microbiota at the phylum level. (C) Relative abundance of gut microbiota at the genus level. (D) Linear discriminant analysis (LDA) score for taxa differing between groups. (E) LEfSe evolutionary branch graph. CON: glucose as carbon source, PSDF: purified SDF as carbon source. Reproduced with permission from ref. 96, copyright 2023 Elsevier.

$\pm$ 6.70 mg mL^{-1} for lemon juice, suggesting a potential link between phenolic acid abundance and antioxidant capacity.[59] This also supports their inclusion in the formulation of nano-carriers with improved bioactivity.

Due to their amphiphilic nature, phenolic acids have also been incorporated into nanoemulsion systems, liposomes, and biopolymer-based NPs, enhancing their bioavailability and release kinetics in pharmaceutical and food applications.

2.1.2. Flavonoids. Flavonoids are the most prominent subclass of phenolic compounds in CPW, accounting for a significant portion of its bioactivity, with a quantity ranging from 2.5 to 5.5 g/100 g dry weight, depending on the citrus species.[60] These polyphenolic molecules are widely distributed in the flavedo and albedo layers of the citrus peel and play essential roles in plant defense, pigmentation, and growth regulation. Their health-promoting effects in humans include antioxidant, anti-inflammatory, antiviral, and anticancer activities.[61,62]

Structurally, flavonoids consist of a 15-carbon skeleton arranged in a C6–C3–C6 configuration, forming two aromatic rings (A and B) and a heterocyclic ring (C). Based on variations in oxidation and substitution patterns of the C ring, flavonoids are classified into several subclasses: flavanones, flavones, flavonols, flavanols (catechins), anthocyanidins, and isoflavones.[61]

Although flavonoids are generally regarded as non-nutritive agents, their potential role in the prevention of major chronic diseases has attracted increasing research interest. For example, Lai *et al.* (2007) employed 5-Hydroxy-3,6,7,8,3′,4′-hexamethoxyflavone (5-OH-HxMF), a polymethoxyflavone found exclusively in the genus *Citrus*, particularly in sweet orange (*C. sinensis*) peels, to study the effects of 12-*O*-tetradecanoylphorbol 13-acetate (TPA) on skin inflammation and tumor promotion in mice. Their results demonstrated that pre-application of 5-OH-HxMF significantly suppressed TPA-induced iNOS and COX-2 mRNA and protein expression in a dose-dependent manner. Moreover, topical application of 1 and 3 μmol of 5-OH-HxMF prior to TPA treatment during tumor promotion markedly reduced both the number and size of papillomas, consistent with reduced levels of pro-inflammatory markers.[62]

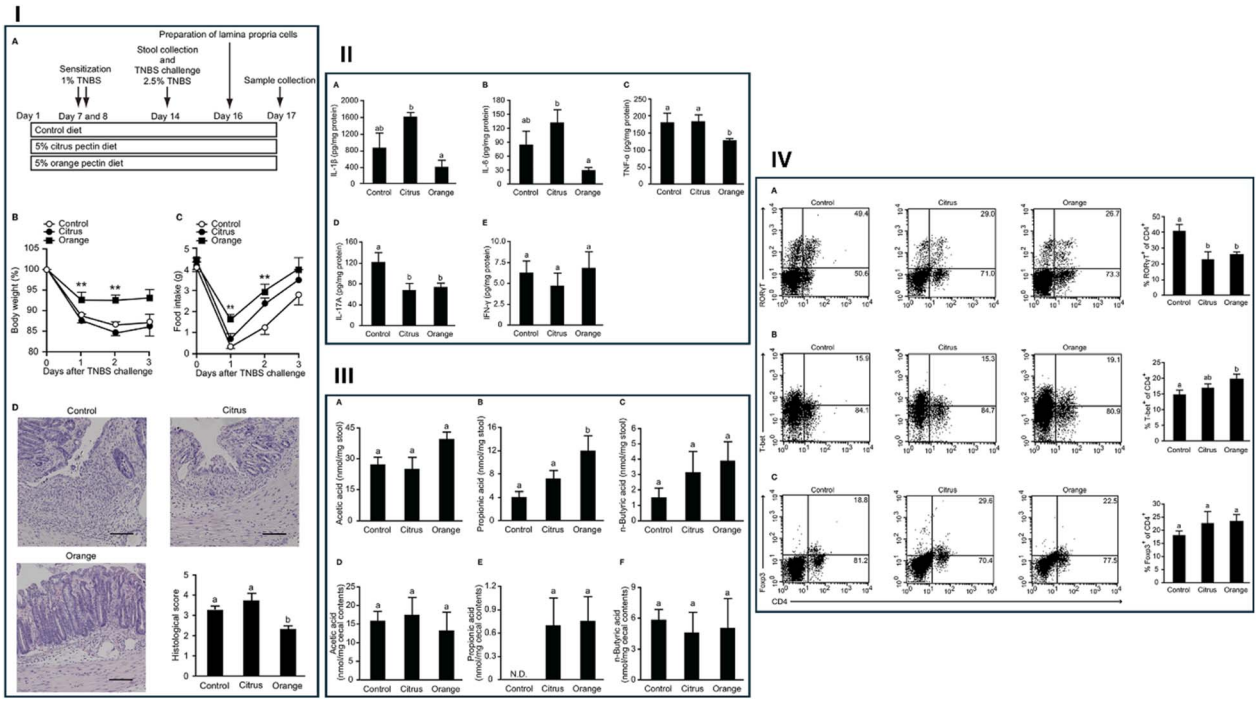

Fig. 10 Effects of pectin feeding on TNBS-induced colitis in mice. (I) Impact of pectin on disease severity in TNBS-induced colitis: (A) Experimental design and treatment timeline, (B) changes in body weight, (C) changes in food intake, (D) histological score of colonic tissue. Scale bars: 100 μm. (II) Effect of pectin on colonic inflammatory cytokine production in TNBS-induced colitis. Levels of (A) IL-1β, (B) IL-6, (C) TNF-α, (D) IL-17A, and (E) IFN-γ in colon tissue 3 days post-TNBS administration. (III) Effect of pectin feeding on intestinal short-chain fatty acid (SCFA) production. Concentrations of (A) fecal acetic acid, (B) fecal propionic acid, (C) fecal butyric acid, (D) cecal acetic acid, (E) cecal propionic acid, and (F) cecal butyric acid. (IV) Effect of pectin on colonic T cell differentiation in TNBS-induced colitis. Flow cytometry analysis of colonic lamina propria cells 2 days post-TNBS challenge: (A) CD4+RORγt+ cells, (B) CD4+T-bet+ cells, (C) CD4+Foxp3+ cells. Reproduced from ref. 97, copyright 2019 Frontiers.

Citrus fruits include two types of flavonoids: polymethoxylated flavones (*e.g.*, sinensetin, nobiletin, and tangerine) and flavanone glycosides (*e.g.*, hesperidin, neohesperidin, and naringin).[60] The total flavonoid content (TFC) of citrus peels is mainly composed of flavanones and polymethoxylflavones (PMFs), including naringin, hesperidin, narirutin, nobiletin and neohesperidin.[63] PMFs from orange peel comprise approximately 75.1% non-hydroxylated PMFs and 5.44% hydroxylated PMFs, both of which demonstrate a wide spectrum of biological activities.[64]

The dominant flavonoids vary among citrus species: *C. reticulata* (mandarins) and hybrids are rich in hesperidin, *C. grandis* (pummelos) contain more naringin, and *C. limon* (lemon) is rich in eriocitrin.[65,66] Citrus peels, in general, contain higher levels of PMFs compared to other fruit parts.[67,68]

Flavonoids in citrus peel are well-recognized as potent dietary antioxidants, exhibiting mechanisms such as hydrogen atom transfer, free radical scavenging, and divalent metal ion chelation.[69] These molecules also help regulate metabolic syndrome and type 2 diabetes by mechanisms including α-glucosidase inhibition, insulin sensitization, and blood lipid reduction.[70]

Furthermore, Shehata *et al.* (2021) investigated the potential of orange peels as natural antioxidants and antibacterial agents. The solvent used for extraction had a significant impact on flavonoid and polyphenol yield. Methanolic extraction yielded the highest total flavonoid content in sweet orange peel (approximately 16 g/100 g), while ethanolic extraction enhanced the total phenolic (345 mg GAE/100 g DW) and flavonoid content (80 mg CE/100 g DW). The ethanolic extract exhibited the highest DPPH and ABTS scavenging activity, while the methanolic extract showed stronger hydroxyl radical scavenging. Notably, all extracts displayed excellent antimicrobial activity against both Gram-positive and Gram-negative bacteria, as well as fungi. The sweet orange peel extract showed the strongest antibacterial performance. Further UPLC-ESI-MS/MS analysis revealed the presence of narirutin (~29 μg g^{-1}), quinic acid (~13 μg g^{-1}), naringin (~27 μg g^{-1}), hesperetin-7-*O*-rutinoside naringenin (~15 μg g^{-1}), datiscetin-3-*O*-rutinoside (~11 μg g^{-1}), and hesperetin (~17 μg g^{-1}).[71]

These findings underscore the therapeutic versatility of citrus-derived flavonoids, not only for direct bioactivity but also for their potential role in nanotechnology applications, such as serving as reducing agents in NPs synthesis or as encapsulated bioactives in nanoformulations. Their dual function, as bioactives and green synthesis mediators, adds significant value to CPW-based nanomaterial platforms.

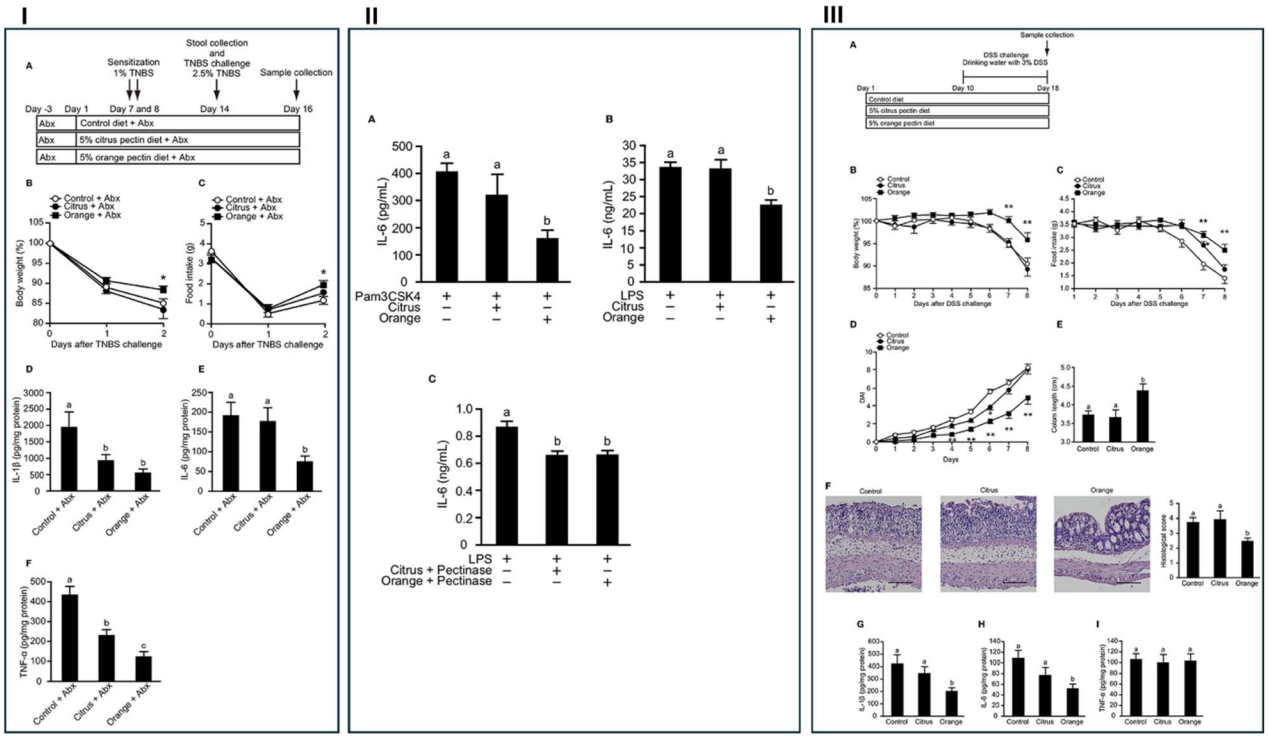

Fig. 11 Effects of pectin on colitis in mice and macrophage responses. (I) Effects of pectin feeding on TNBS-induced colitis in mice pre-treated with antibiotics: (A) experimental design and treatment timeline, (B) changes in body weight, (C) changes in food intake, (D) colonic IL-1β levels, (E) colonic IL-6 levels, (F) colonic TNF-α levels. (II) Effect of pectin pre-treatment on IL-6 production in RAW264.7 macrophages: (A) cells were stimulated with Pam3CSK4, (B) cells were stimulated with LPS, (C) cells were pre-treated with polysaccharides derived from pectin side chains and stimulated with LPS. (III) Effects of pectin feeding on DSS-induced colitis in mice: (A) experimental design and treatment timeline, (B) changes in body weight, (C) changes in food intake, (D) disease activity index (DAI) score, (E and F) colon length and representative histological sections, (G) colonic IL-1β levels, (H) colonic IL-6 levels, (I) colonic TNF-α levels. Scale bars: 100 μm. Reproduced from ref. 97, copyright 2019 Frontiers.

2.2. Essential oils (EOs)

Citrus EOs are an important biologically active compounds, mainly concentrated in the oil glands of citrus peels.[43] On average, they represent approximately 0.5–5% of the fresh weight of citrus peels. These volatile oils contain diverse phytochemicals, including monoterpene and sesquiterpene hydrocarbons, along with their oxygenated derivatives (*e.g.*, aldehydes, ketones, acids, alcohols, and esters).[72]

Limonene and γ-terpinene, the major constituents of citrus EO, exhibit a broad spectrum of biological activities, including antimicrobial, antioxidant, and anticancer effects.[73,74] The key phytochemical components commonly identified in citrus EO include D-limonene (~90%), citral, *n*-dodecanal, α-pinene, *n*-decanal, citronella, and linalyl acetate.[75] These compounds contribute not only to the distinct aroma but also to their wide use in the perfume, food, and pharmaceutical industries due to their low cost and multifunctionality.[76]

Citrus EOs also exhibit strong antioxidant, insecticidal, antifungal, and antibacterial properties, making them relevant in applications across food preservation, sanitation, cosmetics, and medicine.[22] For instance, tangerine EO has been linked to hypolipidemic and anti-inflammatory properties, and is widely used for its antidepressant effects.[41] In support of this, Castro *et al.* demonstrated tangerine EO's potential to prevent atherosclerosis by inhibiting lipid production and reducing LDL peroxidation.[77] Bergamot EO is well known for its anticancer activities and usefulness in food preservation.[78] Orange EO has demonstrated a variety of health benefits, including an anti-obesity properties with a reported 17% reduction in total cholesterol,[79] as well as antidepressant, anxiolytic,[80] apoptotic and anti-angiogenesis effects on colon cancer cells,[81,82] anti-inflammatory, neuroprotective, and analgesic effects.[82,83]

Koochi *et al.* (2022) investigated the antioxidant, α-glucosidase, and α-amylase inhibitory activities of EOs derived from fresh peels of bitter orange, grapefruit, lime, mandarin, lemon, sweet orange, and pomelo. Citrus EO is primarily composed of linalool (18.26–29.08%), linalool acetate (17.17–30.47%), limonene (17.08–22.44%), α-geraniol (2.05–6.30%), geranyl acetate (1.89–2.80%), β-ocimene (1.52–5.02%), terpineol (6.08–11.06%), nerolidol (2.93–4.00%), β-pinene (2.71–3.29%), and farnesol (2.08–2.97%). These extracts exhibited high antioxidant capacity (375–643 mg Trolox equivalents per g) and demonstrated substantial α-amylase (520–738 mg acarbose equivalents

per g) and α-glucosidase inhibitory activity (470–780 mg acarbose equivalents per g).[84]

Despite their promising bioactivities, citrus EOs face several formulation challenges due to their high volatility, photosensitivity, and low water solubility. To address these limitations, nanoencapsulation techniques have been employed to improve stability, bioavailability, and controlled release. For example, orange peel oil (OPO), widely used as a flavoring agent, is prone to degradation under heat, light, and oxidative conditions. Encapsulation in biopolymer-based nanocomposites has been shown to protect OPO and enhance its functional properties. Ghasemi *et al.* (2023) evaluated the release behavior of freeze-dried OPO nanocomposite powders under varying pH (3, 7, 11) and temperature (30, 60, 90 °C) in a simulated salivary system (Fig. 6). Their findings demonstrated an encapsulation efficiency ranging from 70–88%, with particle size confirmed in the nanoscale range *via* AFM.[85]

In another study, Ahmed *et al.* (2023) explored the use of nano-formulated lemon peel EO (LPEO) encapsulated in polyethylene glycol (PEG) NPs to enhance its insecticidal activity against *Agrotis ipsilon*. The nanoformulation significantly improved performance compared to free LPEO: at 75 mg mL^{-1}, larval mortality reached 90% with LPEO-NPs *versus* 80% for free LPEO. TEM imaging validated the successful formulation, and the results highlighted the enhanced bioefficacy of EO upon nano-delivery (Fig. 7).[86]

These findings emphasize the potential of citrus EO as both bioactive agents and nanocarrier-friendly compounds, making them highly valuable in sustainable applications ranging from insect control and disease prevention to functional foods and targeted therapy.

2.3. Dietary fiber

Citrus peels contain a variety of useful active compounds, with dietary fiber (DF) accounting for more than 50%.[87] DF is a complex polymer composed of various monomeric units and is either part of plant cell walls or extracted from intracellular regions. While indigestible by human enzymes, DF plays a crucial role in modulating gut microbiota and overall metabolic health. Studies confirm that adequate DF intake can lower blood sugar and cholesterol levels, thus reducing cancer risk.[88]

DF is generally categorized as soluble (SDF) or insoluble (IDF), based on its water solubility. Among the two, SDF exhibits stronger antioxidant potential, likely due to its polysaccharide content.[89–91] Carbohydrates account for nearly 80% of citrus fiber composition, predominantly as pectin (~42.25%) and cellulose (~15.95%).[92] Owing to its acidic and charged nature (*e.g.*, galacturonic acid), pectin imparts viscosity and gelling properties, thus contributing significantly to fiber functionality. Hemicellulose, another major DF component (~10.06%), has

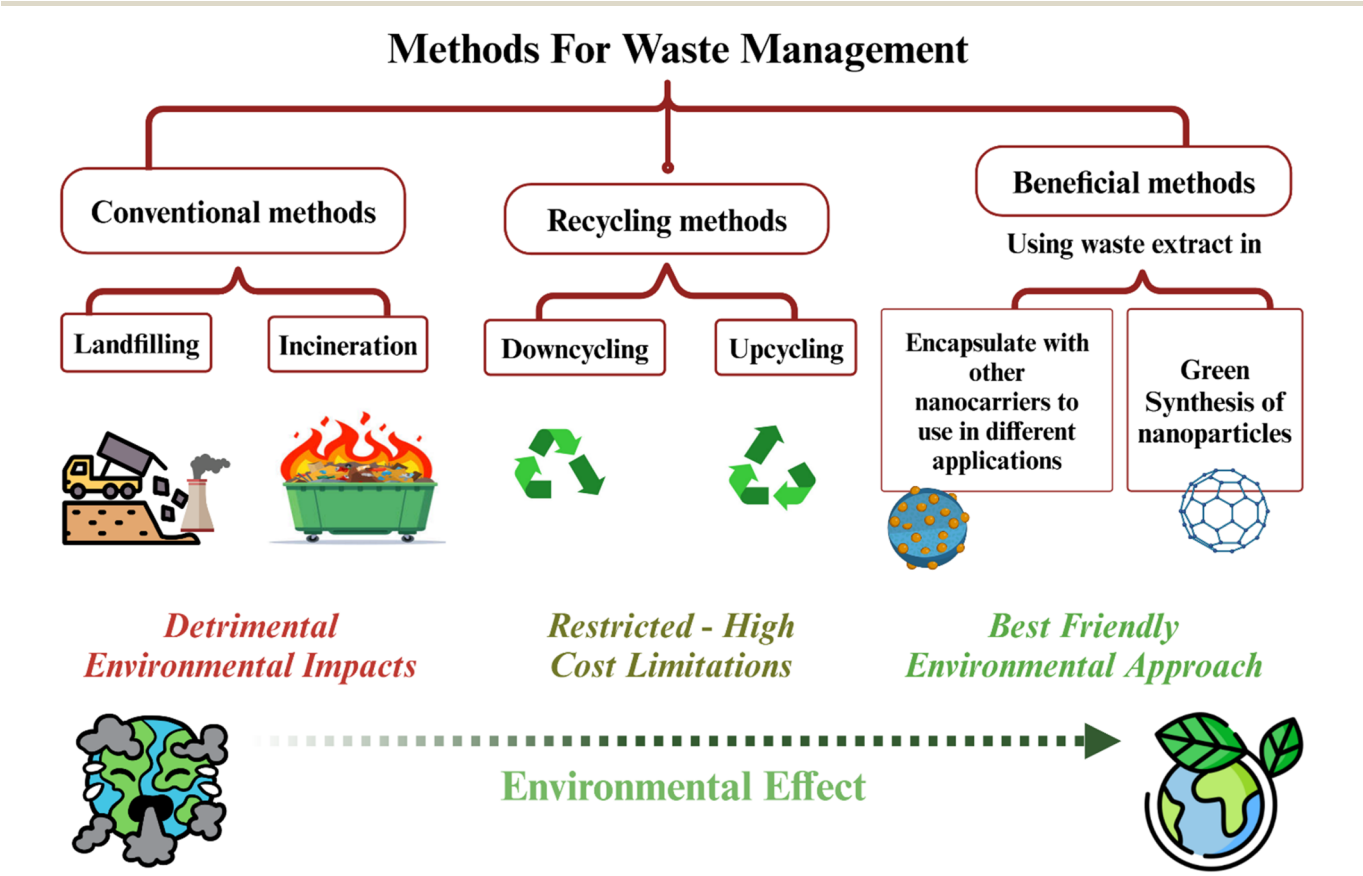

Fig. 12 Management approaches of citrus peel waste along with their impact on the environment. Figure created in Biorender.

a highly branched, amorphous, and non-crystalline structure that provides high viscosity and water-holding capacity.[93,94] These physicochemical features collectively make citrus DF a valuable multifunctional additive in health-promoting formulations.

For example, Fu *et al.* (2024) investigated the antioxidant and microbiota-regulating effects of purified SDF (PSDF) from *C. unshiu* in a mouse model of oxidative stress. The authors conducted their investigation on 8-week-old mice that were artificially aged for 42 days by subcutaneous injections of a 200 mg per kg per day D-galactose solution, followed by a 28-day feeding intervention with varied dosages of PSDF, insoluble dietary fiber (PIDF), and vitamin C. Following the intervention, they observed significant reductions in D-galactose-induced oxidative stress, as seen by weight normalization and decreased oxidative damage. PSDF drastically altered the makeup of intestinal flora, raising Firmicutes and decreasing Bacteroidota ratios while enriching colonic short-chain fatty acids. Further Spearman correlation analysis revealed a positive link between Firmicutes and isovaleric acid, as well as negative correlations between Muribaculaceae and acetic acid and Lachnospiraceae NK4A136 group and caproic acid (Fig. 8). These data refer to Citrus PSDF's ability to reduce oxidative damage.[95]

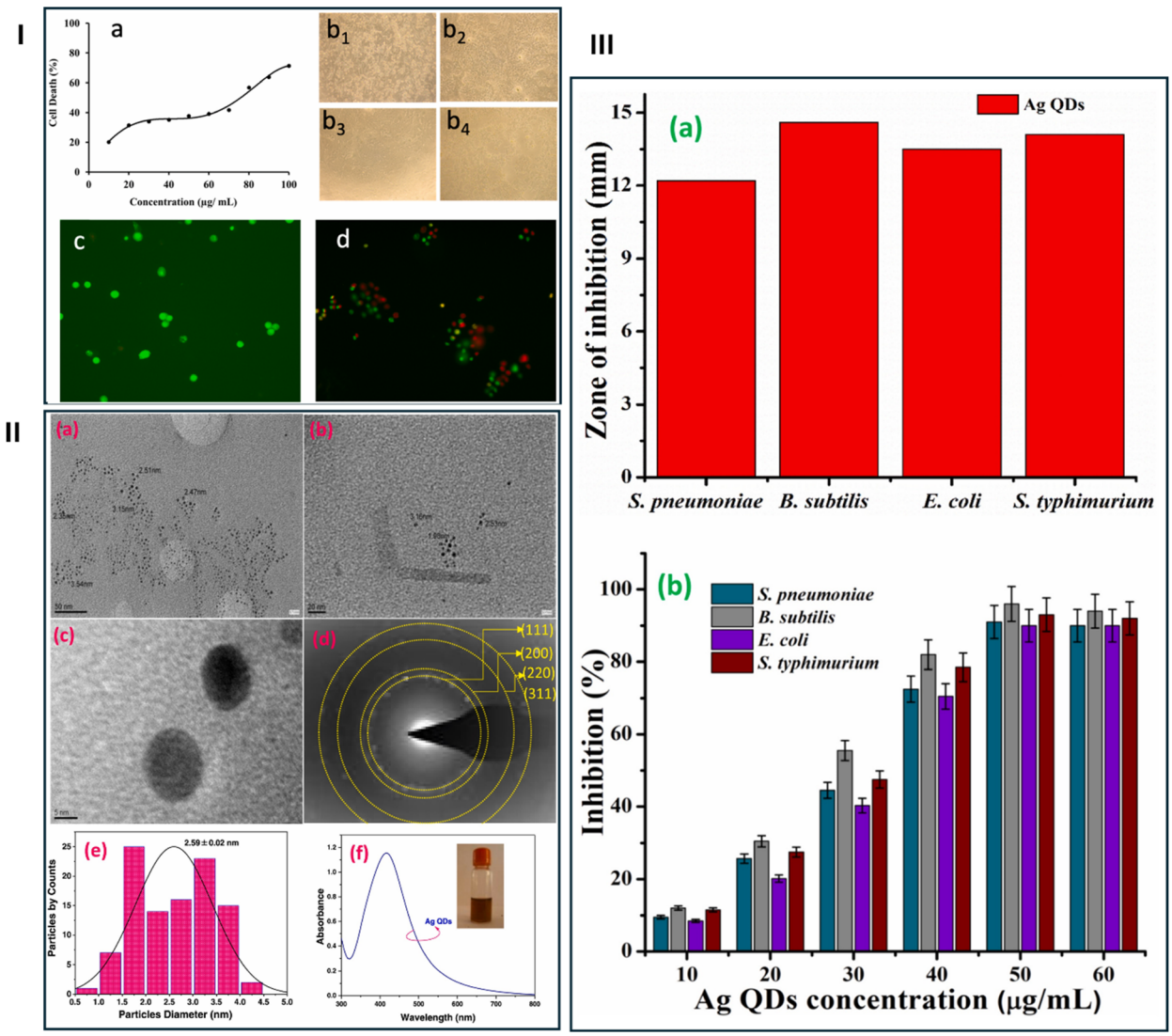

Fig. 13 (I) *In vitro* evaluation of Ag QD cytotoxicity and antibacterial activity. (a) Dose–response curve illustrating the effect of Ag QDs on the viability of MCF-7 human breast cancer cells. (b1–b4) Light microscopic images of control cells and cells treated with 10, 50, and 100 μg mL^{-1} of Ag QDs. (c) Fluorescence microscopic images of control cells. (d) Fluorescence microscopic images of cells treated at the IC50 value of Ag QDs using AO-EB dual staining. (II) Characterization of synthesized Ag QDs. (a and b) Transmission electron microscopy (TEM) images, (c) high-resolution TEM (HRTEM) image, (d) selected area electron diffraction (SAED) pattern, (e) size distribution analysis, and (f) UV-vis absorption spectrum of Ag QDs and a photograph of the Ag QD reaction solution. (III) Antibacterial activity of Ag QDs against Gram-positive bacteria and Gram-negative bacteria. (a) Antibacterial activity of Ag QDs at a concentration of 50 μg mL^{-1}. (b) Bacterial growth inhibition of selected pathogenic bacteria at various Ag QD concentrations. Reproduced with permission from ref. 104, copyright 2021 Elsevier.

In another study, Gu *et al.* (2023) compared purified and crude SDF extracted from *C. unshiu* peel using ultrasound-assisted alkaline extraction. Unpurified soluble dietary fiber (CSDF) was compared to purified soluble dietary fiber (PSDF) in terms of content, molecular weight, physicochemical characteristics, antioxidant activity, and intestinal regulating ability. The PSDF exhibited higher molecular weight (>15 kDa), shear-thinning properties, and greater thermal stability under 200 °C. PSDF also demonstrated enhanced antioxidant activity, including DPPH, $ABTS^{+}$, and hydroxyl radical scavenging, and promoted SCFA production and Bacteroides abundance in fermentation trials (Fig. 9). These results support PSDF's potential in functional food applications and intestinal health enhancement.[96]

Beyond antioxidant and prebiotic effects, citrus DF, especially pectin, has shown therapeutic promise in gastrointestinal conditions such as inflammatory bowel disease (IBD). Ishisono *et al.* (2019) examined how pectin's side-chain

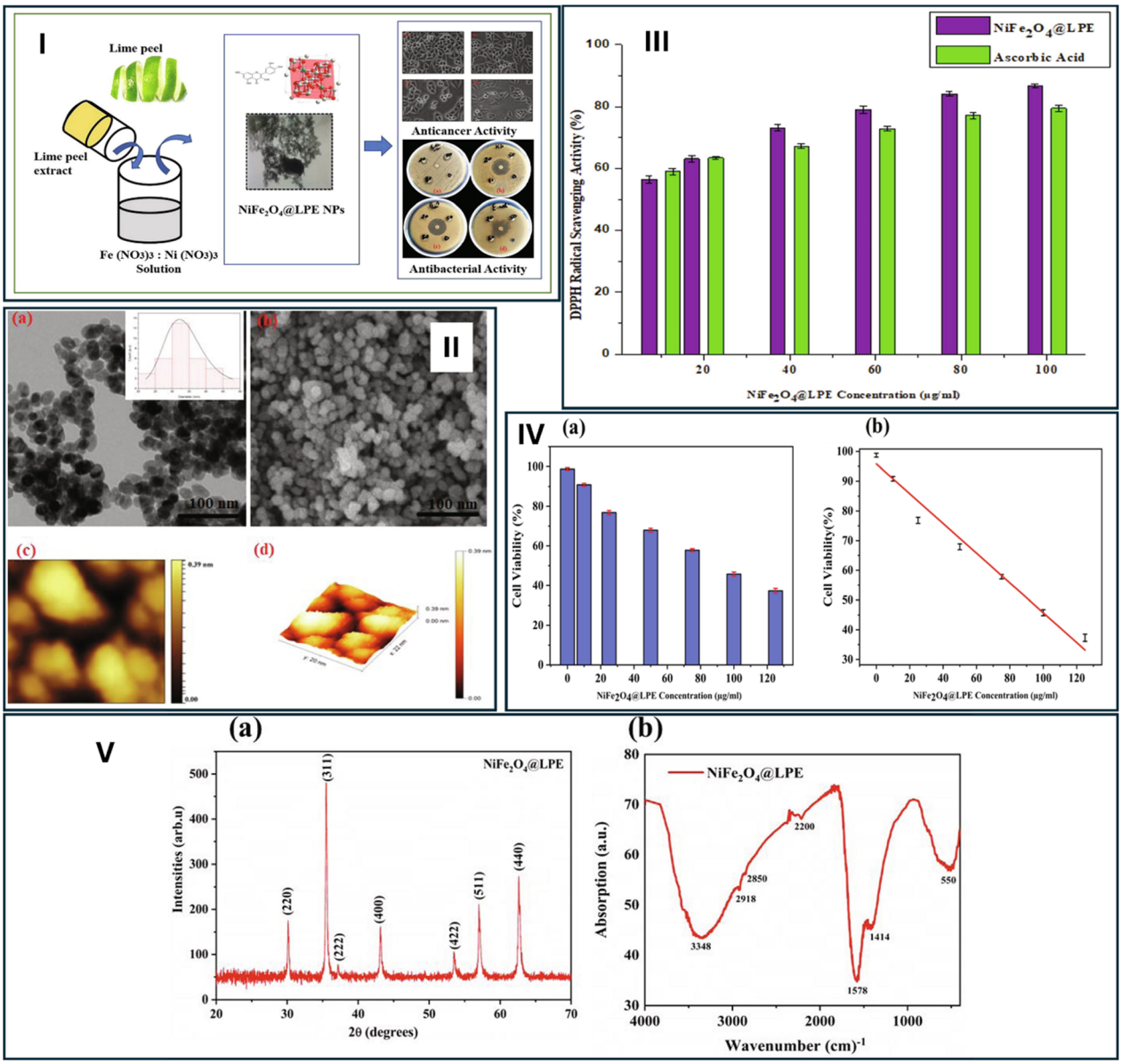

Fig. 14 (I) Schematic representation of the green synthesis of $NiFe_2O_4$@LPE NPs using lime peel extract and their potential applications in anticancer and antibacterial activities. (II) Morphological characterization of green synthesized $NiFe_2O_4$@LPE NPs. (a) Transmission electron microscopy (TEM) image revealing internal structural morphology. (b) Scanning electron microscopy (SEM) image showing surface morphology. (c) Two-dimensional atomic force microscopy (2D AFM) image revealing surface topography. (d) 3D view of $NiFe_2O_4$@LPE NPs. (III) Evaluation of antioxidant activity of green synthesized $NiFe_2O_4$ NPs mediated by lime peel extract using DPPH radical scavenging assay. Ascorbic acid was used as a positive control. (IV) *In vitro* cytotoxicity assessment of $NiFe_2O_4$@LPE NPs on HeLa cells. (a) Cell viability (%) of HeLa cells treated with $NiFe_2O_4$@LPE NPs after 24 h. (b) Linear calibration plot of $NiFe_2O_4$@LPE NPs concentration *versus* cell viability. (V) XRD (a) and FTIR (b) spectra of $NiFe_2O_4$@LPE NPs depicting their chemical constituents. Reproduced from ref. 105, copyright 2022 Elsevier.

composition modulates colitis severity in mice. Orange and citrus pectin diets were compared in two colitis models (TNBS and DSS). Male C57BL/6 mice were provided with pectin-free diet, diet enriched with high (5% orange pectin) or low (5% citrus pectin) side chain content for ten to fourteen days before being given 2,4,6-trinitrobenzene sulfonic acid/dextran sulfate sodium to induce colitis. Mice fed orange pectin exhibited less colon damage and reduced levels of IL-1β and IL-6, despite similar immune cell profiles. Orange pectin also slightly increased fecal propionic acid concentrations. The protective effect extended even to antibiotic-treated mice and macrophage cell models, where orange pectin significantly suppressed IL-6 production (Fig. 10 and 11). These findings suggest that pectin's structural features, particularly its neutral sugar side chains, play a dual role: enhancing prebiotic effects and directly modulating host inflammatory responses, even independently of microbiota.[97]

Recent advances have highlighted additional green valorization approaches for citrus pectin. Notably, IntegroPectin, a novel phyto complex pectin produced *via* hydrodynamic

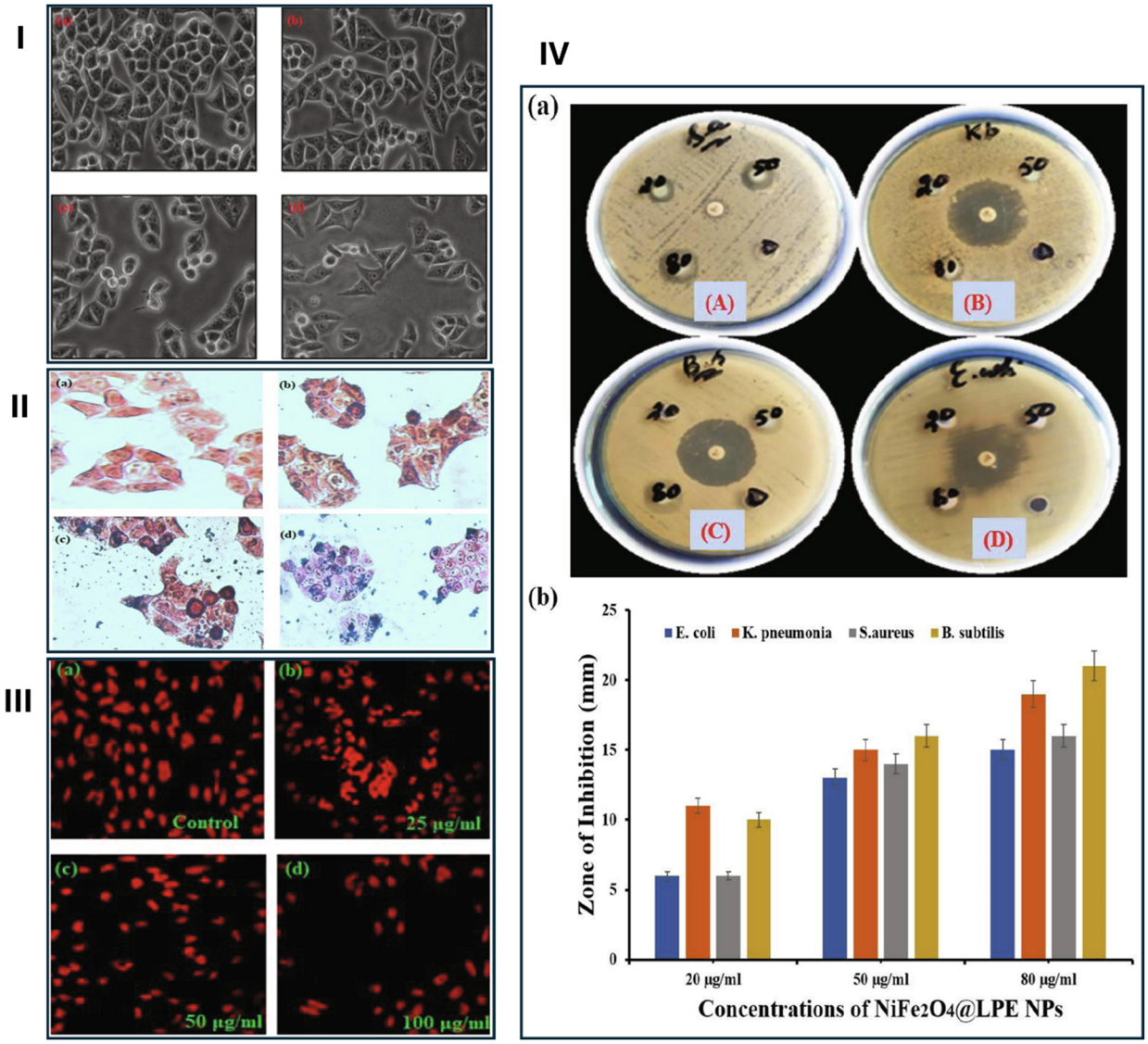

Fig. 15 (I) Morphological changes in HeLa cells induced by $NiFe_2O_4$@LPE NPs. Microscopic images of HeLa cells treated with various doses of $NiFe_2O_4$@LPE NPs: (a) control, (b) 25 μg mL^{-1}, (c) 50 μg mL^{-1}, (d) 100 μg mL^{-1}. (II) Prussian blue staining of HeLa cells to visualize intracellular iron uptake after treatment with $NiFe_2O_4$@LPE NPs. (a) Control, (b) 25 μg mL^{-1}, (c) 50 μg mL^{-1}, (d) 100 μg mL^{-1}. (III) Morphological variations displaying $NiFe_2O_4$@LPE NPs induced morphological changes (MMP) in HeLa cells in a dose-dependent manner: (a) control, (b) 25 μg mL^{-1}, (c) 50 μg mL^{-1}, (d) 100 μg mL^{-1}. (IV) Antibacterial activity of $NiFe_2O_4$@LPE NPs against different microbial strains employing different concentrations compared to controls. (a): (A) *S. aureus*, (B) *K. pneumoniae*, (C) *B. subtilis*, (D) *E. coli*. (b) Histogram representing the comparison of zones of inhibition for increasing concentrations of $NiFe_2O_4$@LPE NPs. Reproduced from ref. 105, copyright 2022 Elsevier.

cavitation, exhibits markedly enhanced antioxidant, antimicrobial, and neuroprotective properties at the molecular and cellular levels. Computational modeling further supports its broad-spectrum bioactivity, including anticancer and anti-inflammatory potential. Additionally, the use of pressurized CO_2 extraction has been demonstrated as an acid-free and sustainable method to obtain pectin from citrus peel waste, delivering oligosaccharides with distinctive structural attributes and bioactive profiles.[98–101]

These chemical families (Table 1, and Fig. 1) serve as the molecular basis for downstream valorization strategies and specifically support the green synthesis approaches discussed in the following section.

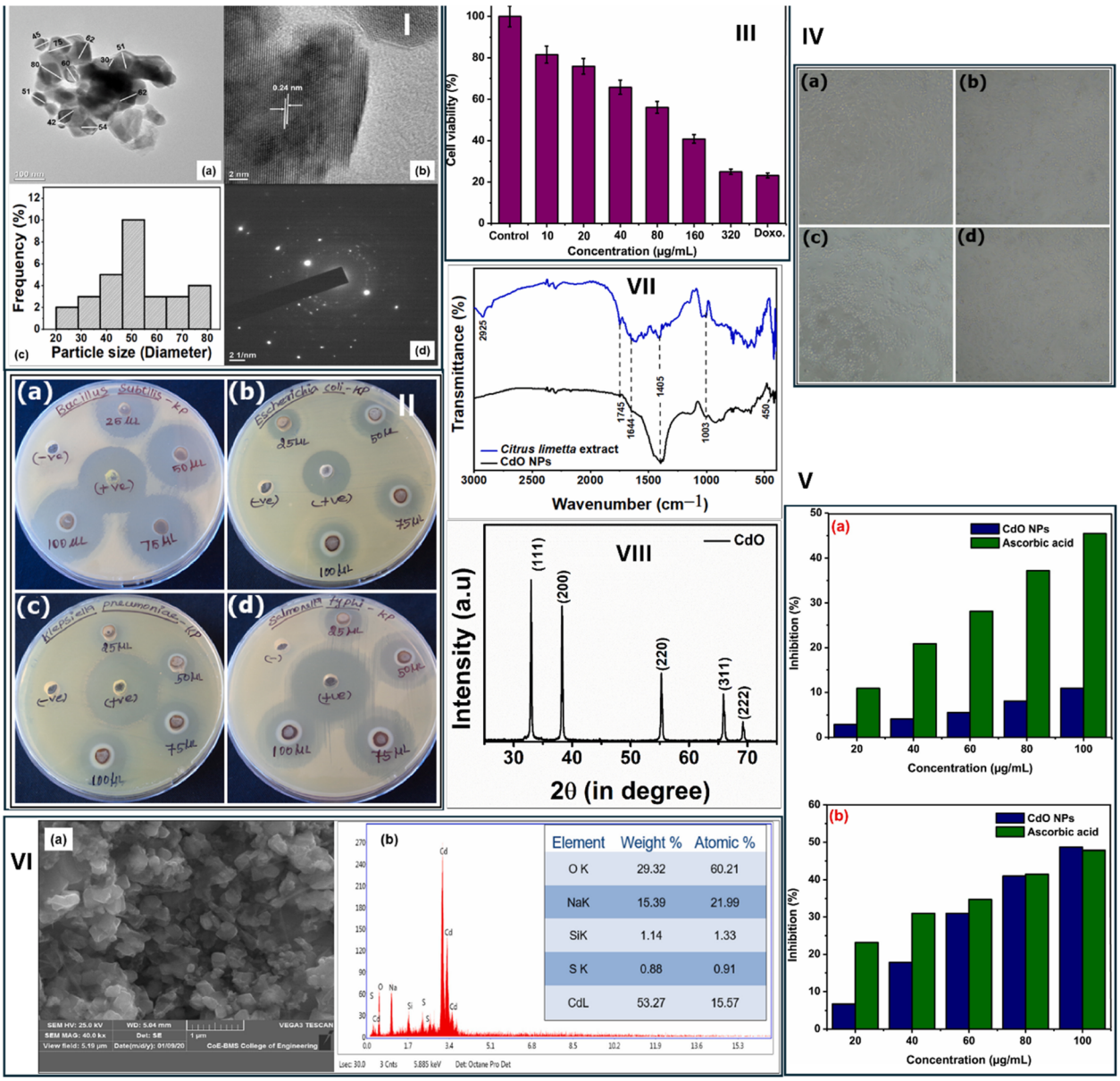

Fig. 16 Characterization and biological evaluation of CdO NPs. (I) Characterization of CdO NPs. (a) Transmission electron microscopy (TEM) image of CdO NPs. (b) High-resolution TEM (HRTEM) image of CdO NPs displaying the lattice fringes. (c) Particle size distribution graph (histogram). (d) Selected area electron diffraction (SAED) pattern of CdO NPs. (II) Antibacterial activity of CdO NPs against various bacterial strains. (a) *B. subtilis*, (b) *E. coli*, (c) *K. pneumoniae*, and (d) *Salmonella typhi*. (III) *In vitro* anticancer activity of CdO NPs against A549 human lung cancer cell line. (IV) Cytotoxicity of CdO NPs on A549 cells. Light microscopic photographs of *C. limetta* peel extract mediated-CdO NPs tested at (a) control, (b) 10 μg mL^{-1}, (c) 320 μg mL^{-1}, and (d) doxorubicin 3.12 μg mL^{-1}. (V) Antioxidant activity of CdO NPs. (a) DPPH assay. (b) ABTS assay. (VI) SEM micrograph (a) and elemental data analysis (EDX) (b) of CdO NPs. FTIR (VII) and XRD (VIII) profiles of CdO NPs green synthesized using *C. limetta* peel extract. Reproduced with permission from ref. 106, copyright 2023 Elsevier.

3. Conventional methods utilized for waste management

Conventional waste management technologies, such as landfilling, incineration, downcycling, and upcycling, are associated with significant environmental drawbacks and high energy demands. These methods often result in the generation of toxins, greenhouse gases, and leachates, which pose threats to both ecosystems and public health.[102]

Landfilling, a widely practiced method, contributes substantially to global anthropogenic greenhouse gas (GHG) emissions, primarily due to the anaerobic decomposition of organic matter, which releases large quantities of carbon dioxide (CO_2) and methane (CH_4). In addition to GHG emissions, landfilling is linked to groundwater and surface water contamination, stemming from volatile organic compounds and landfill leachate, especially in facilities lacking adequate liners. Other common nuisances include noise from landfill operations, bioaerosol emissions, and persistent foul odors. These factors collectively harm nearby ecosystems and negatively affect communities situated close to landfill sites. Njoku *et al.* (2019) investigated the environmental and social implications of landfill proximity, highlighting its adverse impact on public well-being.[102]

Incineration, another conventional method, also presents serious concerns. Depending on the waste composition, incinerators emit a complex mixture of pollutants, including nitrogen oxides, sulfur dioxide, acid gases, heavy metals, particulate matter, and persistent organic pollutants. These emissions are associated with respiratory diseases, cancer risks, hormonal disruptions, congenital abnormalities, and other health issues. From an ecological perspective, incineration contributes to smog formation, global warming, acidification, and toxicity to terrestrial and aquatic life.[103]

Downcycling and upcycling, while often considered more sustainable alternatives, are not without limitations. Downcycling involves converting waste into lower-quality materials, which may degrade more rapidly or pose environmental hazards over time. Upcycling, on the other hand, creates higher-value products from waste but often lacks scalability due to labor-intensive processing and the inconsistent quality

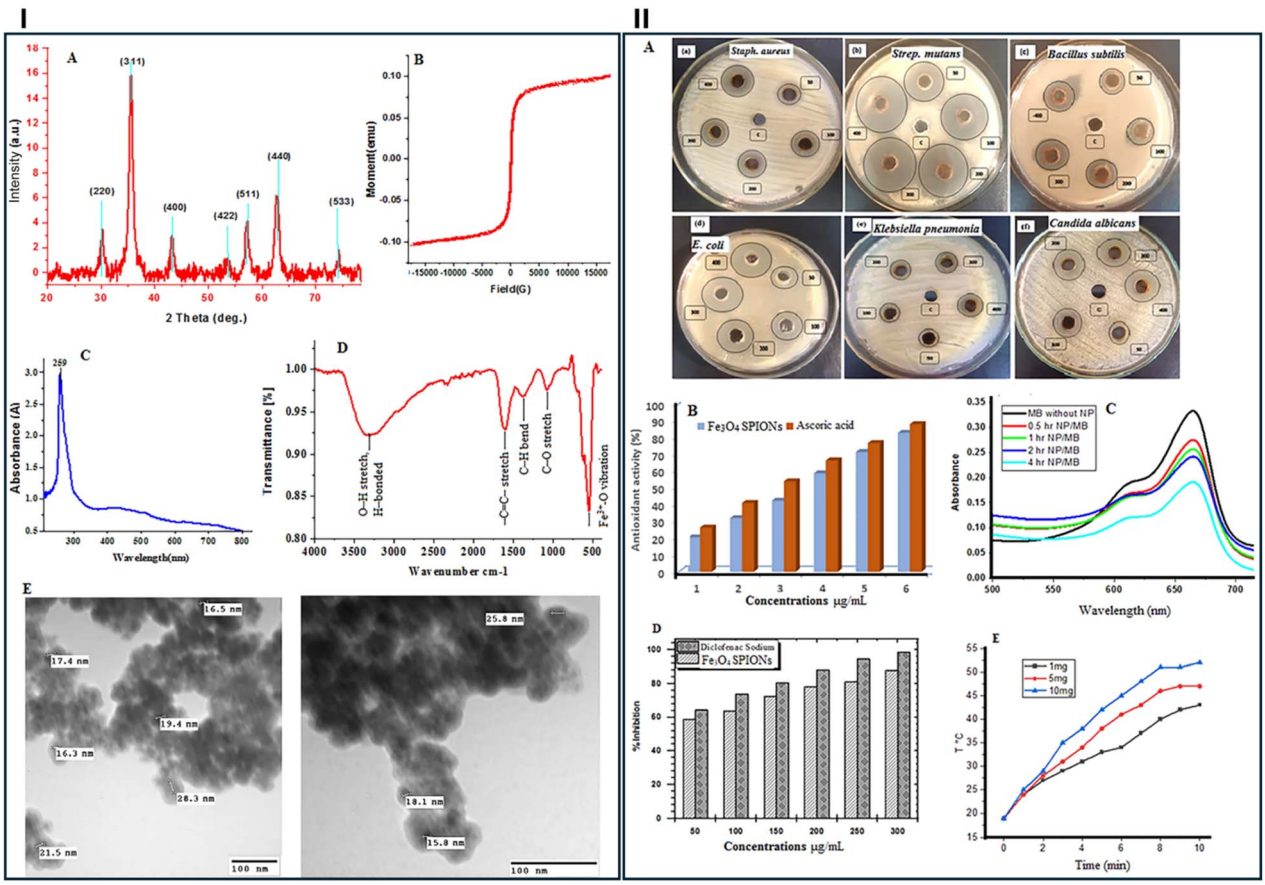

Fig. 17 Characterization and evaluation of the multifunctionality of the synthesized NPs. (I) (A) X-ray diffraction (XRD) pattern, (B) Vibrating Sample Magnetometry (VSM) curve, (C) UV-vis absorption spectrum, (D) Fourier Transform Infrared (FTIR) spectrum, and (E) Transmission Electron Microscopy (TEM) image of the synthesized NPs. (II) Antimicrobial activity (A) against *S. aureus* (a), *S. mutans* (b), *B. subtilis* (c), *E. coli* (d), *K. pneumonia* (e), and *C. albicans*; antioxidant activity (B); catalytic dye degradation (C); inhibition percentage of protein denaturation (D); and temperature-dependent behavior of the NPs (E). Reproduced from ref. 40, copyright 2023 Scientific Reports – Nature.

of input materials. Consequently, both processes can incur high operational costs and limited industrial applicability.

Fig. 12 depicts commonly utilized techniques for citrus peel waste management and their impact on the environment.

4. Green synthesis of nanomaterials from CPW

Building on the chemical classes summarized in Section 2, this section reviews green synthesis approaches that employ CPW extracts and polysaccharides as reducing, templating, and capping agents to fabricate carbon-based, metallic, metal-oxide, and polymeric nanomaterials. Conventional physical and chemical methods for nanoparticle synthesis are often energy-intensive, hazardous, and environmentally burdensome. In contrast, CPW-derived phytochemicals such as flavonoids, phenols, tannins, carotenoids, anthocyanins, vitamin C, and essential oils possess intrinsic antioxidant and reducing properties that make them attractive for sustainable biosynthesis of nanomaterials. These bioactive compounds enable simple, cost-effective, and environmentally benign fabrication of functional nanomaterials with potential applications in therapeutics, diagnostics, and environmental remediation.

For example, Pugazhenthiran *et al.* (2021) successfully green-synthesized monodispersed silver quantum dots (Ag QDs) under 5 nm using sweet lime (*C. limetta*) peel extract. Characterization using XRD confirmed a face-centered cubic structure, while TEM and SAED (selected area electron diffraction) affirmed their nanoscale morphology. The QDs exhibited strong SPR absorption (~415 nm) and photoluminescence quenching, indicating a low recombination rate and prolonged electron lifetime. Biochemical analyses (FTIR, LC-MS, and NMR) of the peel extract identified citrate and carbohydrate macromolecules as potential capping/reducing agents (Fig. 13). These Ag QDs showed significant cytotoxicity (71% reduction in MCF-7 breast cancer cell viability at 100 μg mL^{-1}) and antimicrobial efficacy with an MIC of 50 μg mL^{-1} against selected bacteria (Fig. 13), supporting their use as eco-friendly biocidal agents.[104]

Furthermore, Malik *et al.* (2022) green-synthesized nickel ferrites NPs ($NiFe_2O_4$) using lime peel extract (LPE). The face-

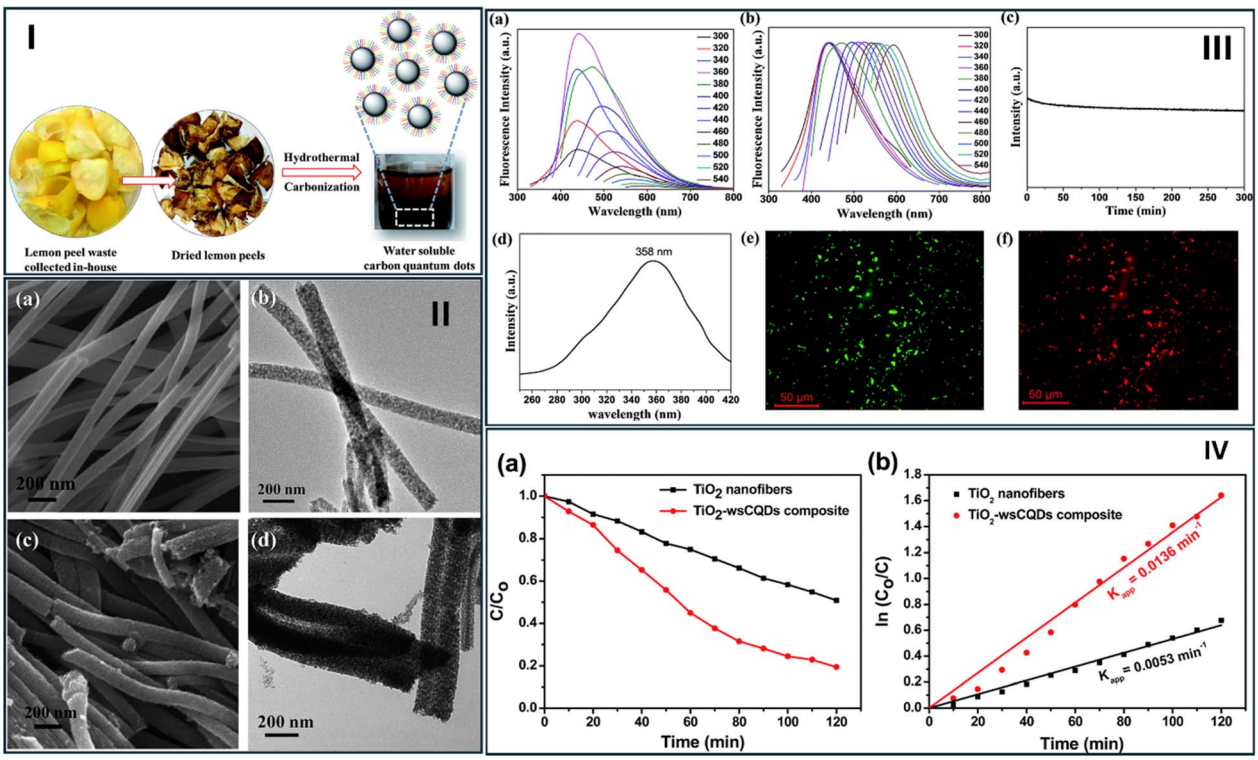

Fig. 18 Synthesis, characterization and photocatalytic activity of water-soluble carbon quantum dots (wsCQDs) derived from lemon peel waste and their composites with TiO_2 nanofibers. (I) Illustration of wsCQDs synthesis employing hydrothermal treatment of lemon peel as a waste precursor. (II) Morphological characterization of TiO_2 nanofibers and TiO_2–wsCQDs composites. (a) Field Emission Scanning Electron Microscopy (FESEM) and (b) Transmission Electron Microscopy (TEM) micrograph of TiO_2 nanofibers. (c) FESEM and (d) TEM micrograph of TiO_2–wsCQDs composites. (III) Photoluminescence properties of wsCQDs. (a) Fluorescence spectra of wsCQDs obtained at different excitation wavelengths progressively increasing from 300 to 540 nm in 20 nm increments. (b) Normalized fluorescence intensity. (c) Photostability test of wsCQDs on continuous 360 nm excitation for 5 h. (d) Excitation spectra at $\lambda_{em} = 441$ nm. (e) Digital fluorescence images of green-emitting wsCQDs ($\lambda_{ex} = 488$ nm, $\lambda_{em} = 535$ nm). (f) Digital fluorescence images of red-emitting wsCQDs ($\lambda_{ex} = 540$ nm, $\lambda_{em} = 605$ nm). (IV) Photocatalytic degradation of methylene blue (MB) dye. (a) Photocatalytic degradation of MB in the presence of TiO_2 nanofibers and TiO_2–wsCQDs composite under UV light irradiation. (b) Photocatalytic reaction kinetics of MB degradation in the presence of TiO_2 nanofibers and TiO_2–wsCQDs composite. Reproduced with permission from ref. 107, copyright 2016 RSC.

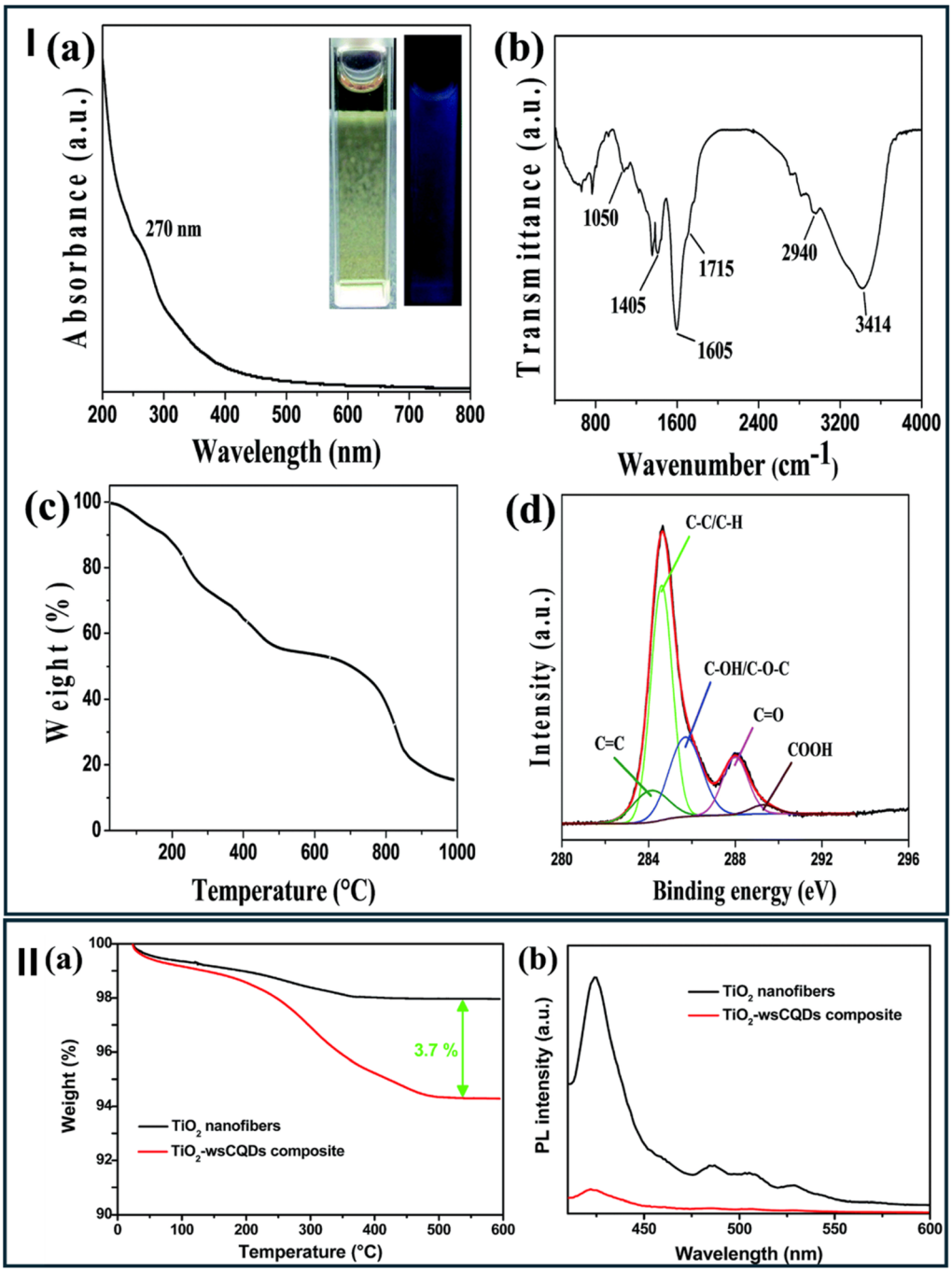

Fig. 19 (I) (a) UV-vis absorption spectrum of wsCQDs in aqueous medium; the inset displays photographic images of the solution under natural light (left) and UV illumination (right). FTIR analysis (b), TGA profile (c), and high-resolution XPS spectrum (d) of wsCQDs, focusing on the C1s region. (II) (a) TGA curves comparing TiO_2 solid nanofibers with the TiO_2–wsCQDs composite. (b) Photoluminescence (PL) spectra of TiO_2 nanofibers and the TiO_2–wsCQDs composite. Reproduced with permission from ref. 107, copyright 2016 RSC.

centered cubic crystal structure of the obtained NPs (31 nm) was confirmed by XRD and supermagnetic behavior by vibrating sample magnetometer (VSM), while FTIR analysis assessed the related functional groups (Fig. 14). TEM and SEM studies revealed that the average diameter of the NPs was 31–35 nm, while AFM evaluated the surface morphology in three dimensions (Fig. 14). Their cytotoxicity against HeLa cells revealed dose-dependent mitochondrial membrane potential alterations, linked to oxidative stress-mediated anticancer activity (Fig. 14 and 15). Additionally, these NPs exhibited broad-spectrum antibacterial activity (against *B. subtilis*, *E. coli*, *P. aeruginosa*, and *S. aureus*) and significant DPPH antioxidant activity, confirming their multifunctional therapeutic promise (Fig. 14 and 15).[105]

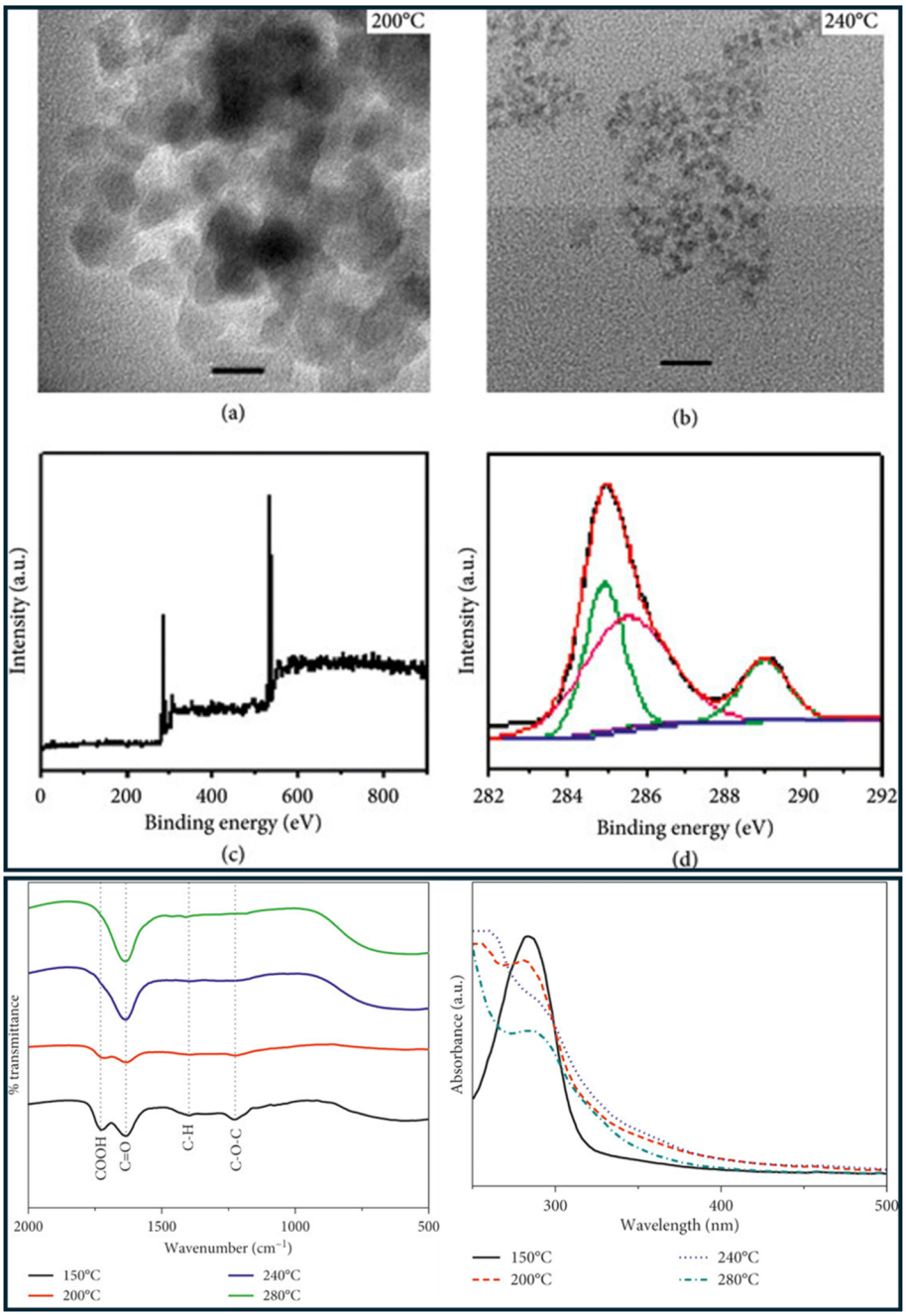

Fig. 20 Carbon dots (C-dots) morphological assessment and chemical characterization. (a and b) High-Resolution Transmission Electron Microscopy (HRTEM) images (scale bar: 20 nm), (c) X-ray Photoelectron Spectroscopy (XPS) spectrum, and (d) high-resolution XPS spectra of C1s of C-dots. The lower panel shows the FTIR spectrum and UV-vis spectra of C-dots synthesized from lemon juice. Reproduced with from ref. 109, copyright 2019 John Wiley & Sons.

In another study, Pagar *et al.* (2023) utilized *C. limetta* peel extract as a reducing and stabilizing agent for cadmium oxide (CdO) NPs green synthesis. The physicochemical properties of the produced CdO NPs were thoroughly investigated by XRD, FTIR, SEM, EDX, HR-TEM, photoluminescence (PL), and UV-DRS analysis (Fig. 16). The resulting NPs (average size 51.5 nm) showed a face-centered cubic structure and a bandgap of 2.6 eV (UV-DRS). FTIR analysis confirmed the functional groups of the active compounds found in *C. limetta* peel extract. Moreover, several biological tests of the green synthesized CdO NPs were investigated, including their antibacterial (*B. subtilis*, *E. coli*, *K. pneumoniae*, and *S. typhi*), antioxidant, anticancer (A549 cells), DNA damage, and biocompatibility activities. The obtained NPs demonstrated promising antibacterial activity (particularly against *B. subtilis*), anticancer efficacy against A549 lung cancer cells (IC50 = 152.2 μg mL^{-1}), and notable

antioxidant potential (DPPH IC50 = 94.47 μg mL; ABTS IC50 = 68.98 μg mL^{-1}). Furthermore, DNA damage and biocompatibility assessments suggested their safe therapeutic applicability (Fig. 16).[106]

Eldeeb *et al.* (2023) employed *C. sinensis* peel extract to synthesize superparamagnetic iron oxide NPs (SPIONs). UV-visible, TEM, FTIR, VSM, and XRD were all employed to characterize the manufactured SPIONs (Fig. 17). The UV-vis spectra investigation revealed a peak at 259 nm due to surface plasmon resonance. TEM examination revealed that green-produced SPIONs were spherical, with particle sizes ranging from 20 to 24 nm. The FTIR spectrum exhibited prominent bands at 3306 cm^{-1} and 1616 cm^{-1}, indicating the role of the extract in NPs formation and capping. Magnetization measurements show that the produced SPIONs have superparamagnetic properties at normal temperatures. Furthermore, SPIONs' antibacterial activity, antioxidant potential, anti-inflammatory effect, and catalytic degradation were investigated. The results showed that SPIONs have varying antibacterial properties against several pathogenic multidrug-resistant bacteria. SPIONs inhibited all target isolates at the maximum concentration (400 μg mL^{-1}), with zones ranging from 14.7–37.3 mm. The MICs of

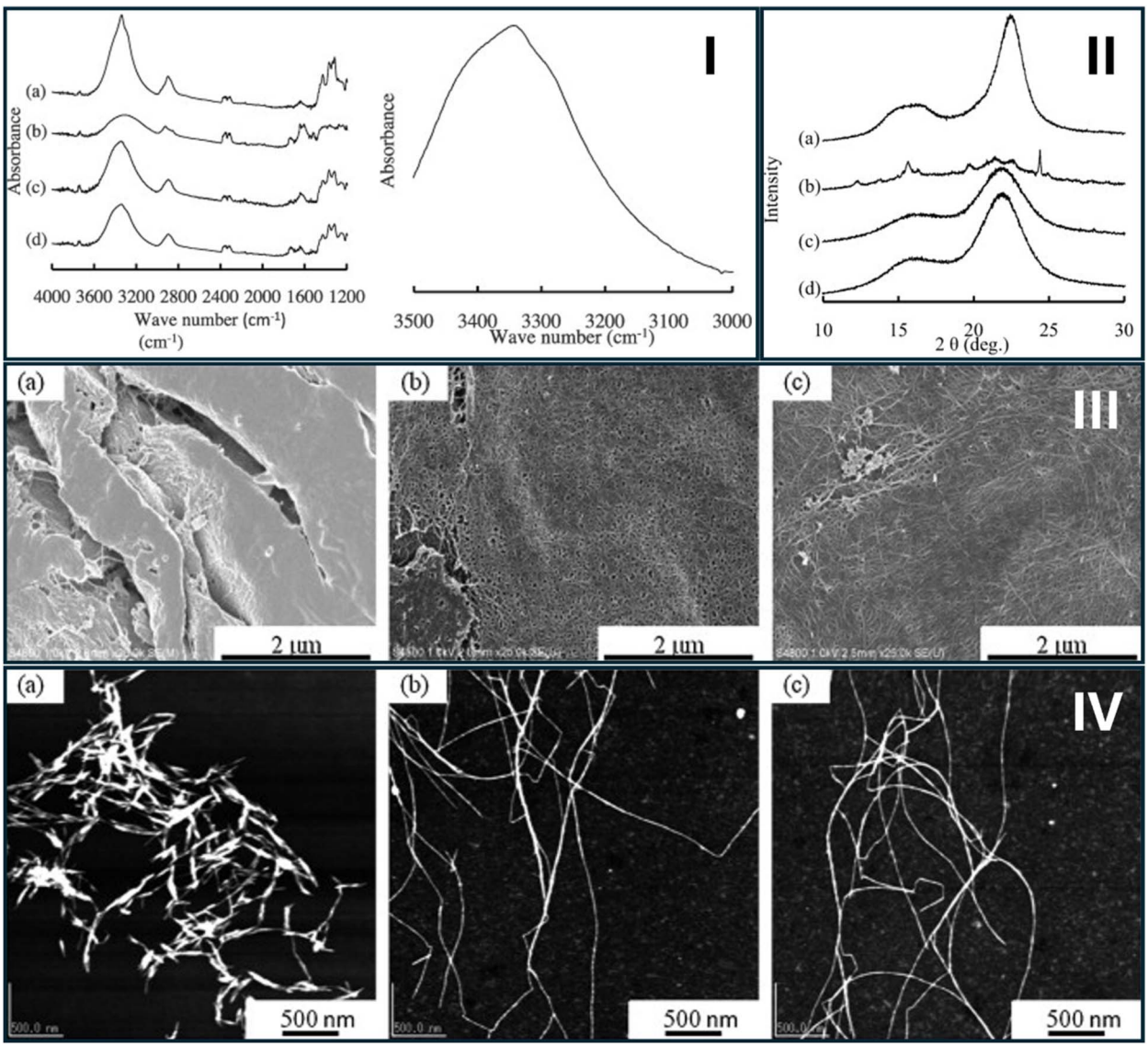

Fig. 21 (I) Left panel shows the FTIR analysis of wood cellulose (a), untreated mandarin peel waste (b), multistep treated mandarin peel waste (c), hydrothermally treated mandarin peel waste (d) (4000–1200 cm^{-1}). The right panel reveals the FTIR analysis of the hydrothermally treated mandarin peel waste (3000–3500 cm^{-1}). (II) XRD patterns of the same components: wood cellulose (a), untreated mandarin peel waste (b), multistep treated mandarin peel waste (c), hydrothermally treated mandarin peel waste (d). (III) SEM micrographs of untreated mandarin peel waste (a), multistep treated mandarin peel waste (b), hydrothermally treated mandarin peel waste (c). (IV) AFM analysis of disk-milled wood cellulose (a), sonicated multistep treated mandarin peel waste (b), and hydrothermally treated mandarin peel waste (c).[110] Reproduced with permission from ref. 110, copyright 2014 Elsevier.

Fig. 22 Green synthesis methods of citrus peel NPs. Figure created in Biorender.

the produced SPIONs against *S. aureus*, *Streptococcus mutans*, *B. subtilis*, *E. coli*, *K. pneumonia*, and *Candida albicans* were 3, 6.5, 6.5, 12.5, 50, and 25 μg mL^{-1}. SPIONs showed significant antioxidant, anti-inflammatory, and dye degradation properties (Fig. 17). Remarkably, SPIONs showed excellent magnetic hyperthermia efficiency in an alternating magnetic field (AMF), with specific absorption rates (SAR) of 164, 230, and 286 W g^{-1} at doses of 1, 5, and 10 mg mL^{-1}, respectively, supporting their candidacy for biomedical applications including targeted drug delivery and cancer hyperthermia therapy.[40]

In the carbon-based nanomaterials domain, Tyagi *et al.* (2016) reported a simple hydrothermal synthesis of water-soluble carbon quantum dots (wsCQDs) from lemon peel. The spherical CQDs (1–3 nm) exhibited a 14% quantum yield and high photostability. wsCQDs were further employed to serve as a cost-effective, environmentally friendly, and highly sensitive fluorescent probe for Cr6+ ions detection, with a detection limit of around 73 nM. This fluorescent probe based on wsCQDs had the potential to provide a simple, quick, and convenient method for sensitive and selective Cr6+ detection in water purification operations. Furthermore, wsCQDs were immobilized on electrospun TiO_2 nanofibers, and the photocatalytic activity of the TiO_2-wsCQDs composite was tested using methylene blue dye as a model pollutant. The photocatalytic activity of the TiO_2-wsCQDs composite was approximately 2.5-fold higher than TiO_2 alone (Fig. 18 and 19). This study suggests wsCQDs as scalable, low-cost nanomaterials for environmental sensing and remediation.[107]

Baig *et al.* (2023) also used the pyrolysis method to synthesize nano graphite materials (NGMs) from lemon and orange peel powders. The structural and compositional properties of the NGMs were confirmed using XRD and FTIR. The XRD examination validated the crystalline nature of the NGMs, whilst the FTIR analysis revealed the functional groups contained in the materials. The findings indicated that NGMs derived from lemon and orange peel powders have potential applications in energy storage and heterogeneous catalysis, underlining the high carbon yield potential of citrus peels.[108]

Hoan *et al.* (2019) developed highly luminescent carbon dots (C-dots) from lemon juice using a one-pot hydrothermal technique. The luminosity of C-dots was controlled by varying temperatures, time, precursor aging, and diluted solvents. HR-TEM, XRD, FTIR, DLS, UV-vis spectrophotometry, and photoluminescent spectrophotometry were all used to describe the C-dots (Fig. 20). The C-dots emitted intense green light with quantum yields ranging from 14.86 to 24.89% as hydrothermal

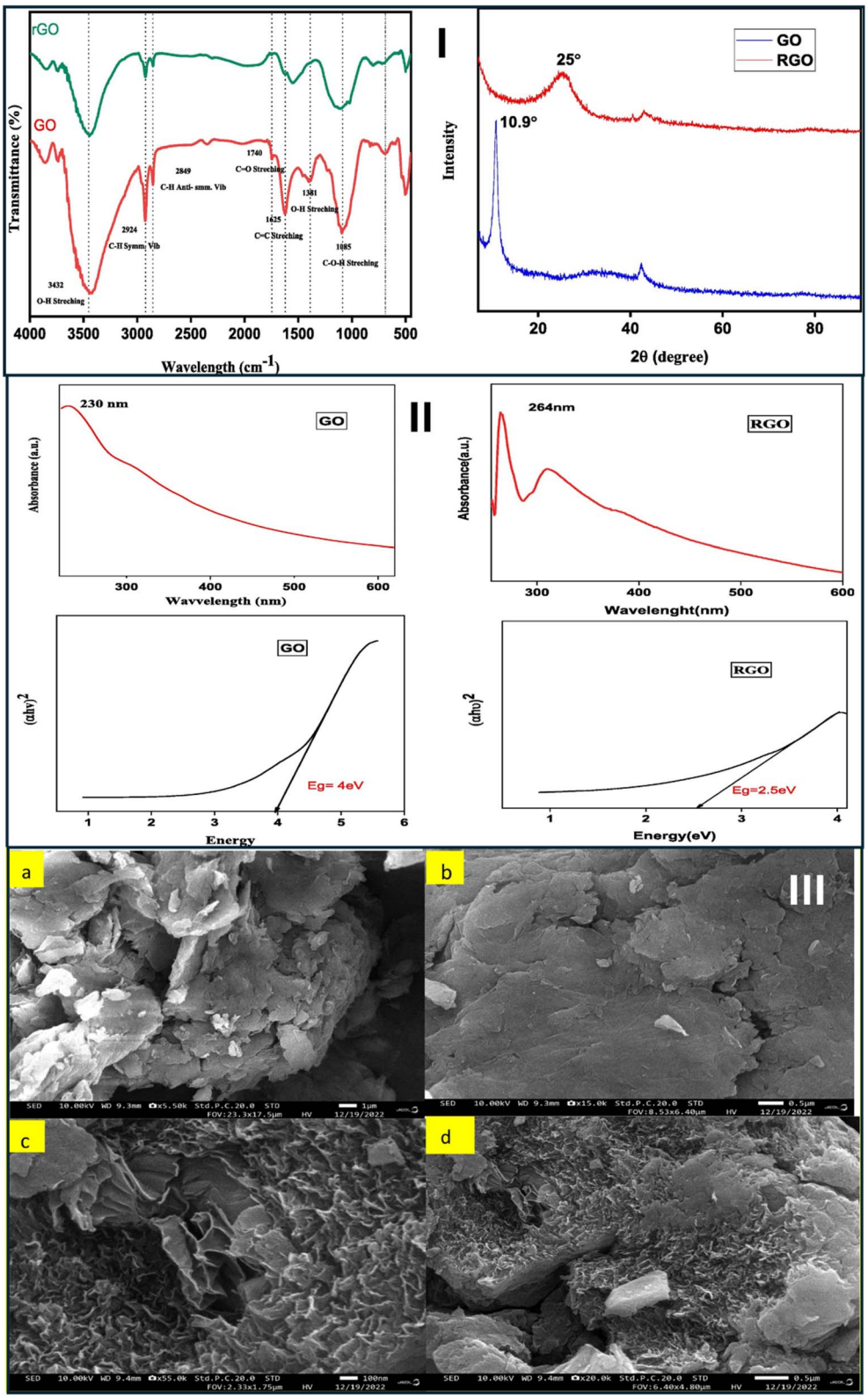

Fig. 23 (I) FTIR analysis (left panel) and XRD patterns (right panel) of graphene oxide (GO) and reduced graphene oxide (rGO) green synthesized using citrus lemon. (II) UV-vis spectrophotometers (upper panel) and Tauc's plots (lower panel) of GO and rGO for the purpose of determining the optical band gap. (III) SEM micrographs of GO (a and b) and green synthesized rGO (c and d).[113] Reproduced with permission from ref. 113, copyright 2023 Elsevier.

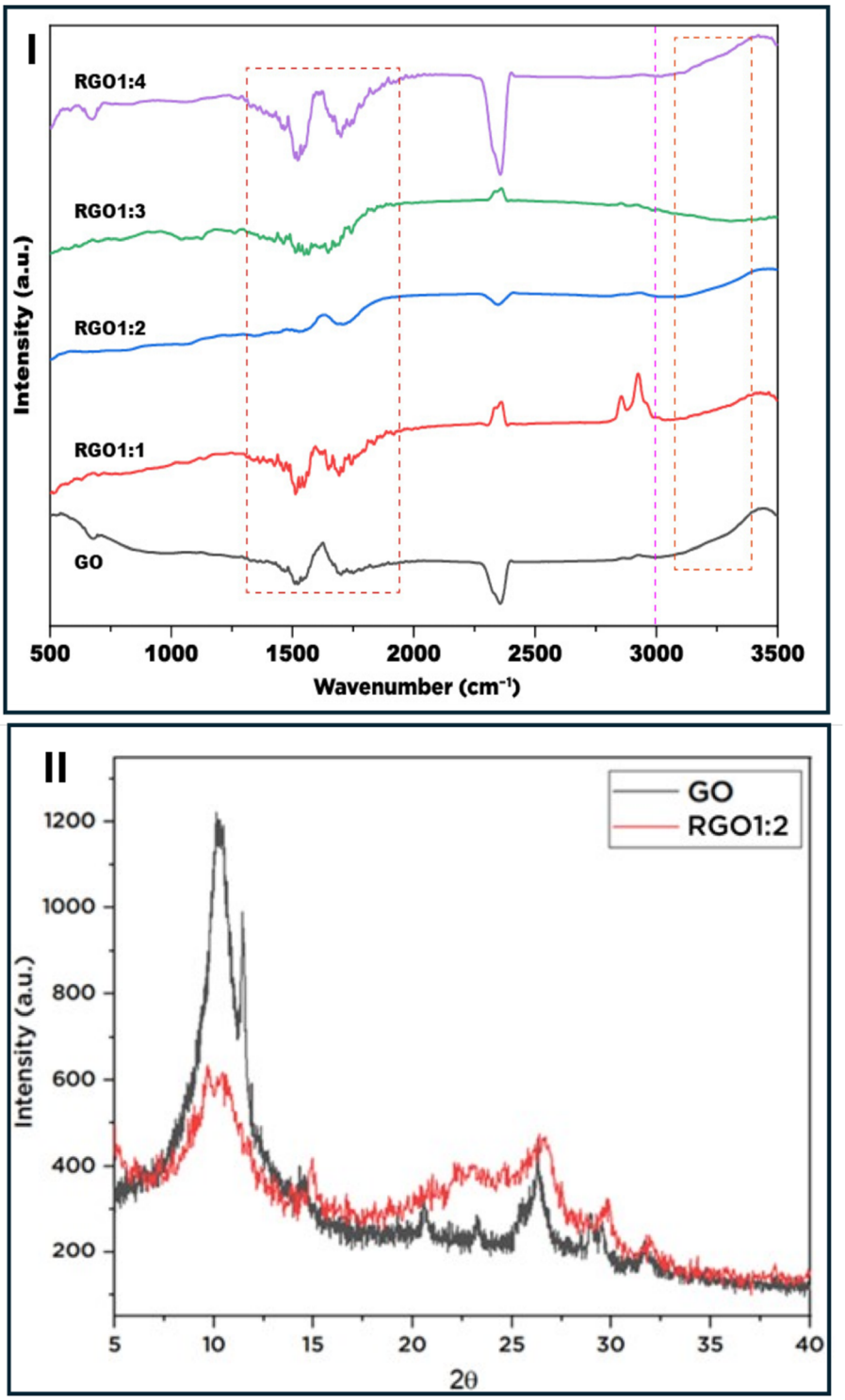

Fig. 24 FTIR (I) and XRD (II) spectra of GO and green synthesized rGO, revealing their chemical and crystalline structures. Reproduced from ref. 114, copyright 2022 MDPI.

temperatures increased (Fig. 20). Furthermore, light emission was found to be dependent on hydrothermal time, precursor age, and diluted solvent. With their green light emission and excellent physicochemical properties, they have potential for use in bioimaging and optoelectronics.[109]

Hiasa *et al.* (2014) isolated cellulose nanofibrils (CNFs) from *C. unshiu* peels *via* multistep and hydrothermal pectin removal. The process involved removing metal from pectin, and depolymerizing and dissolving it. Following that, hydrothermal treatment was applied using a solution of 0.18 wt% hydrochloric

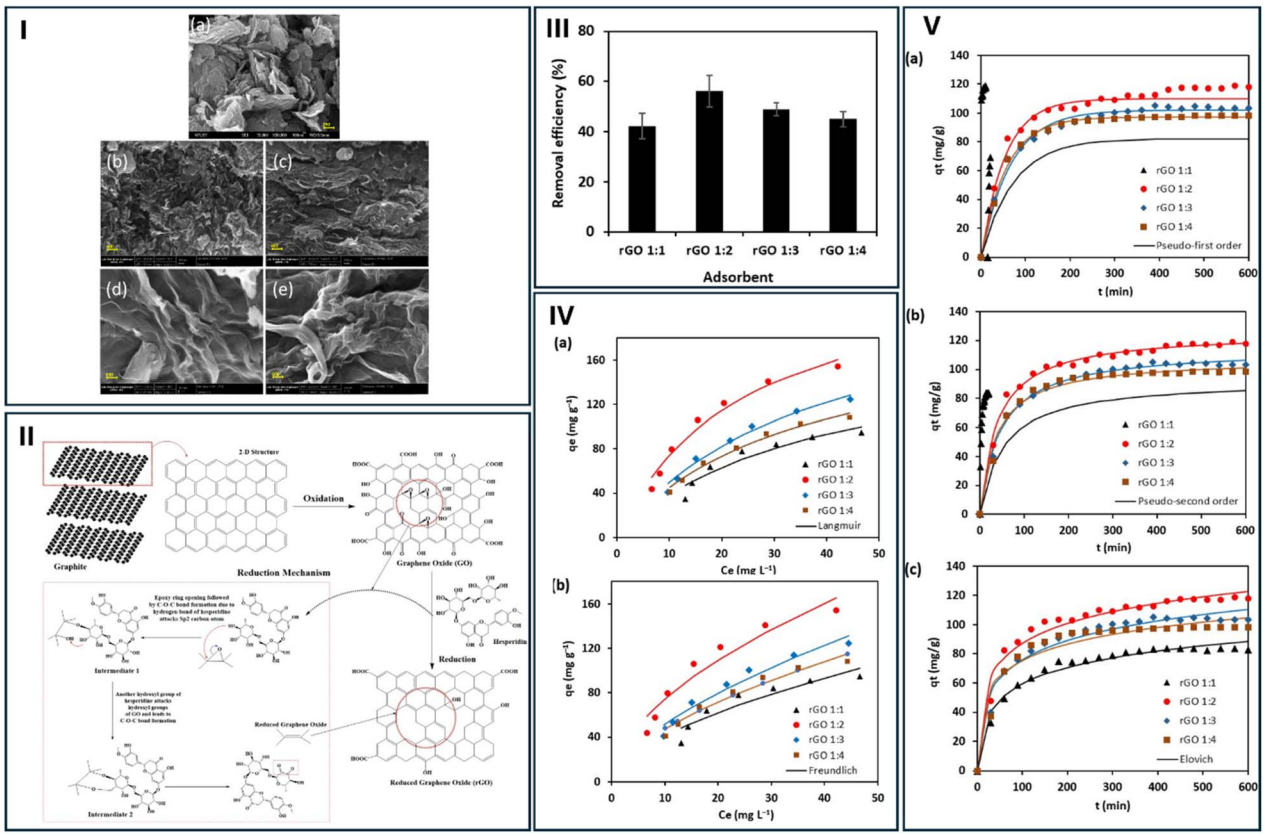

Fig. 25 (I) Morphological characterization of reduced graphene oxide (rGO) obtained from different graphene oxide (GO)–extract ratios. (a) GO, (b) 1 : 1 GO : extract, (c) 1 : 2 GO : extract, (d) 1 : 3 GO : extract, (e) 1 : 4 GO : extract. (II) Proposed mechanism for the reduction of graphene oxide (GO) by polyphenols present in kaffir lime peel extract. Hesperidin was used as a representative polyphenol. (III) Methylene blue removal efficiency using rGO. Initial methylene blue concentration (C_o) = 50 mg L^{-1}. Adsorbent dosage of 5 mg was utilized for 400 min. (IV) Methylene blue adsorption isotherms onto rGO (Langmuir (a) and Freundlich (b) models). (V) Methylene blue adsorption kinetics onto rGO. Pseudo-first-order (a), pseudo-second order (b), and Elovich kinetic (c) models. Reproduced from ref. 114, copyright 2022 MDPI.

acid. FTIR spectroscopy and neutral sugar content analysis of the purified cellulose, from mandarin peel waste, revealed that the hydrothermal treatment was more effective in purifying cellulose than the multistep treatment. XRD showed that the purified cellulose had a smaller crystal width (2.5 nm) than wood cellulose (3.9 nm) (Fig. 21). Following pectin removal, the purified cellulose from mandarin peel waste was sonicated to produce cellulose nanofibrils, resulting in cellulose fibers with diameters of 2–3 nm, as measured by atomic force microscopy (Fig. 21). The detected fiber width matched the crystal width, showing that the cellulose nanofibrils were totally individualized by sonication (Fig. 21). These cellulose nanofibrils are ideal for bio-based packaging and medical materials.[110]

Similarly, Hideno *et al.* (2019) used pectinase to produce cellulose nanofibers from Japanese citrus peels (*C. iyo* and *C. unshiu*), and the resulting nanofibers were studied in terms of shape and other features. First, pectinase treatment and diluted alkali treatment were applied as pretreatments for the mechanical nanofibrillation of Japanese orange peels. Second, surface morphology was used to characterize and compare the nanofibrillated peels. When cellulose from Japanese citrus inner peels was treated with pectinase, it was easier to fibrillate than cellulose from other materials, such as woody pulp. Nanofibers obtained from citrus inner peels were easier to mix with the oil and kept the oil drops smaller than cellulose nanofibers derived from hardwood pulp. These findings showed cellulose nanofibers with superior emulsification properties, maintaining small oil droplets, making them suitable as stabilizers in food and cosmetic formulations.[111]

The following figure (Fig. 22) illustrates the green synthesis of various NPs employing the waste of Citrus peels extracts.

4.1. Carbon-based nanomaterials

CPW represents a rich, sustainable source of carbon that can be transformed into diverse carbon-based nanomaterials. The abundant bio-organic content, eco-friendliness, biodegradability, and porous structure of CPW make it an attractive precursor for green nanomaterial synthesis. Current strategies

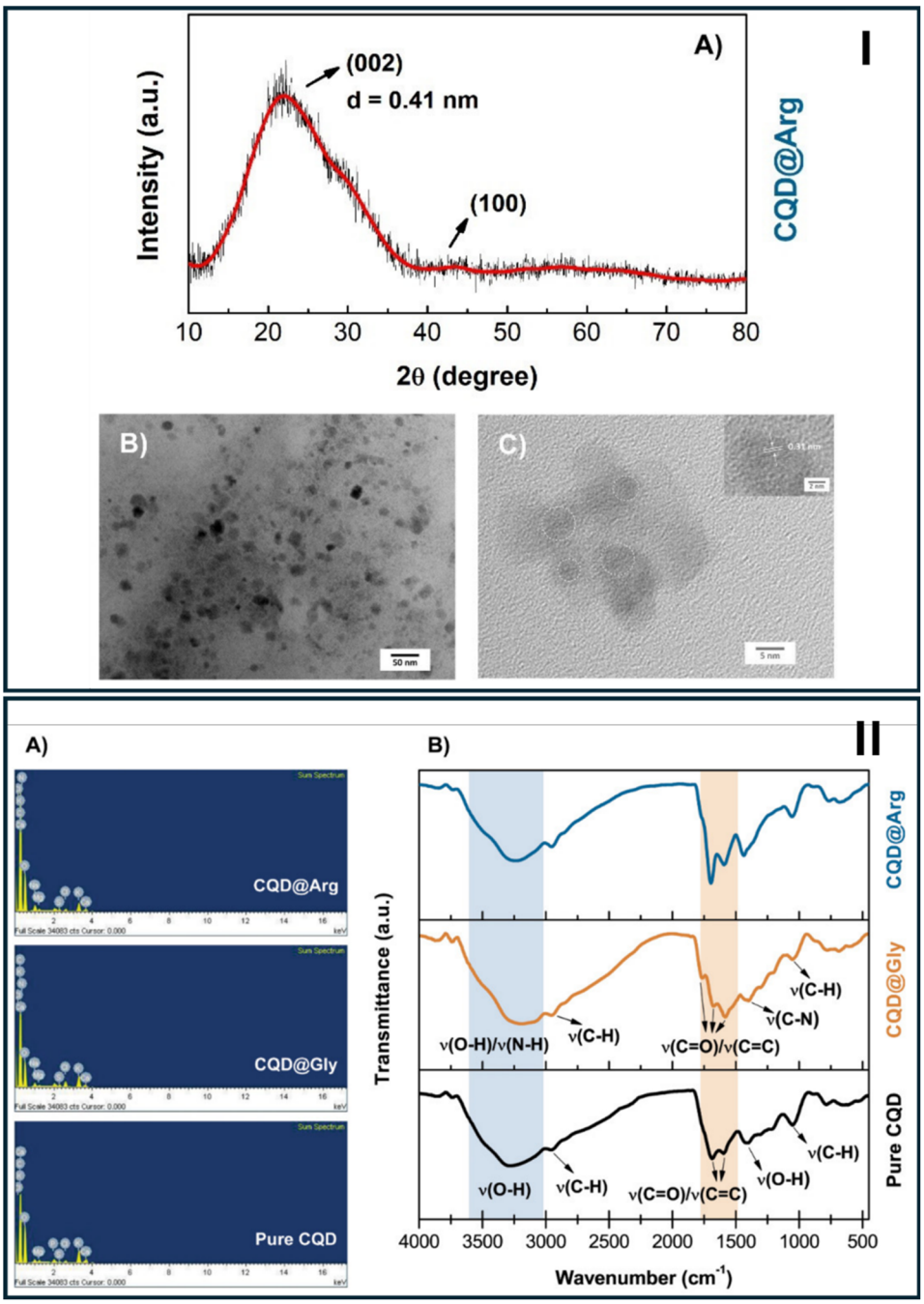

Fig. 26 (I) (A) XRD and (B & C) TEM analyses of CQD@Arg NPs exhibiting lattice spacing of $d = 0.31$ nm. (II) (A) EDS and (B) FTIR spectra of CQDs and N-CQDs. Reproduced from ref. 115, copyright 2021 MDPI.

for converting CPW into carbon-based nanomaterials often involve thermal, hydrothermal, and microwave-assisted techniques to disintegrate complex macromolecules. These approaches not only reduce waste but also provide an economical and sustainable alternative to conventional carbon sources for nanomaterial fabrication.[112]

For example, Rani *et al.* (2023) reported a cost-effective and eco-friendly approach for the reduction of graphene oxide (GO) using *C. limon* (lemon) peel extract. Initially, exfoliated GO sheets were synthesized *via* the Tour method, followed by green reduction using phytochemicals present in the extract as reducing agents. The transformation of GO to reduced GO (rGO) was confirmed through FTIR, XRD, and UV-vis analyses, while SEM revealed changes in surface morphology (Fig. 23). A notable narrowing of the band gap upon reduction was observed, indicating improved electronic properties. This study

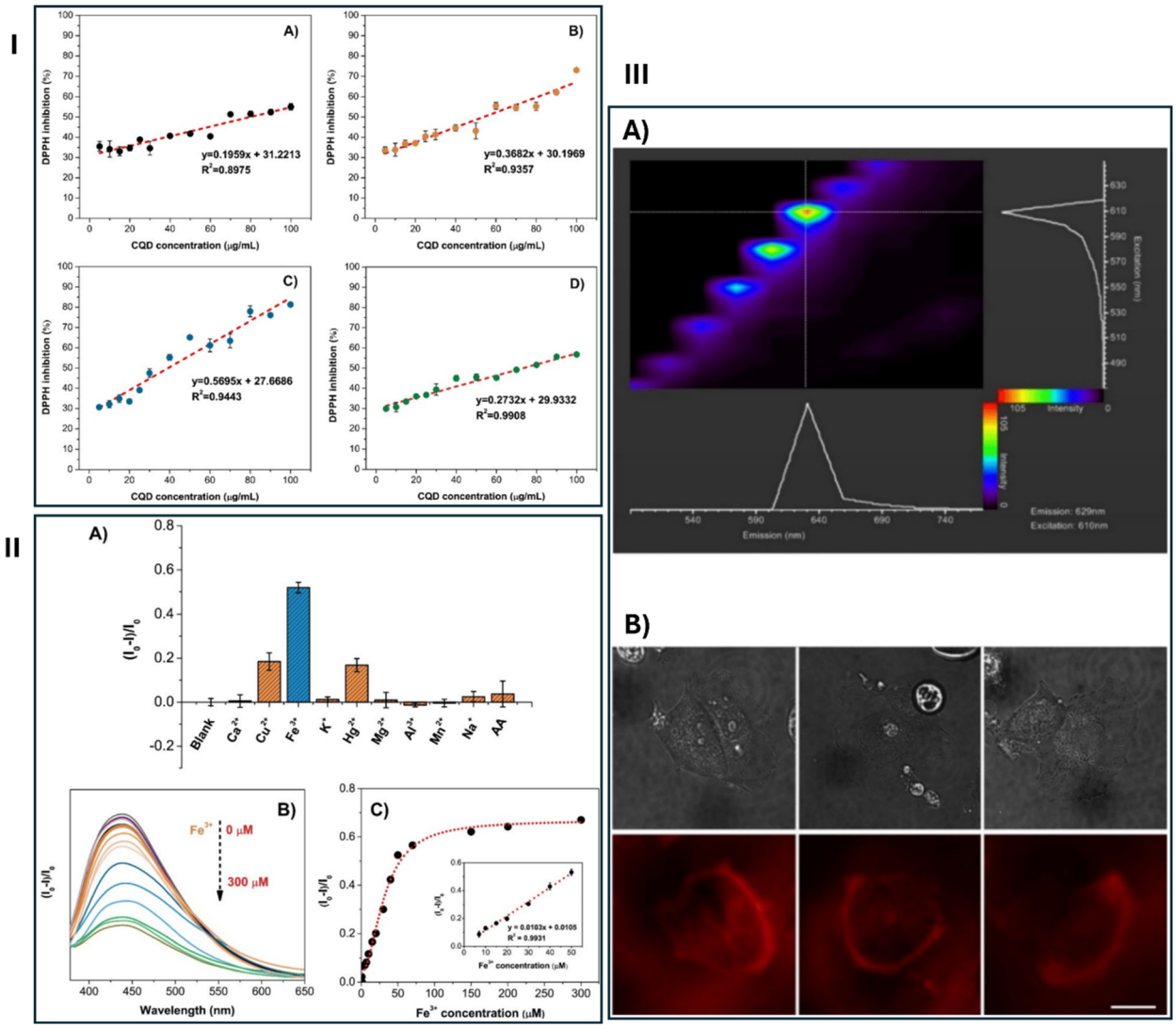

Fig. 27 Characterization and biological applications of CQD@Arg. (I) Evaluation of the antioxidant activity of prepared carbon quantum dots (CQDs) using the DPPH free radical scavenging assay. Antioxidant activity was assessed for (A) pure CQD, (B) CQD@Gly (CQDs coated with glycine), (C) CQD@Arg (CQDs coated with arginine), and (D) *C. clementina* extract. (II) Investigation of the fluorescence properties of CQD@Arg. (A) Fluorescence response of CQD@Arg to different metal ions and ascorbic acid. (B) Fluorescence spectral quenching upon the addition of different Fe^{3+} concentrations (0.5–300 μmol dm^{-3}). (C) Relative fluorescence response $(I_0 - I)/I_0$ of CQD@Arg with the Fe^{3+} addition confirming exponential behavior. (III) Characterization and cellular imaging of CQD@Arg. (A) Microspectrofluorimetry of CQD@Arg in the visible light range. The double-lambda plot of CQD@Arg adhered to the glass surface was obtained using excitation between 470–650 nm and detecting emission of fluorescence between 490–770 nm. The maximum emission was detected using excitation at 610 nm, and those conditions were used for cell imaging. (B) Confocal microscopy images of living MCF-7 cells labeled with CQD@Arg. Images are shown in transmission (upper row) and fluorescence (lower row) channels ($\lambda_{exc} = 610$ nm; $\lambda_{em} = 620–690$ nm). Average fluorescence intensity projections of 3D stacks covering the cell thickness are shown in the fluorescence channel. Scale bar: 20 μm. Reproduced from ref. 115, copyright 2021 MDPI.

supports the utility of citrus-derived phytochemicals as natural reducing agents under hydrothermal conditions for high-quality rGO production.[113]

In another study, Priliana *et al.* (2022) utilized *C. hystrix* (kaffir lime) peel extract to reduce GO into rGO at room temperature through a dispersion method. The GO was produced through the Hummers process, while different GO-to-extract ratios were explored (1 : 1, 1 : 2, 1 : 3, and 1 : 4). The production of rGO was validated by SEM, FTIR, XPS, XRD, and N2 sorption characterization (Fig. 24 and 25). Consequently, the 1 : 2 GO-to-extract ratio yielded rGO with the highest adsorption capacity for methylene blue dye. This was attributed to the greater restoration of C=C bonds and fewer oxygen-containing groups, as validated by XPS and FTIR analyses. Adsorption studies indicated that the Langmuir isotherm model and pseudo-second-order kinetics best described the dye removal

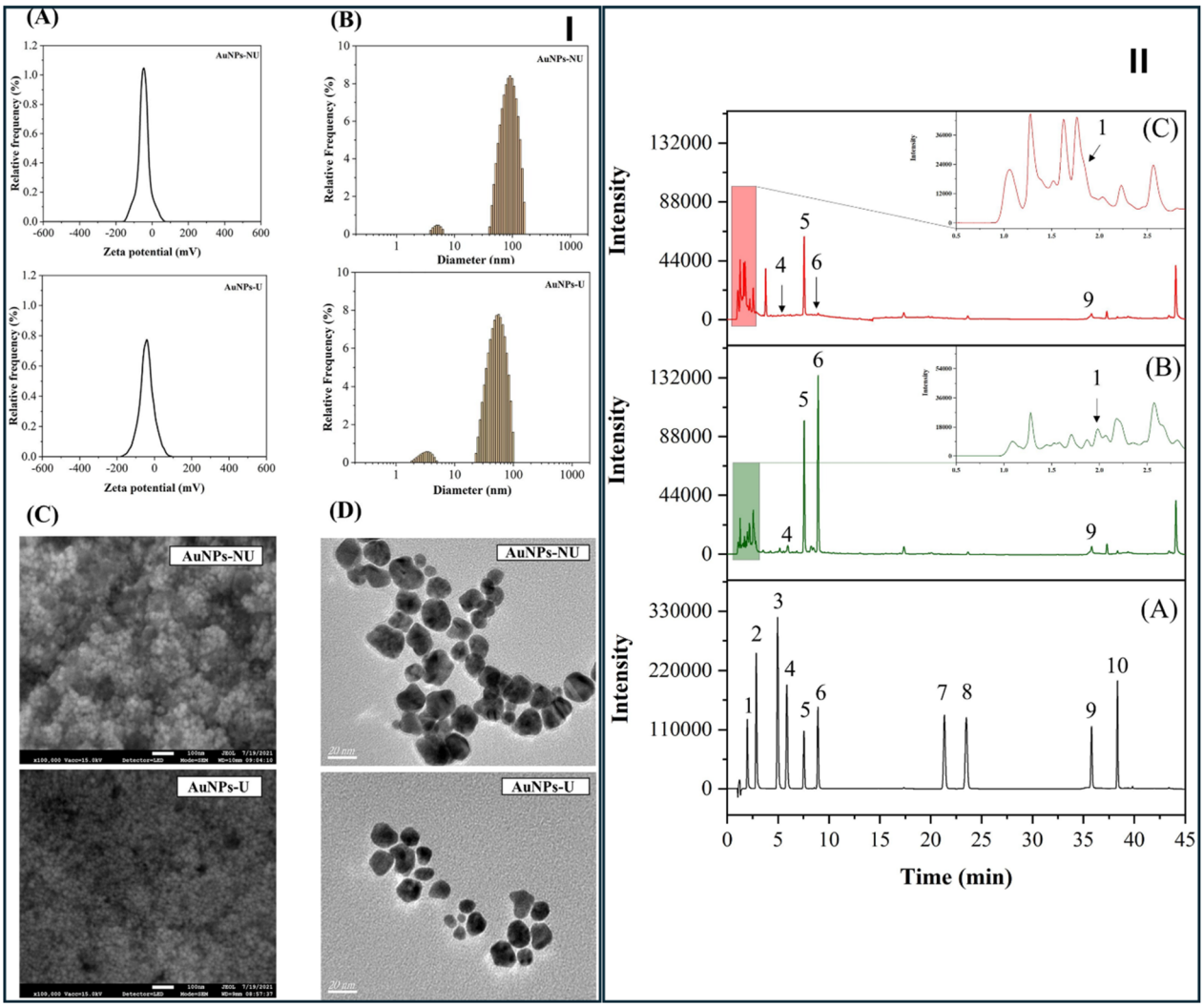

Fig. 28 (I) Characterization of AuNPs green synthesized using citrus peel extract, including zeta potential (A), particle size distribution (B), SEM (C), and (D) FT-TEM. (II) HPLC chromatograph of (A) phytochemical standards, (B) citrus peel extract (CPE) before synthesis, and (C) CPE after synthesis at 280 nm; compounds followed by their peaks numbers shown: chlorogenic acid (1), caffeic acid (2), P-coumaric acid (3), ferulic acid (4), narirutin (5), hesperidin (6), naringenin (7), hesperetin (8), nobiletin (9), tangeretin (10). Reproduced with permission from ref. 117, copyright 2022 Elsevier.

process, with an equilibrium capacity of 118 mg g^{-1}. The results highlight the potential of citrus-extract-reduced GO as an efficient adsorbent for wastewater treatment.[114]

Furthermore, Šafranko *et al.* (2021) synthesized nitrogen-doped carbon quantum dots (N-CQDs) from *C. clementina* peels using glycine (Gly) and arginine (Arg) as N-dopants *via* a hydrothermal process (Fig. 26). The quantum yield of the CQDs increased with nitrogen content. CQDs demonstrated high aqueous stability, biocompatibility, and fluorescence properties. CQD@Gly exhibited inhibitory effects on CFPAC-1 pancreatic cancer cells, while CQD@Arg showed strong antioxidant activity (81.39 ± 0.39% DPPH inhibition) and high sensitivity for Fe^{3+} ion detection (LOD = 4.57 ± 0.27 μmol dm^{-3}) (Fig. 27). These multifunctional CQDs also enabled effective cell imaging, reinforcing their biomedical and sensing potential.[115]

More recently, Aouadi *et al.* (2024) synthesized CQDs from aqueous extracts of lemon and orange peels. The CQDs appeared as small, spherical, closely packed particles with an average size of 2.18 and 2.66 nm. The antioxidant activity tests demonstrated a significant scavenging capacity in CQDs. The IC50 values for lemon-derived CQDs were 2.378 mg mL^{-1} (DPPH) and 2.815 mg mL^{-1} (ABTS), whereas orange-derived CQDs showed values of 3.059 mg mL^{-1} (DPPH) and 3.038 mg mL^{-1} (ABTS). In the total antioxidant capacity test, lemon-derived CQDs exhibited lower antioxidant activity (293.44 mg mL^{-1}) than orange-derived CQDs (277.62 mg mL^{-1}). Additionally, FRAP test revealed lemon-derived CQDs with higher antioxidant activity (382.45 μg mL^{-1}) than orange-derived CQDs (364.542 μg mL^{-1}). Despite similar total antioxidant capacity, differences in radical scavenging efficiency suggested that the

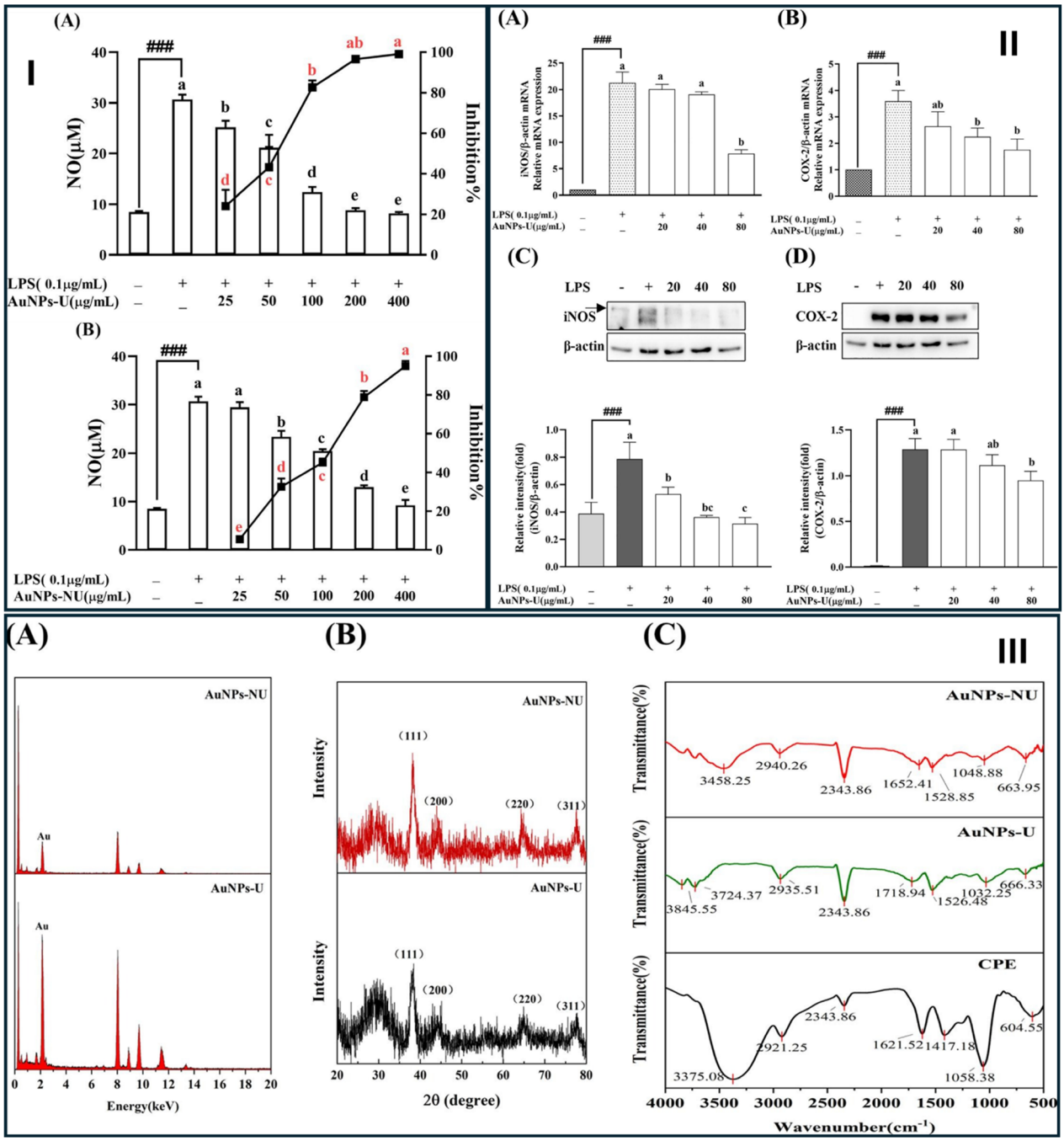

Fig. 29 (I) Effect of ultrasound-treated and untreated AuNPs on nitric oxide (NO) production in LPS-stimulated RAW 264.7 cells. (A) AuNPs-U (ultrasound-treated AuNPs), (B) AuNPs-NU (non-ultrasound-treated AuNPs). RAW 264.7 cells were pre-treated with the indicated concentrations of AuNPs for 1 hour and then stimulated with LPS (0.1 μg mL^{-1}) for 24 hours. (II) Effect of ultrasound-treated AuNPs (AuNPs-U) on the expression of iNOS and COX-2 in LPS-stimulated RAW 264.7 cells. (A) iNOS mRNA; (B) COX-2 mRNA; (C) iNOS protein; (D) COX-2 protein. RAW 264.7 cells were pre-treated with the indicated concentrations of AuNPs for 1 hour and then stimulated with LPS (0.1 μg mL^{-1}) for 24 hours. (III) EDS (A), XRD (B), and FTIR (C) analyses of AuNPs green synthesized using citrus peel extract (CPE). Reproduced with permission from ref. 117, copyright 2022 Elsevier.

composition of the peels influenced the CQDs' bioactivity. These findings support the use of CPW-derived CQDs in antioxidant therapies and functional materials.[116]

4.2. Metallic and plasmonic-based nanoparticles

Metal NPs that are commonly used include gold, silver, copper, platinum, iron, and others. Green synthesis routes using plant-

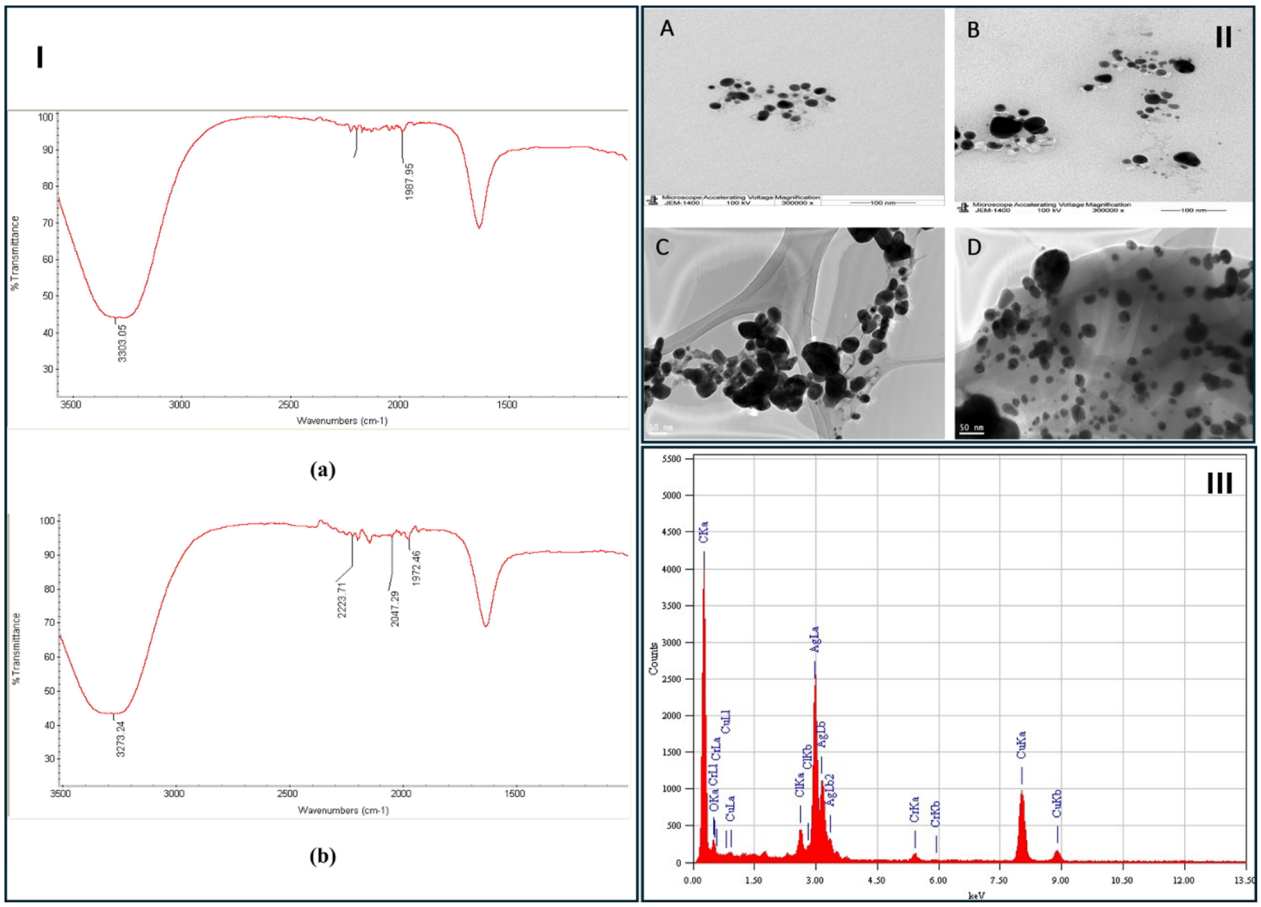

Fig. 30 FTIR (I) and EDX (III) spectra of green synthesized AgNPs using citrus limon peels extract (LPE). For the FTIR spectrum, (a) refers to the LPE extract, while (b) represents green synthesized AgNPs. (II) TEM images (A–D) of green synthesized AgNPs using LPE, depicting spherical appearance of the obtained NPs. Reproduced from ref. 118, copyright 2020 Elsevier.

based materials have emerged as sustainable and eco-friendly methods for producing these NPs. Citrus peels, rich in phenolics, flavonoids, and terpenoids, offer natural reducing and stabilizing agents for NPs formation.

Gao *et al.* (2022) explored the ultrasound-assisted green synthesis of gold NPs (AuNPs) using citrus peel extract and evaluated their anti-inflammatory properties. Characterization *via* UV-vis, DLS, SEM, TEM, EDS, XRD, and FTIR confirmed the successful synthesis of monodispersed, negatively charged spherical AuNPs (Fig. 28 and 29). Compared to non-ultrasound synthesized AuNPs (AuNPs-NU), the ultrasound-treated AuNPs (AuNPs-U) had smaller sizes (13.65 nm *vs.* 16.80 nm) and greater anti-inflammatory activity (IC50, 82.91 *vs.* 157.71 μg mL^{-1}). HPLC analysis revealed hesperidin as the main reductant. AuNPs-U significantly suppressed iNOS and COX-2 mRNA and protein expression in LPS-stimulated RAW 264.7 cells.[117]

In another study, Alkhulaifi *et al.* (2020) synthesized silver NPs (AgNPs) using citrus limon peel extract and assessed their characteristics (UV-vis, TEM, DLS, EDX, and FTIR), antimicrobial, and cytotoxic properties. The AgNPs were spherical (average size 59.74 nm) and showed few agglomerations. FTIR analysis indicated the presence of diverse functional groups contributing to reduction and stabilization (Fig. 30). Additionally, the obtained AgNPs exhibited excellent antibacterial effects against several pathogens (Fig. 31). The cytotoxicity assay revealed dose-dependent effects on human breast (MCF-7) and colon (HCT-116) cancer cell lines with IC50 values of 23.5 ± 0.97 and 37.48 ± 5.93 μL/100 μL, respectively (Fig. 31).[118]

Moreover, Nhi *et al.* (2022) developed an eco-friendly method for synthesizing AgNPs using pectin as both reducing and stabilizing agent. Using response surface methodology, the optimal conditions for NPs synthesis were identified as: 1.64 mg per mL pectin, 3.26 mM $AgNO_3$, 36.6 °C, and 9.6 h. The resulting particles, approximately 6.62 nm in diameter, were confirmed *via* UV-vis, TEM, DLS, XRD, and FTIR. This work demonstrated the feasibility of using citrus-derived pectin for NPs synthesis without toxic chemicals (Fig. 32).[119]

4.3. Metal oxide-based nanoparticles

Green synthesis of metal oxide NPs has gained significant attention due to its environmental compatibility and safety

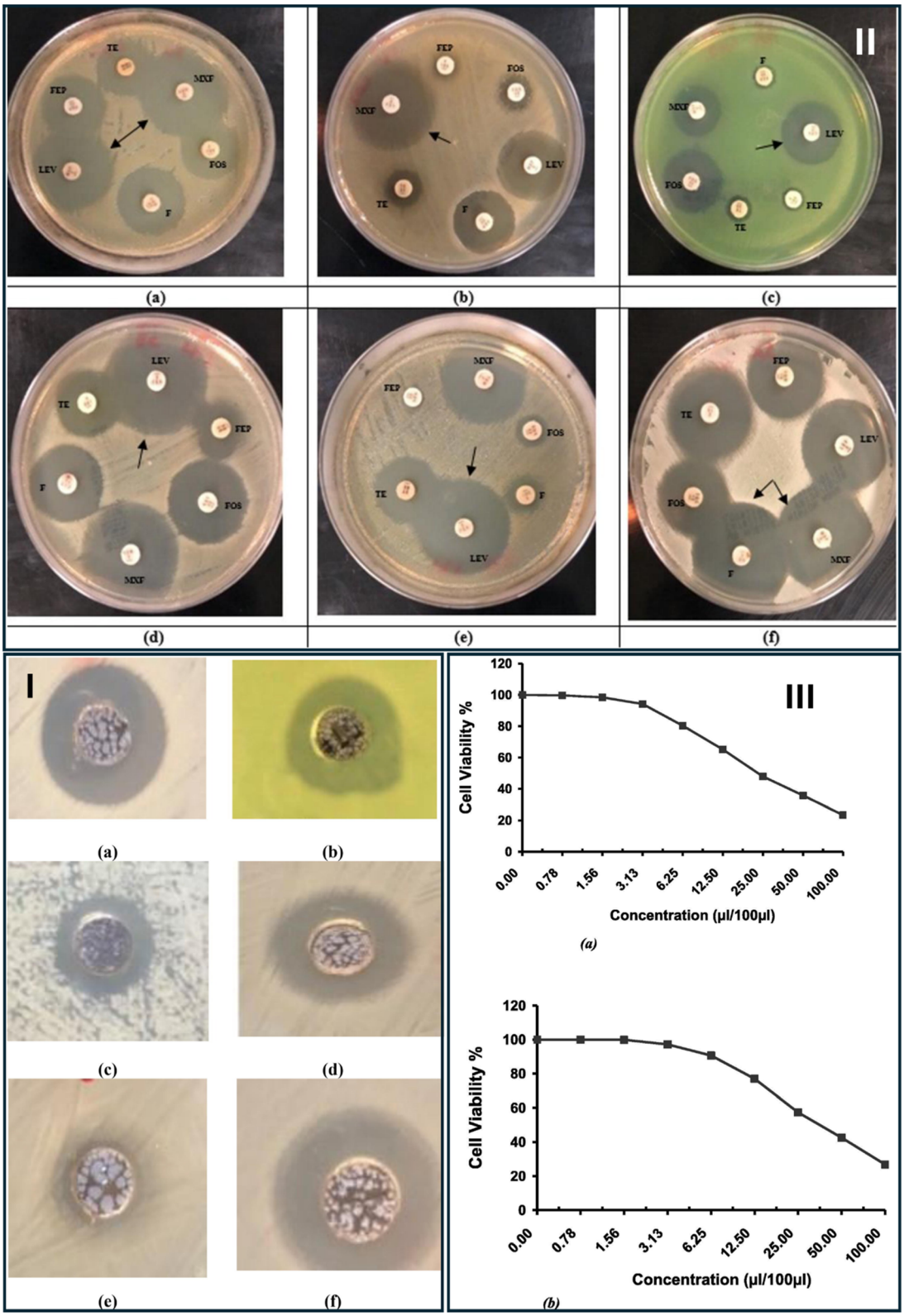

Fig. 31 Evaluation of the antimicrobial and cytotoxic activities of the synthesized AgNPs. (I) Antibacterial activity of the synthesized AgNPs represented by inhibition zones against various bacterial strains: (a) *S. aureus*, (b) *P. aeruginosa*, (c) *Acinetobacter baumannii*, (d) *Salmonella typhimurium*, (e) *Proteus vulgaris*, and (f) *E. coli*. Inhibition zones are visualized. (II) Antimicrobial activity for reference antibiotics against various bacterial strains. (a) *S. typhimurium*, (b) *P. vulgaris*, (c) *P. aeruginosa*, (d) *E. coli*, (e) *A. baumannii*, and (f) *S. aureus*. Arrows indicate the maximum inhibition zones for each antibiotic. F: nitrofurantoin (100 µg); FOS: fosfomycin (50 µg); TE: tetracycline (30 µg); FEP: cefepime (30 µg); MXF: moxifloxacin (5 µg); LEV: levofloxacin (5 µg). (III) cytotoxicity of AgNPs against human cancer cell lines. (a) Cytotoxic effect of AgNPs on MCF-7 human breast cancer cells. (b) Cytotoxic effect of AgNPs on HCT-116 human colon carcinoma cells. Reproduced from ref. 118, copyright 2020 Elsevier.

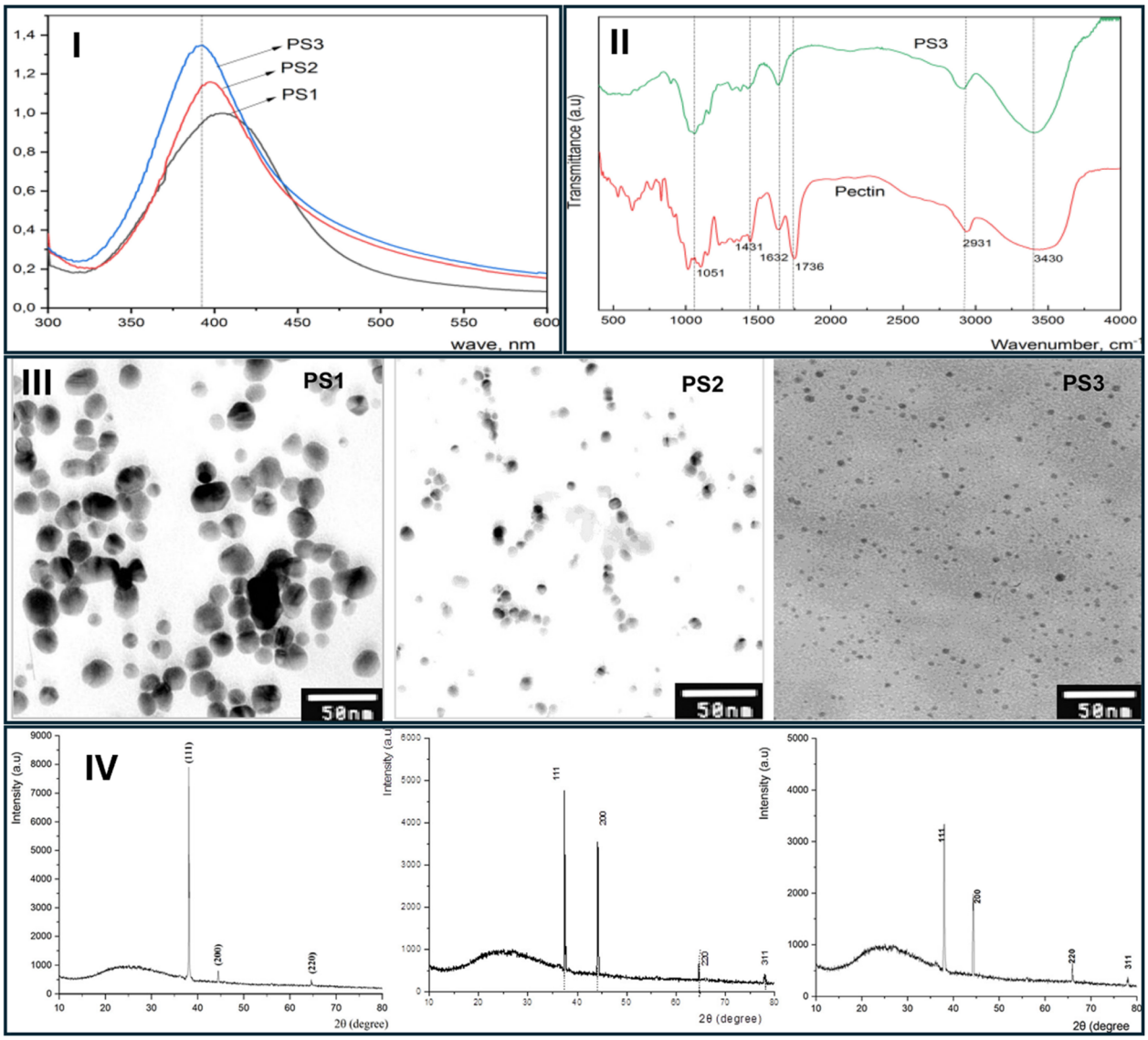

Fig. 32 UV-vis (I), FTIR (II), and XRD (IV) spectra analyses of pectin-silver nanocomposite. (III) TEM images of the obtained pectin NPs, revealing their morphology and size. Reproduced with permission from ref. 119, copyright 2022 John Wiley & Sons.

advantages over traditional chemical and physical routes. In contrast to conventional methods, green synthesis offers lower energy demands, reduced production costs, and minimized use of hazardous reagents, thereby facilitating more sustainable and scalable nanomaterial development.[120]

For example, Supreetha *et al.* (2021) synthesized a citrus pectin–magnesium oxide (MgO) nanocomposite using pectin extracted from *C. sinensis* peels through acid hydrolysis and ethanol precipitation. The extracted pectin (yield: 12.25%) was characterized by its equivalent weight, methoxyl content, anhydrouronic acid content, and molecular weight. The MgO nanocomposite was prepared *via* co-precipitation and characterized by XRD, FTIR, and SEM. The nanocomposite displayed enhanced biological performance compared to pectin alone, showing significant antibacterial activity against *B. subtilis* and *Lactobacillus*, and antifungal effects against *Microsporum gypseum* and *Trichophyton mentagrophytes*. It also demonstrated stronger DPPH radical scavenging activity, suggesting superior antioxidant properties (Fig. 33).[121]

Similarly, Thi *et al.* (2020) developed an eco-friendly method to synthesize ZnO NPs (ZnO NPs) using *C. sinensis* (orange) peel aqueous extract as the reducing agent. The synthesis involved zinc acetate dihydrate as the precursor, and parameters such as pH and annealing temperature were optimized to tune particle size and morphology. At a concentration of 0.025 mg mL^{-1}, the ZnO NPs demonstrated potent antibacterial activity against *E. coli* and *S. aureus* without the need for UV activation. Variations in synthesis conditions notably influenced bactericidal efficiency, highlighting the importance of optimization for biomedical use (Fig. 34).[122]

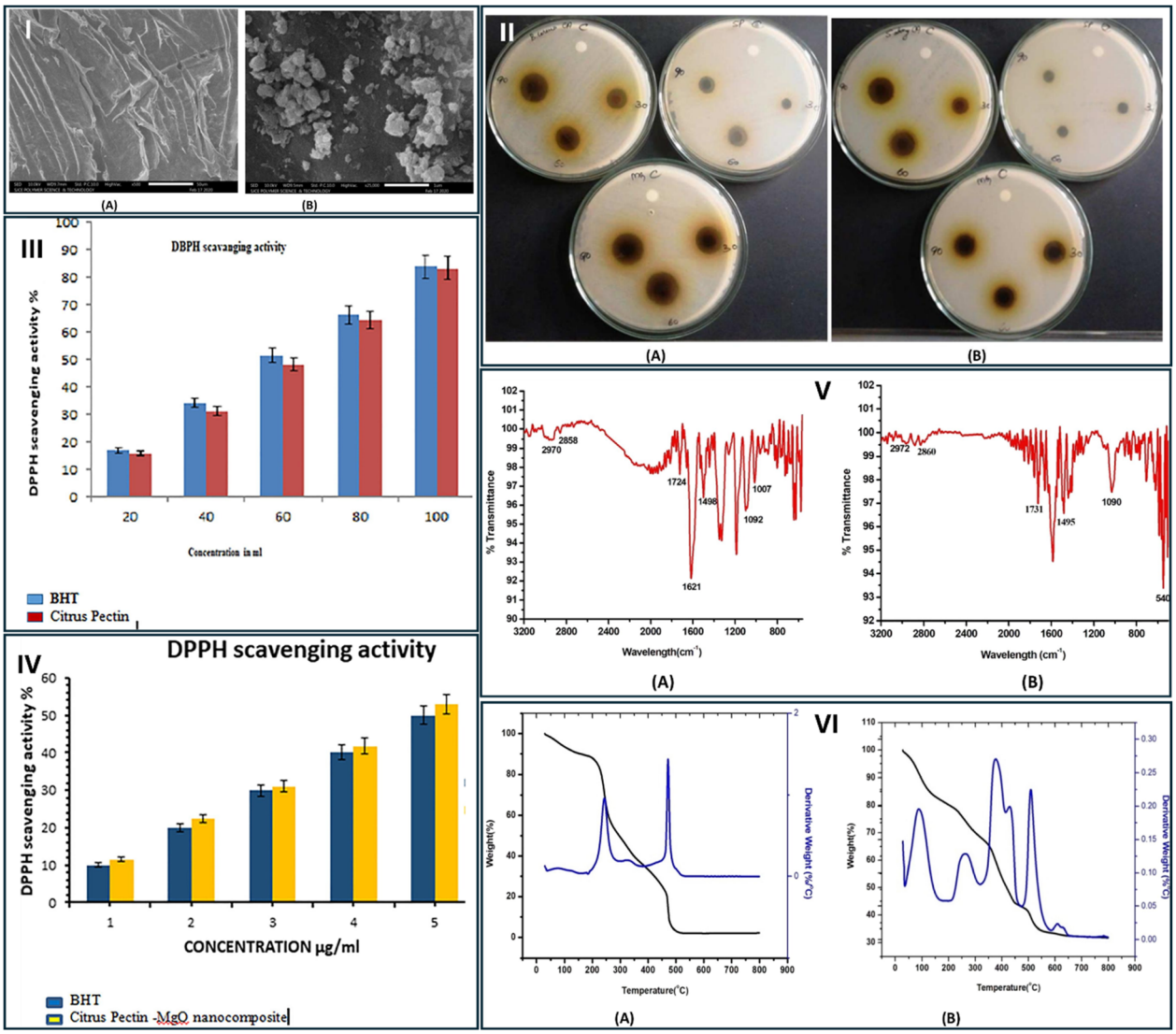

Fig. 33 (I) Microscopic characterization of citrus pectin and citrus pectin-MgO Nanocomposite. (A) Scanning Electron Microscopy (SEM) image of extracted citrus pectin. (B) SEM image of citrus pectin-MgO nanocomposite. (II) Antimicrobial activity of (A) extracted citrus pectin and (B) citrus pectin-MgO Nanocomposite. (III) Evaluation of antioxidant activity of citrus pectin and (IV) citrus pectin-MgO nanocomposite using the DPPH assay. FTIR analysis (V) of extracted citrus pectin (A) and citrus pectin-MgO Nanocomposite (B). TG-DTA thermogram (VI) of (A) extracted citrus pectin and (B) citrus pectin-MgO nanocomposite. Reproduced with permission from ref. 121, copyright 2021 Elsevier.

In another study, Baglari *et al.* (2023) synthesized copper oxide NPs (CuO NPs) from *C. maxima* (pomelo) peel extract. Structural and morphological characterization (XRD, SEM, EDS, FTIR, PL, and UV-vis spectroscopy) confirmed the monoclinic phase and spherical morphology of the CuO NPs, with a mean crystallite size of ~20 nm. The optical bandgap was ~1.5 eV. Electrical characterization revealed a strong photo-response, attributed to enhanced photogenerated electron mobility under light exposure, suggesting potential optoelectronic and sensing applications (Fig. 35).[123]

4.4. Polymeric-based nanoparticles

Biomass-derived polymeric nanomaterials have attracted increasing interest due to their low-cost synthesis, reduced environmental impact, and promising applications as biopolymers. Among these, cellulose and lignin, two abundant components of lignocellulosic biomass, have been widely investigated for the fabrication of nano-sized polymeric particles.

For instance, Matsedisho *et al.* (2024) enhanced the chemical and physical characteristics of cellulose nanofibers derived from chemically modified orange peel (OP) for application in heavy metal adsorption. The peels were modified with phosphoric acid (POP) and sodium hydroxide (NaOP) to improve biosorption performance for Ni(II) ions from wastewater. FTIR spectroscopy confirmed the introduction of carboxyl groups, crucial for metal ion binding, while XRD and TEM/SEM analyses verified increased crystallinity and successful nanofiber

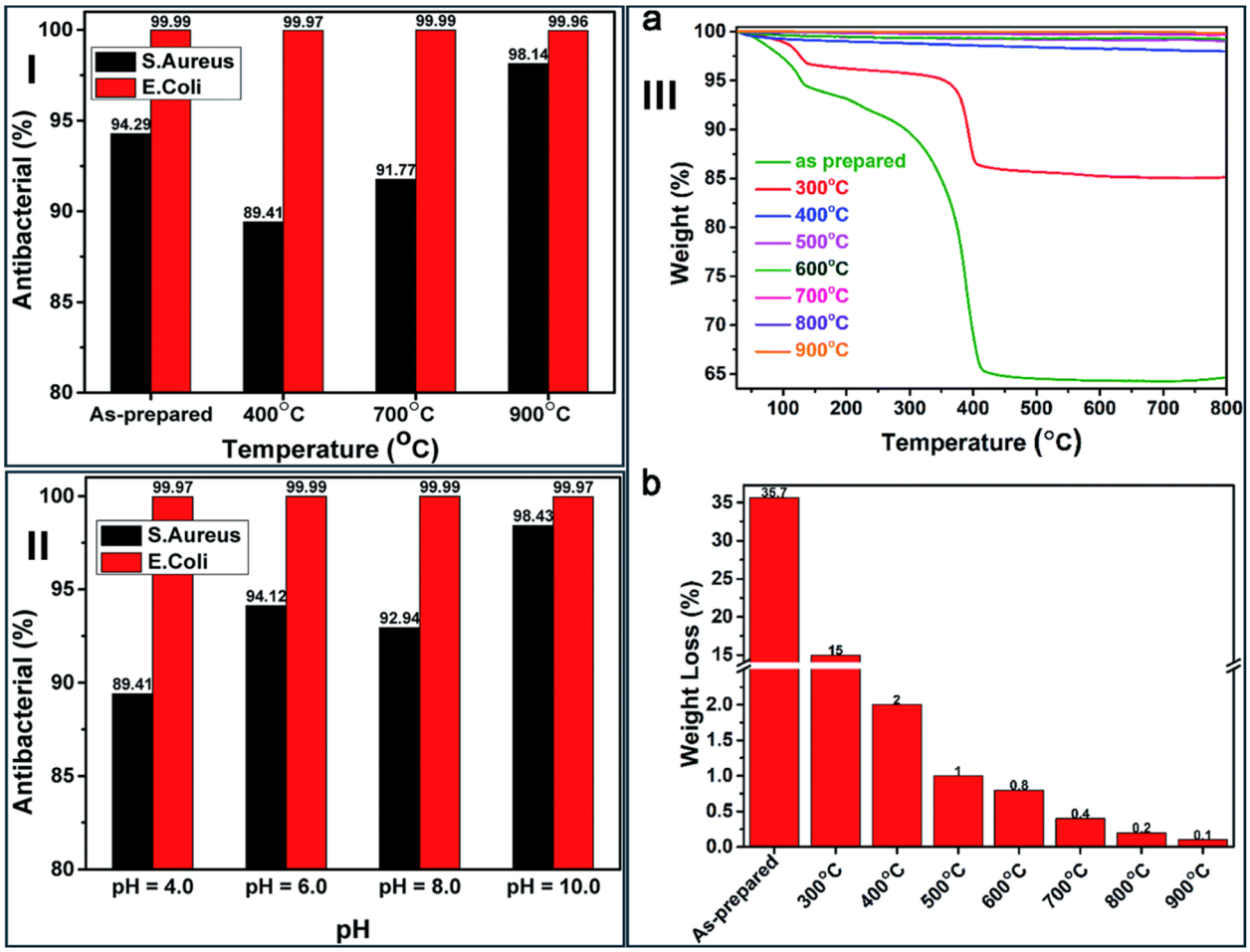

Fig. 34 (I) Bactericidal activity of ZnO NPs against *E. coli* and *S. aureus*. The figure illustrates the bactericidal rates of the as-prepared ZnO NPs and those annealed at various temperatures. (II) Effect of synthesis pH on the bactericidal activity of ZnO NPs. The figure shows the bactericidal rates of ZnO NPs synthesized at different pH values. (III) TGA investigation of the synthesized ZnO NPs was conducted for both as-prepared samples and those annealed at 300–900 °C. (a) Thermogravimetric curves. (b) Weight loss measured at 500 °C. Reproduced from ref. 122, copyright 2020 RSC.

formation (Fig. 36). Surface area analysis revealed improvements from 0.948 $m^2 g^{-1}$ (raw) to 1.428 $m^2 g^{-1}$ (modified). Batch adsorption studies indicated that the POP biosorbent exhibited the highest adsorption capacity (37.5 mg g^{-1}), outperforming NaOP (21.08 mg g^{-1}) and unmodified OP (8.4 mg g^{-1}). Optimal adsorption occurred at pH 5–6, with equilibrium reached within 90 min (Fig. 37).[124]

In another study, Yu *et al.* (2021) prepared nanofibrillated cellulose from grapefruit peel (GNFC) using a TEMPO-mediated oxidation method. The GNFC exhibited rod-like morphology (40–80 nm in diameter, ~200 nm in length), as confirmed by TEM, SEM, and XRD. The incorporation of GNFC into ice cream formulations was explored to enhance texture and reduce fat content by examining their texture, rheological properties, melting resistance, sensory characteristics, microstructure, and gross energy. The addition of 0.4% GNFC yielded the most favorable texture and sensory evaluation, with notable improvements in elasticity and chewiness. Furthermore, GNFC inclusion significantly reduced the gross energy and fat digestibility of ice cream, as demonstrated through *in vitro* simulated digestion, suggesting its utility as a sustainable fat replacer in food products (Fig. 38 and 39).[125]

These examples support the potential of citrus peel-derived polymers in the development of functional nanomaterials with diverse applications in environmental remediation, food formulation, and biomedicine, while supporting waste valorization principles.

A comparative summary of reported methods for synthesizing nanomaterials from CPW, together with particle sizes and representative applications, is presented in Table 2.

5. Biomedical and environmental applications

Citrus peels are managed in a variety of ways (Fig. 12), with the environmental impact ranging from the worst (conventional) to the best (beneficial). Beneficial procedures emphasize making

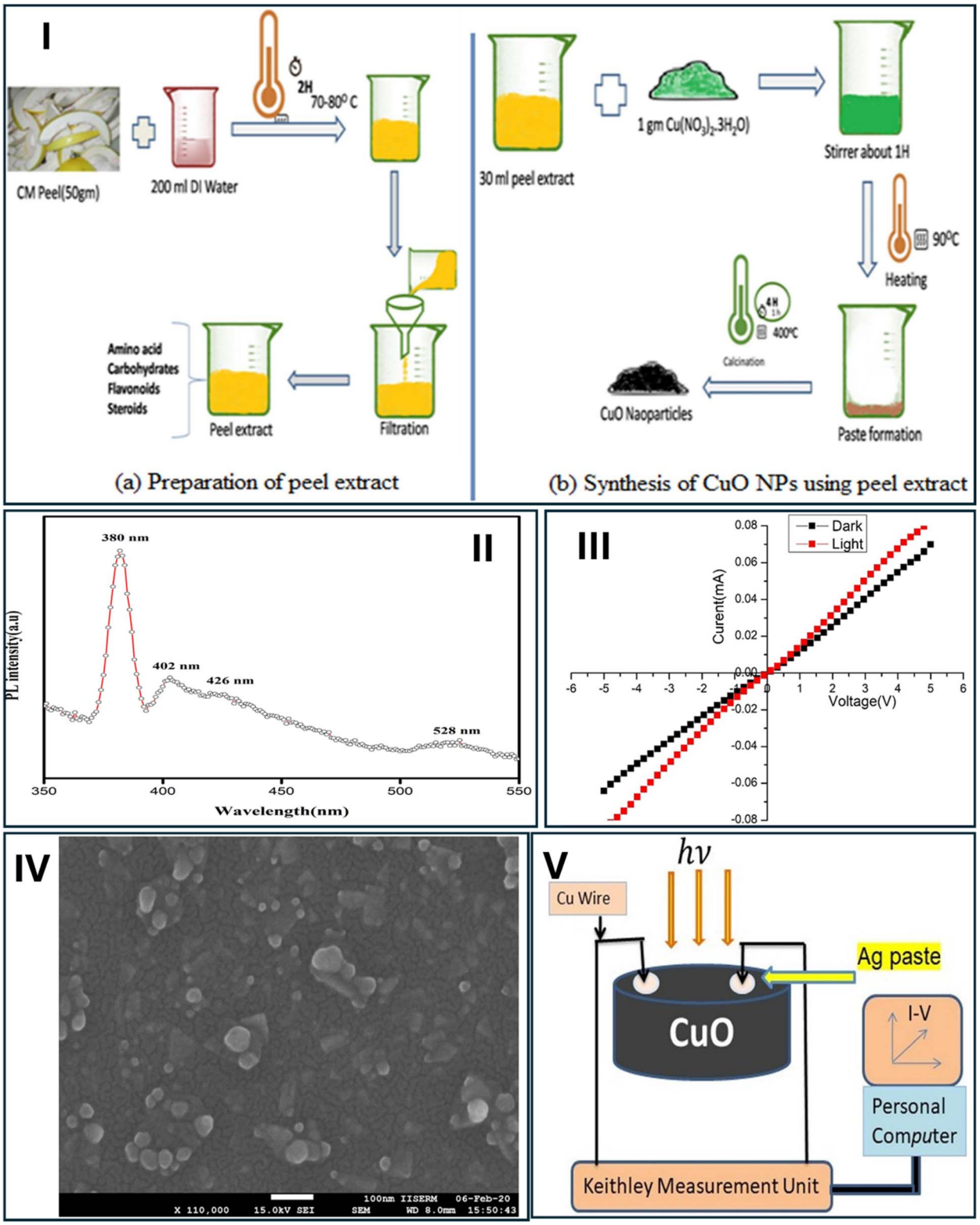

Fig. 35 (I) Schematic representation of the green synthesis of CuO NPs: (a) preparation of the peel extract and (b) synthesis of CuO NPs using peel extract. Photoluminescence spectrum (II) and Scanning electron microscopy (SEM) image (IV) of CuO NPs. (III) Current–voltage (*I–V*) curve for CuO NPs in the dark and under light illumination. (V) Schematic representation of the experimental setup for photo-response *I–V* measurement. Reproduced with permission from ref. 123, copyright 2024 Elsevier.

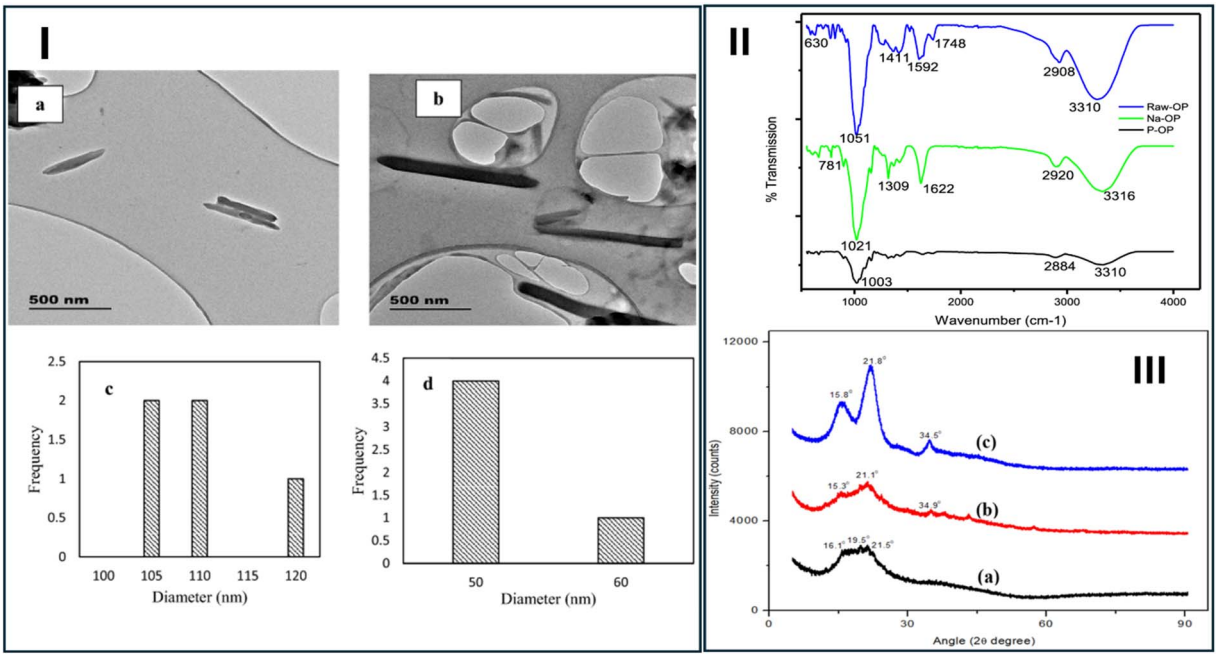

Fig. 36 (I) TEM analysis of unmilled (a) and milled (b) orange peel, in addition to the particle size distribution histograms of unmilled (c) and milled (d) orange peel. FTIR (II) and XRD (III) spectra of (a) raw orange peels (OP), (b) alkali-treated orange peels using sodium hydroxide (NaOP), and (c) acid-treated orange peels using phosphoric acid (POP). Reproduced from ref. 124, copyright 2024 Springer Nature.

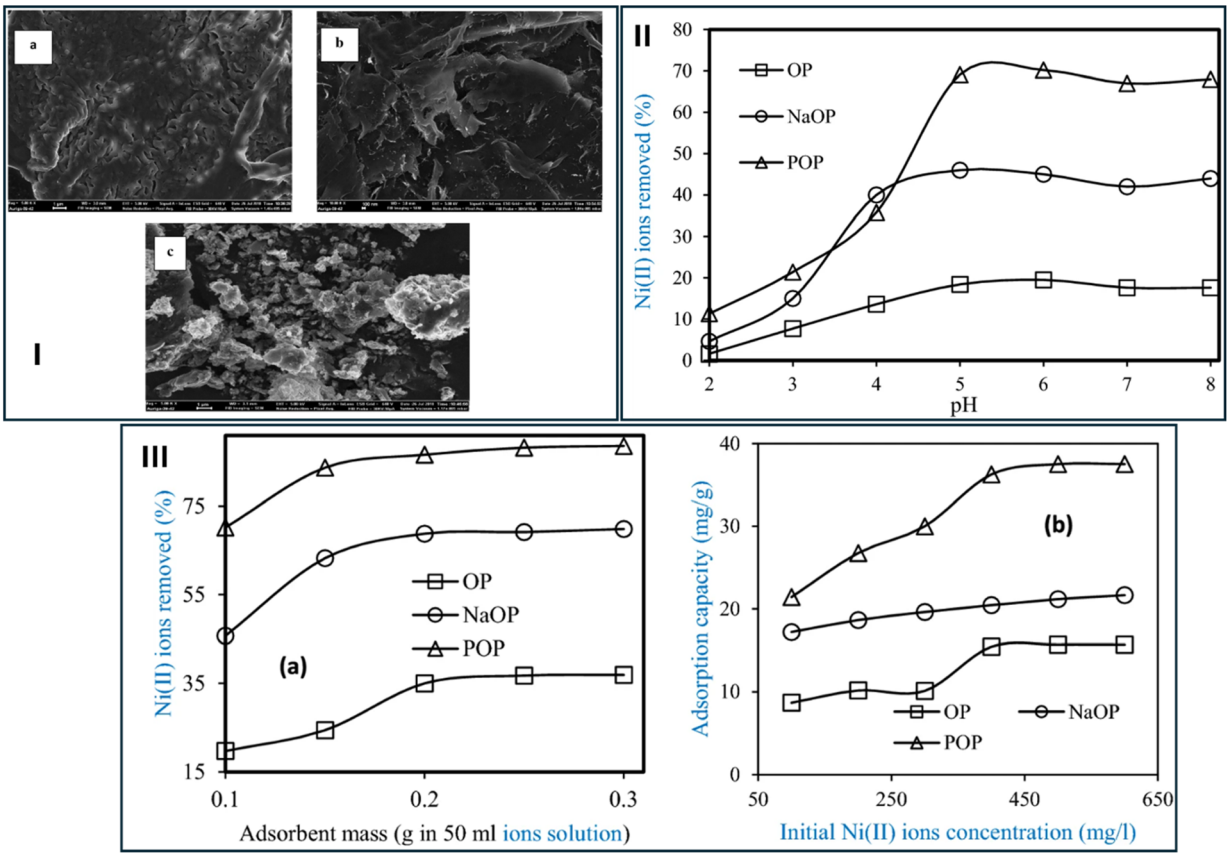

Fig. 37 Characterization of orange peels and their application for nickel II adsorption. (I) Scanning electron microscopy (SEM) images of orange peels: (a) raw, (b) chemically treated, and (c) milled. (II) Effect of pH on the adsorption of nickel II ions by raw and chemically modified orange peels. Experimental conditions: solution volume = 50 mL, contact time = 24 h, agitation speed = 160 rpm, and temperature = 25 °C, initial nickel II concentration = 100 ppm, and adsorbent mass = 0.1 g. (III) Influence of (a) adsorbent mass and (b) initial nickel II ion concentration on the adsorption process. Experimental conditions: pH = 5, solution volume = 50 mL, contact time = 24 h, agitation speed = 160 rpm, and temperature = 25 °C. Reproduced from ref. 124, copyright 2024 Springer Nature.

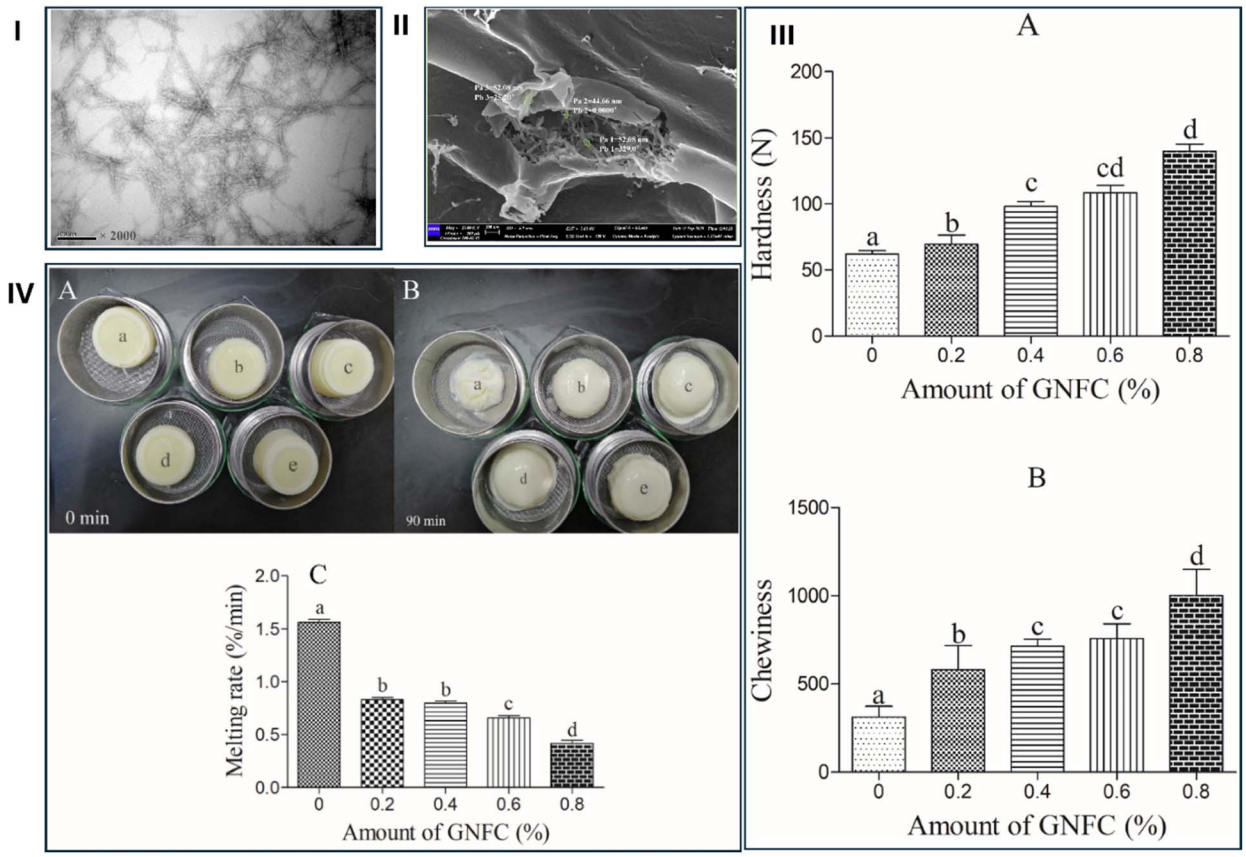

Fig. 38 Characterization and properties of ice cream containing nanofibrillated cellulose from grapefruit peels (GNFC). (I) Transmission electron microscopy (TEM) image of nanofibrillated cellulose from grapefruit peels (GNFC). (II) Scanning electron microscopy (SEM) image of nanofibrillated cellulose from grapefruit peels (GNFC). (III) Effect of GNFC addition and fat reduction on the textural properties of ice cream. (A) Hardness. (B) Chewiness. (IV) Ice cream stability and melting behavior. (A) Comparison of ice cream samples before (A) and after (B) melting at different concentrations of GNFC (a. 0.0%, b. 0.2%, c. 0.4%, d. 0.6%, e. 0.8%) at 0 and 90 minutes. (C) Effect of GNFC addition and fat reduction on the melting rate of ice cream. Reproduced with permission from ref. 125, copyright 2021 Elsevier.

the best use of citrus peels rather than wasting them or expending a lot of energy by recycling them. Recent research has emphasized the multifaceted utility of citrus peel biomass in high-value applications, encompassing biomedical, environmental, and packaging technologies. Citrus peel has recently been the subject of extensive research into its usage in a variety of applications, including antibacterial activity, wound healing, additives in food packaging, membranes for water treatment, scaffolds for bone regeneration, and so on.

Considering scalability and industrial relevance, CPW-derived small molecules (sugars, organic acids, and alcohols) may serve as convenient reductants for lab-scale synthesis of metallic nanoparticles, but the more promising near-term valorization routes for citrus processors are those that generate co-marketable, saleable products (*e.g.*, pectin and essential oils) and then utilize residual streams for materials synthesis or bioenergy. Recent advances in pectin recovery using pressurized CO_2 reduce the need for mineral acids and generate pectin with distinct physicochemical properties that are attractive for biomedical and material applications.[98] Coupling established EO recovery (cold-press/steam methods) with pectin extraction and targeted downstream conversion (*e.g.*, pectin-templated nanocomposites, carbon precursors) improves process economics and is particularly relevant for Egypt, one of the world's largest citrus producers and exporters, where vast amounts of peel waste are generated annually. Adopting such integrated valorization strategies could reduce environmental burdens while strengthening industrial competitiveness in Egypt and other citrus-producing countries.[98,156] These approaches not only improve the economic viability of citrus processing but also create downstream opportunities in biomedical applications (*e.g.*, antimicrobial agents, wound healing scaffolds, drug carriers) and environmental remediation (*e.g.*, biosorbents, membranes, and biopackaging). The following subsections highlight these dual application domains in detail.

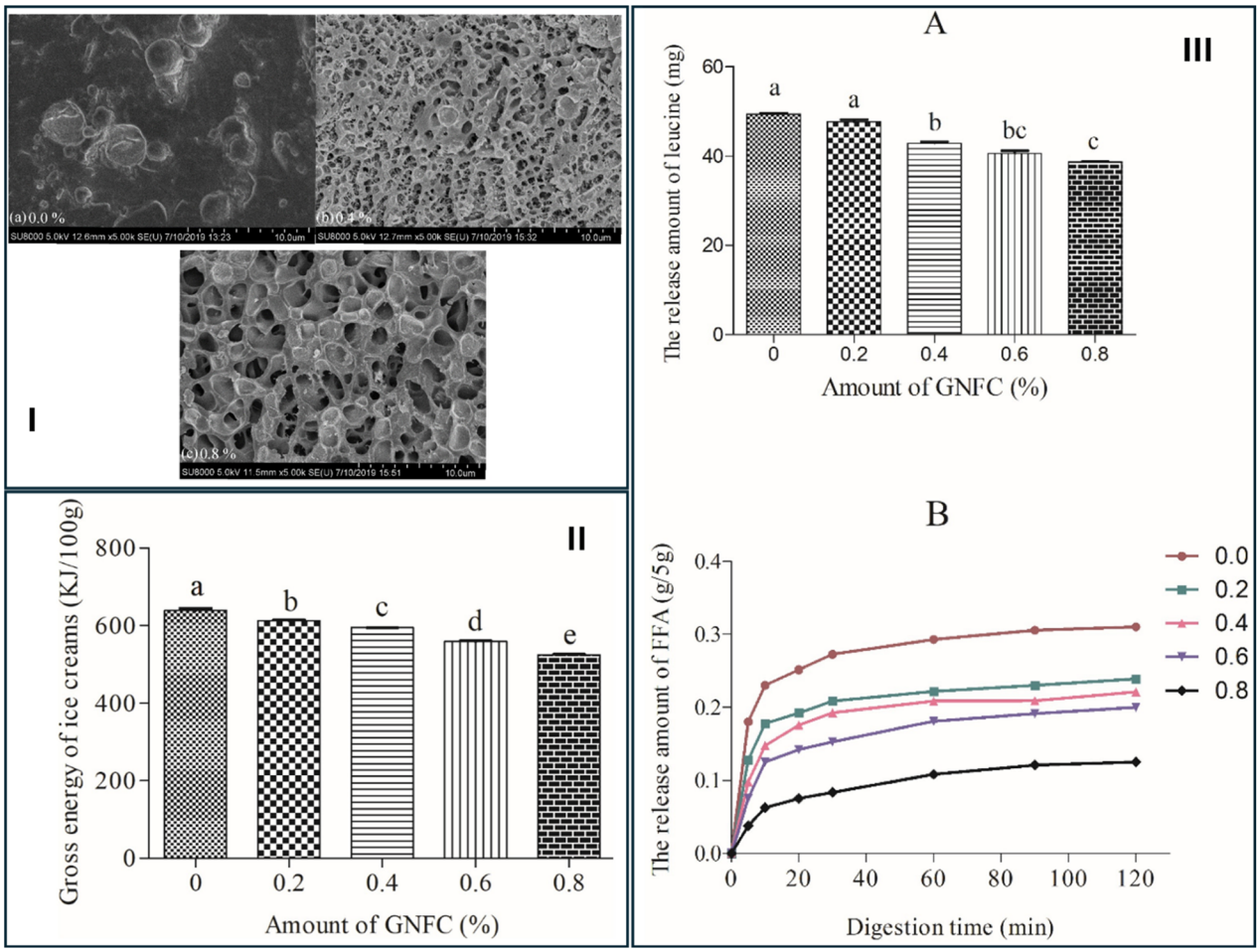

Fig. 39 Characterization and properties of ice cream containing nanofibrillated cellulose from grapefruit peels (GNFC). (I) Microstructure of ice cream. Scanning electron microscopy (SEM) images of ice cream with three representative additions of GNFC: (a) 0.0%, (b) 0.4%, and (c) 0.8%. Scale bar = 10 μm. (II) Effect of GNFC addition and fat reduction on the gross energy of ice cream. (III) Effect of GNFC addition and fat reduction on the release of nutrients during simulated digestion of ice cream. (A) Leucine release. (B) Free fatty acid release. Reproduced with permission from ref. 125, copyright 2021 Elsevier.

For example, Yun *et al.* (2023) employed four different types of citrus peel powder to prepare packaging films (Fig. 40). The structural and functional features of films made from peel powder from four distinct citrus fruits (pomelo, orange, mandarin, and lemon) were compared. The results revealed that the four types of citrus peel powder contained 11.45–15.47 mg GAE per g polyphenols, 5.68–8.23% protein, 2.88–6.27% crude fiber, 3.17–7.65% fat, and 16.36–23.80% pectin. These films had the following characteristics: water contact angle of 51.98–121.64°, thickness of 0.124–0.157 mm, water vapor permeability of 1.34–1.92 $\times$ 10^{-10} g m^{-1} s^{-1} Pa^{-1}, moisture content of 18.16–25.25%, tensile strength of 8.26–9.14 MPa, oxygen permeability of 0.36–0.69 cm^3 mm per m^2 per day per atm, and elongation at break of 8.05–17.18%. Additionally, these films exhibited significant antibacterial and antioxidant properties that delayed the oxidation of corn oil (Fig. 40). Because of its superior light and oxygen barrier capacity as well as antioxidant activity, the mandarin peel powder-based film proved to be the most successful at delaying the oxidation of oil among the other films. This highlights the feasibility of transforming citrus peel into biodegradable packaging with potential to extend food shelf life. The film based on powdered mandarin peel was found to be appropriate for the active packing of corn oil.[157]

Also, according to Dev *et al.* (2020), three waste-derived/low-cost biosorbents, citrus peels (bare), Ca-alginate gel beads, and Ca-alginate-citrus peels composite beads (Ca-alginate@citrus), were used to biosorb Se(IV) from a liquid solution. Citrus peels, Ca-alginate, and Ca-alginate@citrus all had maximal Se(IV) biosorption capacities of 116.2, 72.1, and 111.9 mg g^{-1} overall, with citrus peels (bare and immobilized). These findings support the development of affordable and effective biosorbents for environmental remediation, particularly in treating selenium-contaminated wastewater. This research lays

Table 2 Comparative literature data for different methods to synthesis nanomaterials from citrus peel waste, particle size of prepared nanomaterials, and application

Type of nanomaterials	Synthetic nanomaterials	Source/plant name	Function of citrus peel	Preparation method	Particle size	Application	Ref.
Carbon-based NPs	Water-soluble carbon quantum dots	Lemon peel	Natural-carbon-precursor	Microwave pyrolysis technique	4.4 nm	Detection of tetracycline in the nanomolar range	126
	Water-soluble carbon quantum dots	Lemon peel	Natural-carbon-precursor	Hydrothermal process	1–3 nm	Sensing and photocatalysis	107
	Water-soluble carbon NPs	*Sinensis* peel	Natural-carbon-precursor	Low-temperature carbonization	11.0 nm	Efficient sorbents for methylene blue (MB) and methylene orange (MO) dyes	127
	Nano structured graphene films	*Sinensis* extract	Natural-carbon-precursor	PECVD (RF-PECVD)	10–100 nm	Sensing	128
	Nitrogen and sulfur co-doped carbon dots	Orange-peel waste	Natural-carbon-precursor	Hydrothermal carbonization	2.0–6.5 nm	Nano-booster for enhancing electrocatalytic performance	129
	Nanoporous carbon nanosheets	*J. Citrus* peels	Natural-carbon-precursor	Simple pyrolysis	1–5 nm	Sodium-ion storage	130
	Nanostructured graphene-based material	Orange peels	Natural-carbon-precursor	Hydrothermal carbonization	67.4 nm	Targeted cancer therapy	131
	Porous hard carbon	Pomelo peels	Natural-carbon-precursor	Simple pyrolysis	4–23 nm	Sodium ion batteries	132
Metallic or plasmonic-based NPs	Gold@palladium core–shell NPs	Orange peel extract	Reducing and stabilizing agent	Two-step reduction method	40 nm core size and a 7 nm of shell	Formaldehyde colorimetric sensing performance	133
	Gold NPs	Citrus flavonoids	Reducing and stabilizing agent	One-pot method	15 nm	The role of flavonoids in gold reduction and stabilization	134
	Gold NPs	Orange peel extract	Reducing agent	Ultrasound-assisted green synthesis	13.6 ± 3.9 nm	Anti-inflammatory activity	117
	Selenium NPs	Orange peel extract	Reducing agent	Hydrothermal method	18.3 nm	Antibacterial activity	135
	Silver NPs	Kinnow Mandarin hybrid peel extract	Reducing and capping agent	One-step green synthesis	10–35 nm	Degradation of hazardous dyes from polluted water	136
	Gold NPs	*C. maxima* peel	Reducing and capping agents	Green biosynthesis method	8–25 nm	Catalytic/antibacterial activities	137
	Silver NPs	*Reticulata* peel extract	Reducing agent	Bio-reduction	46.8 nm	Anticorrosion properties	138
	Ag@Cu bimetallic NPs	Lemon peel extract	Stabilizing and reducing agent	Green method	—	Electrochemical characterizations	139
	(Co–Fe–Ag NPs) trimetallic NPs	Limon extract	Bio-reducing agent	Green method	20 nm	Biomedical applications	140
	Silver NPs	*C. maxima* peel extract	Reducing and capping agent	Biosynthesis	4–11 nm	Catalytic, antioxidant and antimicrobial characteristics	141

Table 2 (*Contd.*)

Type of nanomaterials	Synthetic nanomaterials	Source/plant name	Function of citrus peel	Preparation method	Particle size	Application	Ref.
Metal oxide-based NPs	Fe_3O_4 magnetic NPs	*C. sinensis* peel extract	Stabilizing, minimizing and capping agent	Green synthesis	20–24 nm	Biological activities and magnetic-hyperthermia applications	40
	ZnO NPs	Orange fruit peel extract	Biological reducing agent	Green synthesis	10–20 nm	Antibacterial activities	122
	CdO NPs	*limetta* peel extract	Natural reducing/ stabilizing agent	Bio-inspired fabrication	51.5 nm	Biomedical applications	106
	Cobalt oxide NPs	*Reticulata* orange peels	Ligand and a reducing agent	Precipitation method	—	Supercapacitors	142
	CuO NPs	Orange, peel extracts Lemon peel extracts Tangerine peel extracts	Reducing/capping agents	Green synthesis	74 nm 50 nm 70 nm	Combating bacterial resistance	143
	α-MnO_2 crystalline nanorods	Lemon juice and peel	Natural reducing agent	Hydrothermal process	17 nm in diameter and 150 nm in length	Positive electrode for lithium-ion batteries	144
	Silica NPs	Orange peel	Capping/reducing agent	Green synthesis method	20 nm	Combating oxidative stress	145
	MgO NPs	*C. aurantium* peel extract	Capping/reducing agent	Green synthesis method	50–60 nm	Antimicrobial evaluation	146
	TiO_2 NPs	Limon-citrus extract	Capping/reducing agent	Green synthesis method	—	Antibacterial activity	147
	ZnO NPs MgO NPs SiO_2 NPs	Lemon peel extract	Reducing agent	Green synthesis method	60.5 nm 16.7 nm 42.6 nm	Effect on irrigation water, soil properties, and origanum majorana productivity	148
Polymeric-based NPs	Cellulose nanocrystals	Orange peel	Natural-carbon-precursor	Alkaline/H_2O_2 bleaching process and sulfuric acid hydrolysis	Average length and width of 500 nm and 40 nm	Development of nanocomposite films	149
	Nanocellulose fibers (nanofibers)	*C. sinensis* L	Natural-carbon-precursor	Three-step physicochemical and enzymatic procedure	10 nm and a length of 458 nm	—	150
	Pectin NPs	Lime/lemon	Natural-carbon-precursor	Ionotropic gelation method	700 nm–850 nm	—	151
	Cellulose based nanofibers	Lemongrass EOs	Natural-carbon-precursor	Electrospinning	2.8 ± 1.1 μm	Fibrous wound dressings	152
	Hesperidin nanocrystals	Orange peel	Precursor	Nanoemulsion	50–200 nm	Anti-ageing effects	153
	Naringenin NPs	Naringenin powder	Precursor	Single emulsion and solvent evaporation technique	131.2 nm	Sunscreen creams	154
	Nanosized nobiletin	*C. reticulata* Blanco	Precursor	Wet-milling technique	270 nm	Improved oral bioavailability	155

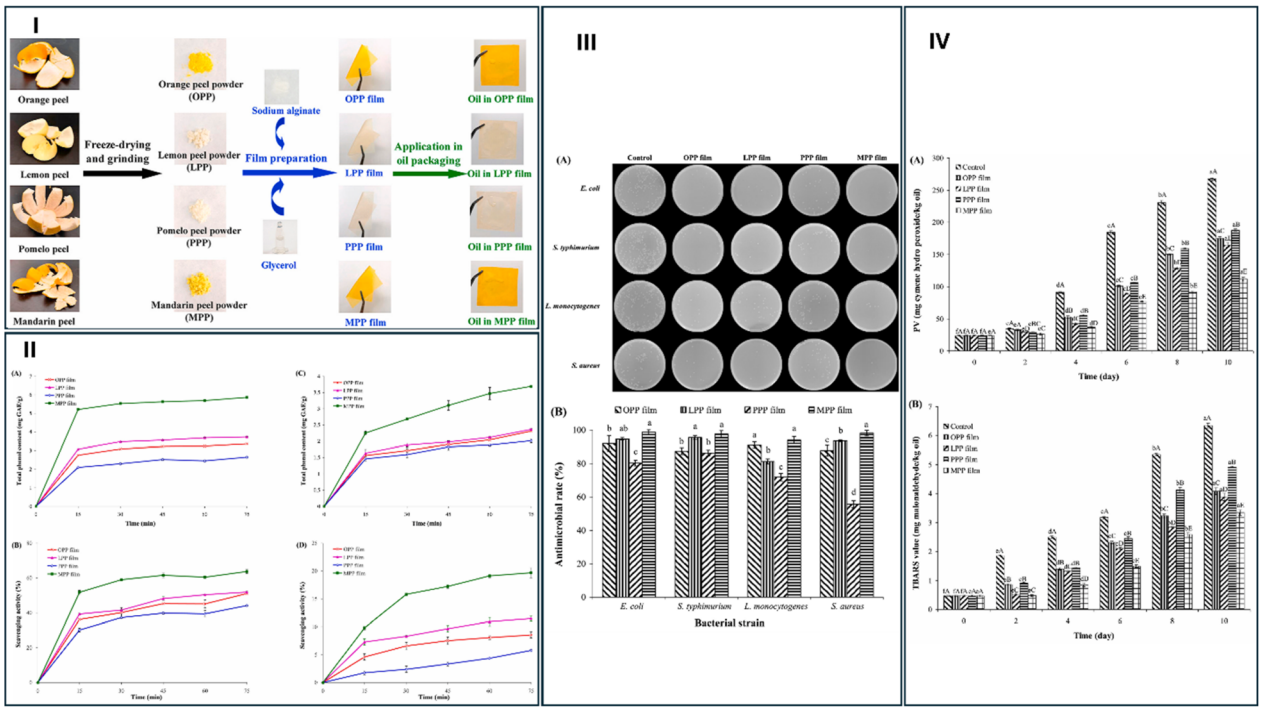

Fig. 40 Characterization and evaluation of citrus peel-based films for edible oil packaging. (I) Citrus peel waste is converted into powder and used to create biodegradable films with antioxidant and antimicrobial properties for improved edible oil packaging. (II) Total phenol content (A and C) and free radical scavenging properties (B and D) of obtained films extracted using ethanol ((A and B): 50%; (C and D): 95%). (III) Antimicrobial properties of obtained films against four bacterial strains: (A) antimicrobial performance; (B) antimicrobial rate. (IV) Oxidative stability of edible oil packaged in developed films: (A) peroxide value (PV); (B) thiobarbituric acid reactive substances (TBARS). Reproduced with permission from ref. 157, copyright 2023 Elsevier.

the groundwork for the future development of an affordable, innovative, and sustainable biosorbent called Ca-alginate@citrus, which may be used to treat Se(IV) contaminated water in an effective filtering system.[158]

In addition, Dahmani *et al.* (2020) found that applying Citrus reticulata peel extract topically resulted in considerable wound healing activity. Biochemical screening revealed that *C. reticulata* peel contains the highest amount of total vitamin C (13.20 mg g^{-1}), polyphenols (13.19 mg g^{-1}), carotenoids (0.032 mg g^{-1}), flavonoids (4.07 mg g^{-1}), and the lowest content of macronutrients (lipids: 1.5%, proteins: 0.40%, reducing sugars: 7.21%). On day 16 of treatment, wound area reduction was 100% for both treated groups (0.5% and 10%), compared to 100% and 98.32% for the positive and negative control groups on day 22. Furthermore, both treated groups showed a higher rate of wound contraction (100% on day 16). The extract also demonstrated promising antibacterial activity and antioxidant potential, confirming the therapeutic relevance of citrus peel constituents in wound management. Furthermore, *C. reticulata* peel showed exceptional antioxidant activity using DPPH and phosphomolybdate techniques, and the extract had antibacterial properties against pathogen microorganisms.[159]

Moreover, Sumathra *et al.* (2024) reported that morphology-focused hydroxyapatite (HAP) was created using pectin derived from the citrus fruit peel (*C. limonum*), which is then utilized to synthesize nano HAP by altering the quantity of pectin as a template (Fig. 41). The chemical structure, crystallinity, and morphology were measured using FTIR, XRD, and SEM, respectively. To improve the biocompatibility of HAP, pectin-aided HAP (tHAP) and HAP/pectin composites were created with varying pectin concentrations. The compatibility of HAP and pectin was tested in a human osteoblast cell line (Fig. 41). These results illustrate the feasibility of utilizing citrus-derived polysaccharides as a natural scaffold to tailor hydroxyapatite nanocomposites for bone regeneration applications. The physicochemical and biocompatibility properties of HAP/pectin revealed that HAP/pectin composites are promising materials for bone tissue engineering applications.[160]

Building on these examples, encapsulation has emerged as a particularly promising strategy to protect citrus peel-derived bioactive compounds, enhance their stability, and enable controlled release under specific physiological conditions. Encapsulation typically involves coating a bioactive substance with a protective polymeric or nanomaterial matrix, which not

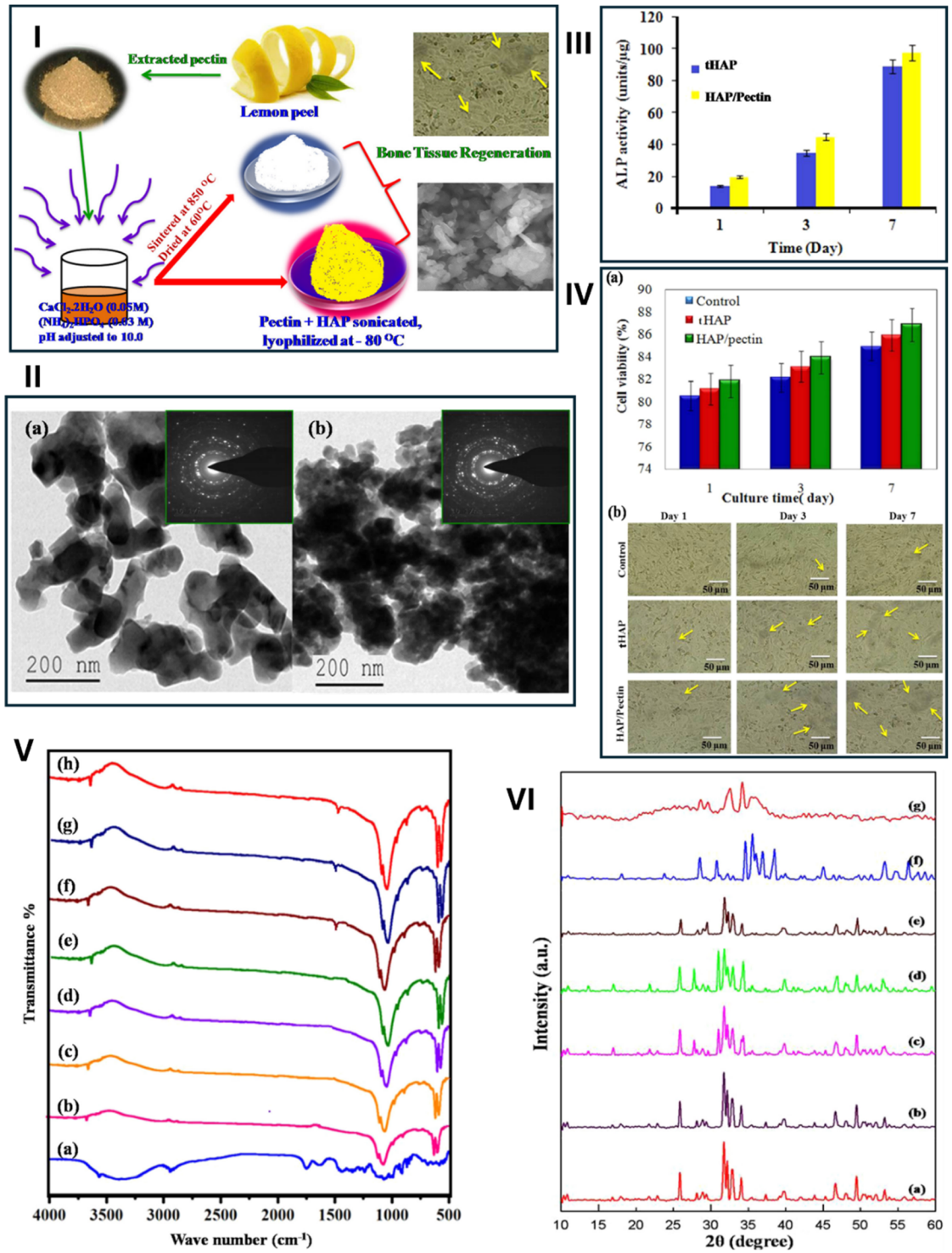

Fig. 41 (I) Schematic representation of the fabrication of HAP/pectin composite and its application in bone tissue regeneration. This figure illustrates the process of extracting pectin from lemon peel, its subsequent use as a template for synthesizing hydroxyapatite (HAP) composites, and their potential application in bone tissue regeneration. (II) Transmission electron microscopy (TEM) images and selected area electron diffraction (SAED) patterns of (a) template-free HAP (tHAP) and (b) HAP/pectin composites synthesized using 0.15% (w/v) pectin template. (III) Alkaline phosphatase (ALP) activity of HAP/pectin composite after 1, 3, and 7 days of culture. (IV) *In vitro* evaluation of cell–material interactions. (a) Cell viability of MG63 cells cultured in the presence of tHAP and HAP/pectin composite. (b) Morphological assessment of MG63 cells cultured on the as-synthesized HAP and HAP/pectin composite, observed by optical microscopy at 1, 3, and 7 days. (V) FTIR spectra of HAP/pectin composite and its corresponding single components of pectin and HAP. Extracted pectin (a), HAP (b), t-HAP 0.01, 0.05, 0.15% (w/v) (c–e), HAP/pectin composite 0.01, 0.05, 0.15% (w/v) (f–h). (VI) XRD spectra of HAP/pectin composite and its corresponding single components of pectin and HAP. Extracted pectin (a), t-HAP 0.01, 0.05, 0.15% (w/v) (b–d), HAP/pectin composite 0.01, 0.05, 0.15% (w/v) (e–g). Reproduced with permission from ref. 160, copyright 2017 Elsevier.

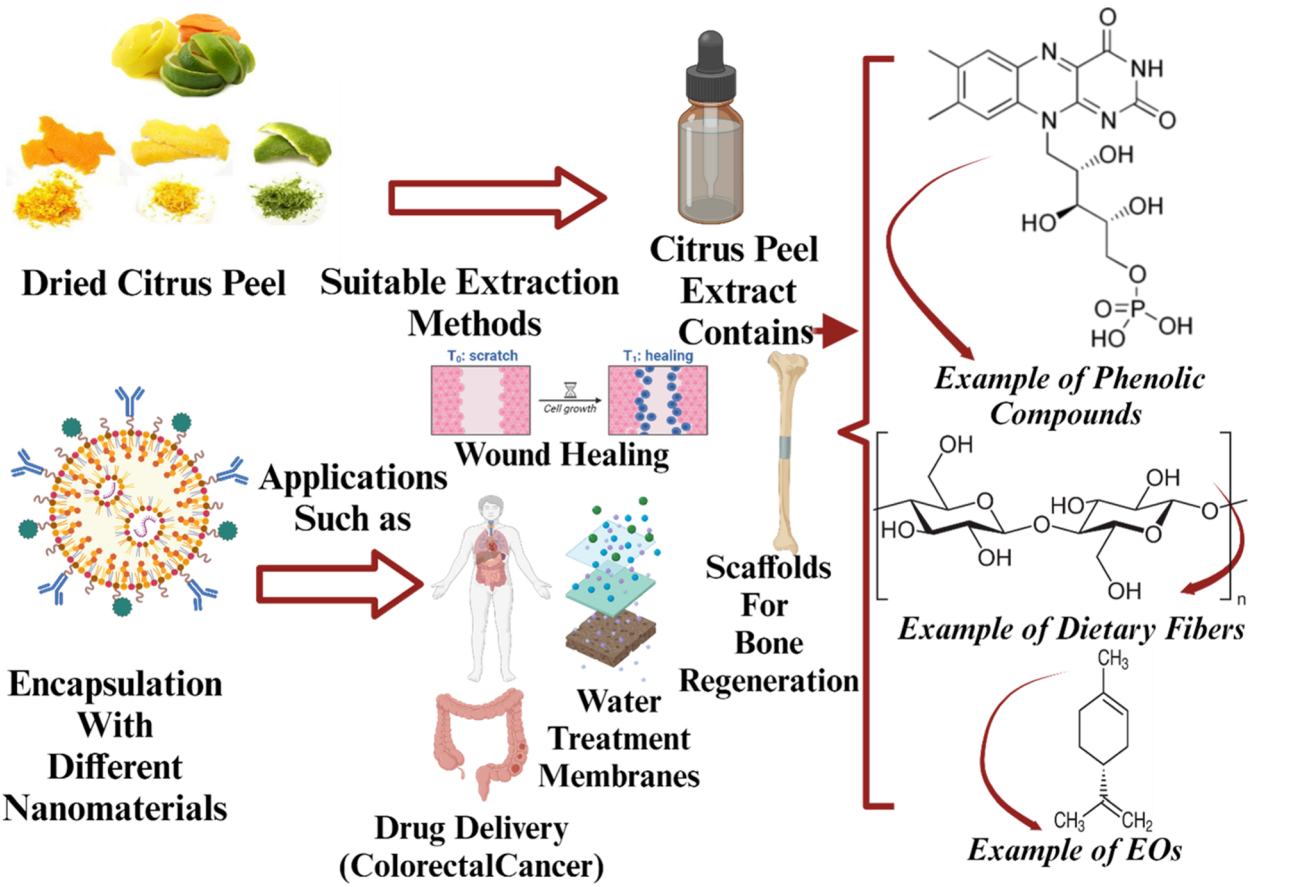

Fig. 42 Encapsulation of bioactive components extracted from citrus peel with different nanomaterials along with their use in different applications.

only shields it from degradation but also improves sensory attributes by masking undesirable odors or tastes. Importantly, the nanoscale dimension of these carriers offers high surface-to-volume ratios, improving encapsulation efficiency, bioavailability, and release kinetics.[161–163] A schematic overview of this concept is provided in Fig. 42.

For instance, Ghasemi *et al.* (2023) investigated the release profile of orange peel oil (OPO) encapsulated in freeze-dried modified nanocomposite powders under varying pH (3, 7, 11) and temperature (30, 60, 90 °C) conditions, as well as within a simulated salivary system. The encapsulated particles, evaluated *via* atomic force microscopy (AFM), exhibited nanoscale dimensions and encapsulation efficiencies ranging from 70% to 88%. The release behavior followed the Higuchi kinetic model across all conditions, with slower release observed at pH 3 and 30 °C and faster release at pH 11 and 90 °C. These findings demonstrate the potential of OPO nanocarriers for flavor-controlled food applications under different environmental and processing conditions.[85]

Similarly, Santos *et al.* (2024) developed nanostructured lipid carriers (NLCs) for delivering *C. sinensis* EO (CSEO) and its primary component, R-limonene, for leishmaniasis treatment. The NLCs were synthesized using microemulsion technique and modified with chitosan to improve surface characteristics. Physicochemical characterization (DSC, XRD, TEM, and DLS) confirmed spherical particles ranging from 97.9 to 111.3 nm in diameter and a positive surface charge (45.8 mV to 59.0 mV) in chitosan-coated systems (Fig. 43). Cytotoxicity tests in L929 and RAW 264.7 cells indicated promising biocompatibility (showing >70% cell viability on L929 cells), while the surface-modified NLCs exhibited significantly enhanced antipromastigote and antiamastigote activity (reducing survival of promastigotes by 93%), compared to uncoated carriers and free compounds (Fig. 44). These findings highlight the therapeutic promise of citrus-based NLCs in parasitic disease treatment.[164]

In another study, Luque-Alcaraz *et al.* (2022) encapsulated orange extract (OE) obtained from orange peels (*C. sinensis*), rich

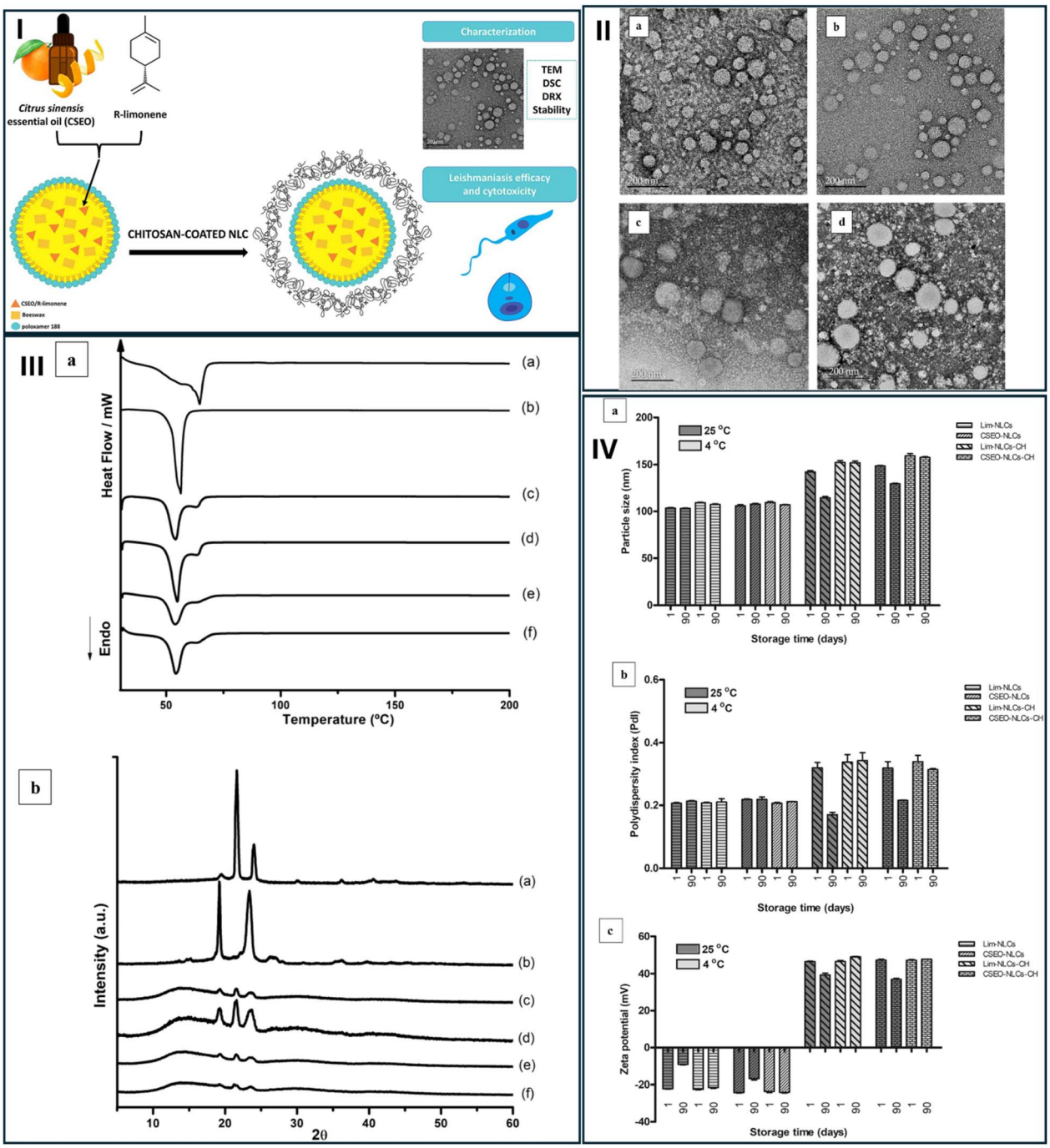

Fig. 43 (I) Schematic representation of the development and characterization of chitosan-coated nanoemulsions (NLCs) loaded with *C. sinensis* EO (CSEO) and R-limonene. (II) TEM photomicrographs of Lim-NLCs (a) and Lim-NLCs-CH (b) CSEO-NLCs (c) CSEO-NLCs-CH (d). (III) Physicochemical characterization of NLCs formulations: (a) DSC investigations of beeswax (a), poloxamer 188 (b), Lim-NLCs (c), CSEO-NLCs (d), Lim-NLCs-CH (e), and CSEO-NLCs-CH (f). (b) XRD profile of beeswax (a), poloxamer 188 (b), Lim-NLC (c), CSEO-NLCs (d), Lim-NLCs-CH (e), and CSEO-NLCs-CH (f). (IV) NLCs stability studies over 90 days of storage employing two different temperatures (25 °C and 4 °C): (a) particle size, (b) polydispersity index, and (c) zeta potential. Reproduced with permission from ref. 164, copyright 2024 Elsevier.

in phenolics and flavonoids, into a zein-based nanoparticulate system. The extract was obtained *via* ultrasound-assisted extraction (UAE), and the encapsulation process used nanoprecipitation. The resulting zein NPs (NpZOE) displayed a hydrodynamic diameter of 159.26 ± 5.96 nm and spherical morphology confirmed by SEM. FTIR and ζ-potential analyses supported successful OE incorporation. Antioxidant assessments using ABTS and DPPH assays revealed comparable or improved activity of NpZOE *versus* unencapsulated OE at lower concentrations, indicating the benefit of encapsulation in enhancing

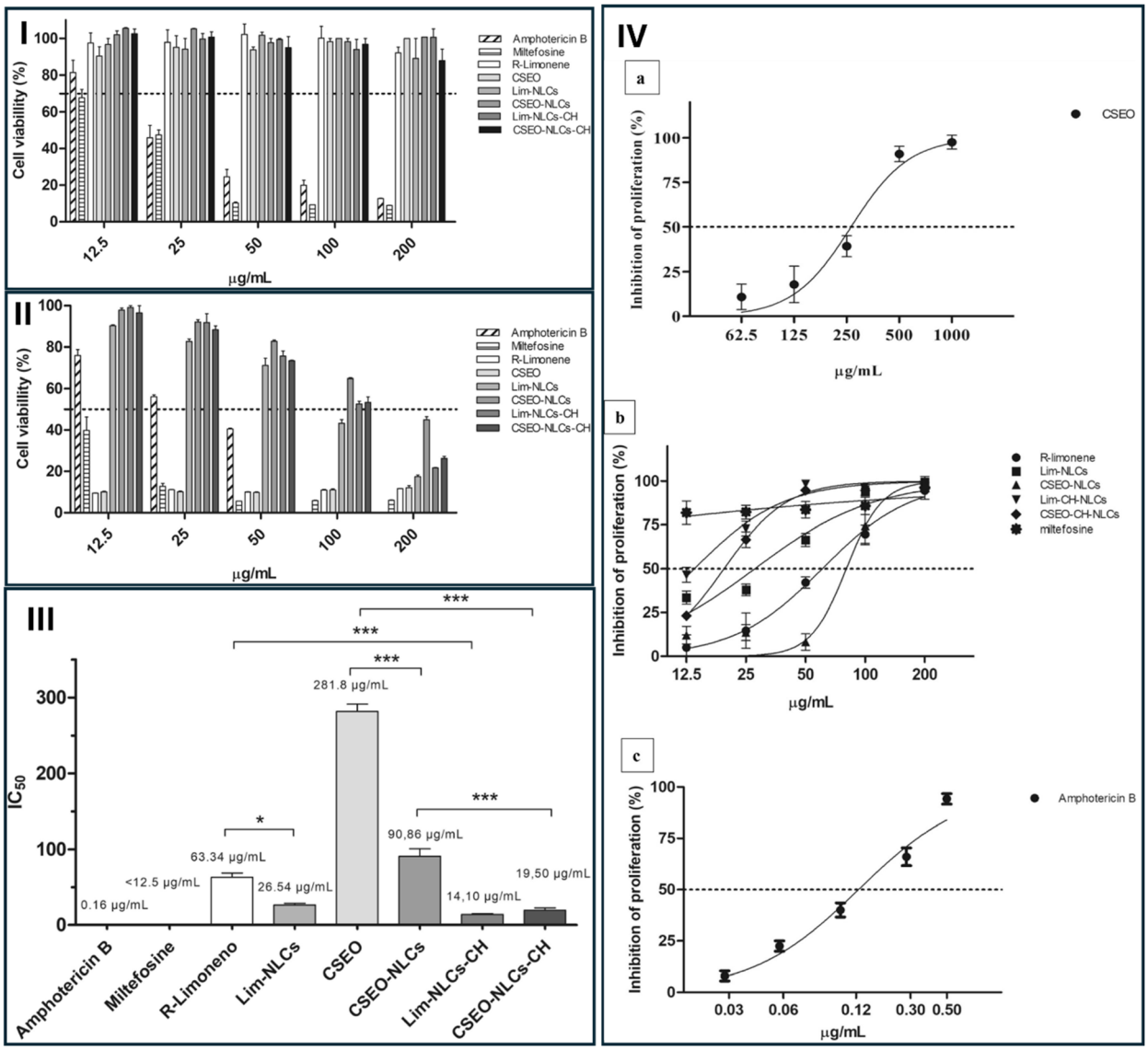

Fig. 44 (I) *In vitro* cytotoxicity evaluation of R-limonene, CSEO, and their NLC formulations on L929 fibroblasts. Cell viability was assessed after 24 h of treatment with concentrations ranging from 12.5 to 200 μg mL^{-1}. Miltefosine and amphotericin B were used as positive controls. Dashed line indicated 70% of L929 cell viability. (II) *In vitro* cytotoxicity evaluation of R-limonene, CSEO, and their NLC formulations on RAW 264.7 macrophages. Cell viability was assessed after 48 h of treatment with concentrations ranging from 12.5 to 200 μg mL^{-1}. Miltefosine and amphotericin B were used as positive controls. Dashed line indicated 50% of RAW 264.7 cell viability. (III) *In vitro* anti-leishmanial activity of R-limonene, CSEO, and their NLC formulations against Leishmania amazonensis promastigotes. The figure shows the inhibitory concentration 50% (IC50) values after 48 h of incubation. Miltefosine and amphotericin B were used as positive controls. (IV) Dose-dependent anti-leishmanial activity of CSEO (a), R-limonene, Lim-NLCs, CSEO-NLCs, Lim-NLCs-CH, and CSEO-NLCs-CH (b), and amphotericin B (c) against Leishmania amazonensis promastigotes after 48 h of incubation. Dashed line indicated 50% of cell viability. Reproduced with permission from ref. 164, copyright 2024 Elsevier.

antioxidant delivery (Fig. 45).[165] These studies collectively support the growing interest in incorporating citrus-derived bioactives into nanocarrier systems for enhanced stability, controlled release, and application-specific performance.

The diverse biomedical applications of citrus-derived bioactive compounds, including citrus flavonoids, citrus EOs, and citrus dietary fibers, in nanomaterial-based formulations are summarized in Table 3.

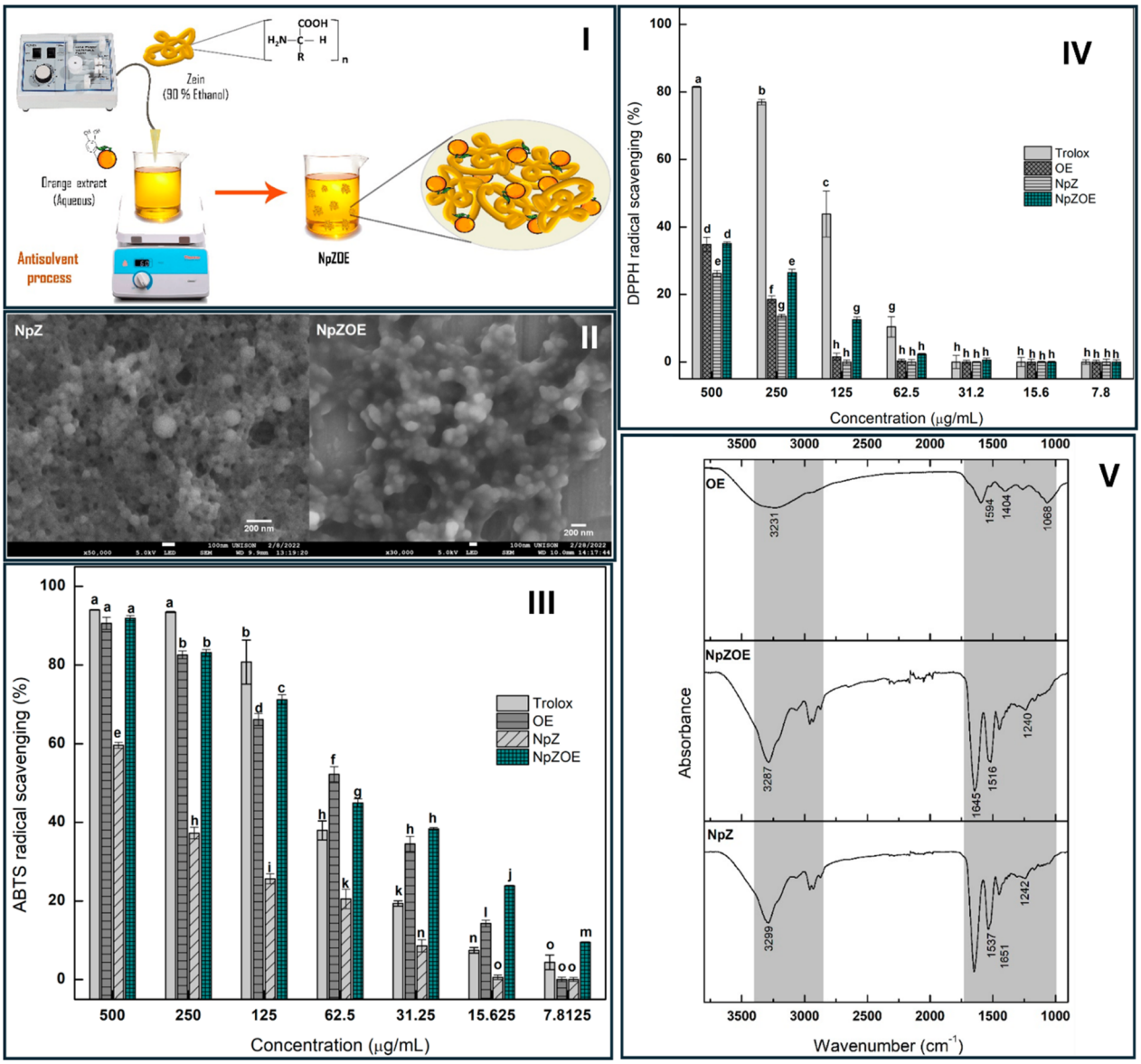

Fig. 45 Synthesis, characterization, and antioxidant activity of zein NPs loaded with orange extract. (I) Schematic representation of the synthesis of zein-loaded orange extract NPs. This figure illustrates the step-by-step process of developing NPs encapsulating orange extract within a zein matrix. (II) Scanning electron microscopy (SEM) micrographs of zein NPs (NpZ) and zein NPs loaded with orange extract (NpZOE). These images provide visual evidence of the morphology and size of the synthesized NPs. (III) Evaluation of antioxidant activity of orange peel extract (OE), zein NPs (NpZ), and zein NPs loaded with orange extract (NpZOE) performing the ABTS free radical scavenging assay. Antioxidant capacity was assessed using a Trolox equivalent antioxidant capacity assay. (IV) Assessment of antioxidant activity of orange peel extract (OE), zein NPs (NpZ), and zein NPs loaded with orange extract (NpZOE) using the DPPH free radical scavenging assay. Trolox was used as a reference antioxidant. (V) FTIR spectra of OE, NpZ, and NpZOE, revealing the chemical structural identities for each component and reflecting the incorporation of OE into NpZ. Reproduced from ref. 165, copyright 2022 MDPI.

Table 3 Citrus-derived bioactive compounds in nanomaterial-based formulations for biomedical and environmental applications

Extracted bioactive component	Source/Plant name	Nanomaterials incorporated	Formulation nanocomposite	Preparation method	Encapsulation efficiency	Application	Ref.
Citrus flavonoids	Naringenin derived from citrus fruits	Polycaprolactone/ polyethylene glycol nanofibers (NFs)	Naringenin-loaded polyethylene glycol/ polycaprolactone electrospun nanofibers	Electrospinning method	98.07%	Evaluation of antibacterial and wound healing activity	166
	C. unshiu	Pectin NPs	Citrus peel extracts-loaded pectin NPs	The ionic gelation technique	91.47%	*In vitro* release and antioxidant activity	167
	Hesperidin derived from citrus fruits	Chitosan NPs	Hesperidin-loaded PLGA-chitosan NPs (HPD/NPs)	Emulsification and evaporation methods	81.02%	Acute lung injury	168
	Naringenin derived from citrus fruits	Chitosan/alginate core–shell NPs	Naringenin loaded chitosan/alginate core–shell NPs	Ionic gelation method	91%	Efficient oral delivery of naringenin in diabetic animals—An *in vitro* and *in vivo* approach	169
	Hesperidin from orange peel	Hesperidin conjugated gold NPs	Hesperidin gold NPs	Chemical reduction method	—	Memory amelioration in diabetes induced cognitive impaired rats	170
	Naringenin derived from citrus fruits	Cysteine conjugated chitosan based green nanohybrid hydrogel embedded with zinc oxide NPs	Naringenin loaded nanohybrid hydrogels	Schiff base crosslinking method	86.09%	Enhanced therapeutic potential of naringenin	171
Citrus EOs	Lemon EOs	Chitosan (CS) and modified starch (Hicap)	Nanoencapsulation of lemon EOs in chitosan-Hicap system	Emulsion	85.44%	*In vitro* release of lemon EOs	172
	Orange EOs	Cross-linked electrospun gelatin nanofibers	Orange EOs using cross-linked electrospun gelatin nanofibers	Emulsion	69 and 52.6%	—	173
	Lemon peel EOs	Guar gum/gelatin based nanogel	Lemon peel extract loaded nanogel made of gelatin and guar gum in casein/basil seed gum film	Inverse miniemulsion approach	—	Active food packaging application	174
	Mandarin	Chitosan NPs	Mandarin EOs incorporated into chitosan NPs	Emulsion	82.35%	Anti-biofilm properties and application in pork preservation	175
	Bitter orange	Chitosan NPs	Chitosan NPs-loaded *C. aurantium* EOs	Ionic gelation technique	4.51–15.33%	Application on antioxidant and antimicrobial characteristics of white button mushroom	176
	Limonene	Solid lipid NPs (SLN)	Limonene 1,2-epoxide-loaded SLNs	Hot high-pressure homogenization (HPH) technique	63%	Evaluation of drug release, antioxidant activity	177
	Pectin	*Citrus limonum* peel			—	Bone tissue engineering	160

Table 3 (*Contd.*)

Extracted bioactive component	Source/Plant name	Nanomaterials incorporated	Formulation nanocomposite	Preparation method	Encapsulation efficiency	Application	Ref.
Citrus dietary fibers			Pectin-aided HAP (tHAP) and HAP/pectin composites	Template-assisted synthesis			
	Pectin	Commercial citrus pectin	Pectin/Guar Gum/Zinc oxide nanocomposites (NCs)	Precipitation method	—	Anticancer activity *via* apoptosis induction, ROS production, and caspase activation	178

6. Conclusions and perspectives

The rapid growth of global food production has led to a proportional increase in agricultural waste, including citrus peels, which present notable environmental management challenges. As a major byproduct of the food processing industry, citrus peel waste has attracted considerable attention due to its rich content of bioactive compounds and potential as a low-cost, sustainable feedstock for value-added applications. This review evaluated recent advances in the utilization of citrus peel waste, particularly its role in the green synthesis of nanomaterials and extraction of bioactive compounds for biomedical, environmental, and technological purposes.

Among the most promising approaches is the green synthesis of nanomaterials using citrus peel extracts, which act as reducing and stabilizing agents. Compared to conventional chemical synthesis methods, this strategy offers advantages such as reduced toxicity, environmental compatibility, and cost-effectiveness. Studies have demonstrated successful fabrication of various nanomaterials, including carbon-based nanostructures, metallic and plasmonic NPs, metal oxide NPs, and polymeric nanomaterials, using citrus peel extracts. These nanomaterials have been investigated for potential applications in drug delivery, antimicrobial therapies, wound healing, water treatment, and biosensing.

In parallel, citrus peels serve as a valuable source of bioactive compounds, notably flavonoids, EOs, polyphenols, and dietary fibers, that exhibit antioxidant, antimicrobial, and anti-inflammatory activities. These compounds can be directly applied or encapsulated within nanocarriers to improve their stability, bioavailability, and targeted ability in diverse fields, including pharmaceuticals, nutraceuticals, food packaging, and cosmeceuticals.

Despite the growing body of literature supporting the value of citrus peel-derived nanomaterials and bioactives, several challenges must be addressed to facilitate broader industrial and clinical adoption, including scalability (developing robust, reproducible, and cost-effective green synthesis methods suitable for large-scale NPs production), comprehensive characterization (standardizing protocols for evaluating physicochemical properties such as size, surface charge, stability of the synthesized nanomaterials), *in vivo* validation (conducting systematic preclinical studies to assess the biosafety, toxicity, and therapeutic efficacy of citrus peel-derived nanomaterials), expanding applications (exploring emerging uses in biosensors, catalysis, energy storage, and smart packaging), and life cycle analysis (implementing full cycling analysis models to assess the environmental and economic sustainability of citrus peel valorization approaches).

The valorization of citrus peel waste offers not only environmental benefits but also economic feasibility. Many of the reviewed studies demonstrated the use of simple, cost-effective extraction and synthesis methods, such as ethanol precipitation, hydrothermal treatments, and aqueous extraction, that eliminate the need for costly purification steps. Furthermore, by transforming low- or zero-cost waste streams into functional

nanomaterials with high value in biomedicine, packaging, and remediation, these approaches support economically viable circular bioeconomy models.

In conclusion, citrus peel waste presents a viable and underutilized biomass for sustainable material development. Continued interdisciplinary research will be essential for optimizing these processes, understanding long-term implications, and translating laboratory findings into real-world solutions that align with circular economy principles and global sustainability goals.

Conflicts of interest

The authors declare no potential competing interests.

Data availability

No primary research results, software or code have been included and no new data were generated or analysed as part of this review.

References

1 S. J. Bharathiraja, J. Suriya, M. Krishnan, P. Manivasagan and S.-K. Kim, Production of Enzymes From Agricultural Wastes and Their Potential Industrial Applications, *Adv. Food Nutr. Res.*, 2017, **80**, 125–148, DOI: **10.1016/bs.afnr.2016.11.003**.

2 UNEP, Global Waste Management Outlook 2024 the United Nations Environment Programme28 FEBRUARY 2024, available from, **https://www.unep.org/resources/global-waste-management-outlook-2024**.

3 M. Wadhwa, and M. Bakshi, *Utilization of Fruit and Vegetable Wastes as Livestock Feed and as Substrates for Generation of Other Value-Added Products*, RAP publication, 2013, vol. 4, p. 67.

4 G. M. Á. Alarcón, J. H. López Vargas and D. A. Restrepo Molina, Agro-industrial fruit co-products in Colombia, their sources and potential uses in processed food industries: a review, *Rev. Fac. Nac. Agron.*, 2015, **68**(2), 7729–7742, DOI: **10.15446/rfnam.v68n2.50993**.

5 P. D. Pathak, S. A. Mandavgane and B. D. Kulkarni, Fruit peel waste as a novel low-cost bio adsorbent, *Rev. Chem. Eng.*, 2015, **31**(4), 361–381, DOI: **10.1515/revce-2014-0041**.

6 P. D. Pathak, S. A. Mandavgane and B. D. Kulkarni, Valorization of pomegranate peels: A biorefinery approach, *Waste Biomass Valorization*, 2017, **8**, 1127–1137.

7 P. D. Pathak, S. A. Mandavgane and B. D. Kulkarni, Fruit peel waste: characterization and its potential uses, *Curr. Sci.*, 2017, **113**, 444–454DOI: **https://www.jstor.org/stable/26294001**.

8 N. Mahato, M. Sinha, K. Sharma, R. Koteswararao and M. H. Cho, Modern Extraction and Purification Techniques for Obtaining High Purity Food-Grade Bioactive Compounds and Value-Added Co-Products from Citrus Wastes, *Foods*, 2019, **8**(11), 523, DOI: **10.3390/foods8110523**.

9 R. Ravindran, S. S. Hassan, G. A. Williams and A. K. Jaiswal, A review on bioconversion of agro-industrial wastes to industrially important enzymes, *Bioengineering*, 2018, **5**(4), 93.

10 P. Sharma, V. K. Gaur, S.-H. Kim and A. Pandey, Microbial strategies for bio-transforming food waste into resources, *Bioresour. Technol.*, 2020, **299**, 122580, DOI: **10.1016/j.biortech.2019.122580**.

11 Y. Dai, Q. Sun, W. Wang, L. Lu, M. Liu, J. Li, *et al.*, Utilizations of agricultural waste as adsorbent for the removal of contaminants: A review, *Chemosphere*, 2018, **211**, 235–253, DOI: **10.1016/j.chemosphere.2018.06.179**.

12 H. El-Aal, and F. Halaweish, *Food Preservative Activity of Phenolic Compounds in Orange Peel Extracts (Citrus Sinensis L.)*, 2010.

13 S. van Ewijk and J. A. Stegemann, Recognising waste use potential to achieve a circular economy, *Waste Manage.*, 2020, **105**, 1–7, DOI: **10.1016/j.wasman.2020.01.019**.

14 B. Wang, F. Dong, M. Chen, J. Zhu, J. Tan, X. Fu, *et al.*, Advances in Recycling and Utilization of Agricultural Wastes in China: Based on Environmental Risk, Crucial Pathways, Influencing Factors, Policy Mechanism, *Procedia Environ. Sci.*, 2016, **31**, 12–17, DOI: **10.1016/j.proenv.2016.02.002**.

15 J. Bustamante, S. van Stempvoort, M. García-Gallarreta, J. A. Houghton, H. K. Briers, V. L. Budarin, *et al.*, Microwave assisted hydro-distillation of essential oils from wet citrus peel waste, *J. Cleaner Prod.*, 2016, **137**, 598–605.

16 H. Zhang, J. Cui, G. Tian, C. DiMarco-Crook, W. Gao, C. Zhao, *et al.*, Efficiency of four different dietary preparation methods in extracting functional compounds from dried tangerine peel, *Food Chem.*, 2019, **289**, 340–350, DOI: **10.1016/j.foodchem.2019.03.063**.

17 A. K. Maurya, S. Mohanty, A. Pal, C. S. Chanotiya and D. U. Bawankule, The essential oil from Citrus limetta Risso peels alleviates skin inflammation: In-vitro and in-vivo study, *J. Ethnopharmacol.*, 2018, **212**, 86–94.

18 B. Singh, J. P. Singh, A. Kaur and M. P. Yadav, Insights into the chemical composition and bioactivities of citrus peel essential oils, *Food Res. Int.*, 2021, **143**, 110231, DOI: **10.1016/j.foodres.2021.110231**.

19 M. A. Farag, B. Abib, L. Ayad and A. R. Khattab, Sweet and bitter oranges: An updated comparative review of their bioactives, nutrition, food quality, therapeutic merits and biowaste valorization practices, *Food Chem.*, 2020, **331**, 127306.

20 J. M. J. Favela-Hernández, O. González-Santiago, M. A. Ramírez-Cabrera, P. C. Esquivel-Ferriño and MdR. Camacho-Corona, Chemistry and Pharmacology of Citrus sinensis, *Molecules*, 2016, **21**(2), 247.

21 Y. Khane, K. Benouis, S. Albukhaty, G. M. Sulaiman, M. M. Abomughaid, A. Al Ali, *et al.*, Green synthesis of silver nanoparticles using aqueous Citrus limon zest extract: Characterization and evaluation of their antioxidant and antimicrobial properties, *Nanomaterials*, 2022, **12**(12), 2013.

22 H. Bora, M. Kamle, D. K. Mahato, P. Tiwari and P. Kumar, Citrus essential oils (CEOs) and their applications in food: An overview, *Plants*, 2020, **9**(3), 357.
23 S. Y. Kim and K.-S. Shin, Antimicrobial activity of trifoliate orange (Poncirus trifoliate) seed extracts on gram-negative food-borne pathogens, *Prev. Nutr. Food Sci.*, 2012, **17**(3), 228.
24 L. A. Pfaltzgraff, E. C. Cooper, V. Budarin and J. H. Clark, Food waste biomass: a resource for high-value chemicals, *Green Chem.*, 2013, **15**(2), 307–314.
25 Food and Agriculture Organization of the United Nations (FAO), *The State of Food and Agriculture 2013: Food Systems for Better Nutrition*, FAO, Rome, Italy, 2013, p. 114. Available online: **https://www.fao.org/4/i3300e/i3300e.pdf**.
26 N. Mahato, K. Sharma, M. Sinha, E. R. Baral, R. Koteswararao, A. Dhyani, *et al.*, Bio-sorbents, industrially important chemicals and novel materials from citrus processing waste as a sustainable and renewable bioresource: A review, *J. Adv. Res.*, 2020, **23**, 61–82.
27 I. S. Choi, Y. G. Lee, S. K. Khanal, B. J. Park and H.-J. Bae, A low-energy, cost-effective approach to fruit and citrus peel waste processing for bioethanol production, *Appl. Energy*, 2015, **140**, 65–74, DOI: **10.1016/j.apenergy.2014.11.070**.
28 A. Dugrand-Judek, A. Olry, A. Hehn, G. Costantino, P. Ollitrault, Y. Froelicher, *et al.*, The Distribution of Coumarins and Furanocoumarins in Citrus Species Closely Matches Citrus Phylogeny and Reflects the Organization of Biosynthetic Pathways, *PLoS One*, 2015, **10**(11), e0142757, DOI: **10.1371/journal.pone.0142757**.
29 E. González-Molina, R. Domínguez-Perles, D. Moreno and C. García-Viguera, Natural bioactive compounds of Citrus limon for food and health, *J. Pharm. Biomed. Anal.*, 2010, **51**(2), 327–345.
30 M. Talon, and F. G. Gmitter, *Citrus Genomics. International Journal of Plant Genomics*, 2008, p. 2008.
31 H. R. de Moraes Barros, T. A. P. de Castro Ferreira and M. I. Genovese, Antioxidant capacity and mineral content of pulp and peel from commercial cultivars of citrus from Brazil, *Food Chem.*, 2012, **134**(4), 1892–1898, DOI: **10.1016/j.foodchem.2012.03.090**.
32 Y.-S. Huang and S.-C. Ho, Polymethoxy flavones are responsible for the anti-inflammatory activity of citrus fruit peel, *Food Chem.*, 2010, **119**(3), 868–873, DOI: **10.1016/j.foodchem.2009.09.092**.
33 E. Julaeha, W. R. Puspita, N. Permadi, A. Harja, S. Nurjanah, T. Wahyudi, *et al.*, Optimization of Citrus aurantifolia peel extract encapsulation in alginate-gelatin hydrogel microbeads for antibacterial wound dressing applications, *Carbohydr. Polym. Technol. Appl.*, 2024, **7**, 100406, DOI: **10.1016/j.carpta.2023.100406**.
34 E. O. Choi, H. Lee, H. HwangBo, D. H. Kwon, M. Y. Kim, S. Y. Ji, *et al.*, Citrus unshiu peel suppress the metastatic potential of murine melanoma B16F10 cells in vitro and in vivo, *Phytother. Res.*, 2019, **33**(12), 3228–3241.
35 I. Hussain, N. Singh, A. Singh, H. Singh and S. Singh, Green synthesis of nanoparticles and its potential application, *Biotechnol. Lett.*, 2016, **38**, 545–560.
36 G. Benelli, *Green Synthesis of Nanomaterials*, MDPI, 2019, p. 1275.
37 A. Gour and N. K. Jain, Advances in green synthesis of nanoparticles, *Artif. Cells, Nanomed., Biotechnol.*, 2019, **47**(1), 844–851.
38 S. S. Salem and A. Fouda, Green synthesis of metallic nanoparticles and their prospective biotechnological applications: an overview, *Biol. Trace Elem. Res.*, 2021, **199**(1), 344–370.
39 N. Tavker, V. K. Yadav, K. K. Yadav, M. M. Cabral-Pinto, J. Alam, A. K. Shukla, *et al.*, Removal of Cadmium and Chromium by Mixture of Silver Nanoparticles and Nano-Fibrillated Cellulose Isolated from Waste Peels of Citrus Sinensis, *Polymers*, 2021, **13**(2), 234, DOI: **10.3390/polym13020234**.
40 B. A. Eldeeb, W. M. A. El-Raheem and S. Elbeltagi, Green synthesis of biocompatible Fe3O4 magnetic nanoparticles using Citrus Sinensis peels extract for their biological activities and magnetic-hyperthermia applications, *Sci. Rep.*, 2023, **13**(1), 19000.
41 N. Liu, X. Li, P. Zhao, X. Zhang, O. Qiao, L. Huang, *et al.*, A review of chemical constituents and health-promoting effects of citrus peels, *Food Chem.*, 2021, **365**, 130585, DOI: **10.1016/j.foodchem.2021.130585**.
42 N. M'hiri, I. Ioannou, M. Ghoul and N. Mihoubi Boudhrioua, Phytochemical characteristics of citrus peel and effect of conventional and nonconventional processing on phenolic compounds: A review, *Food Rev. Int.*, 2017, **33**(6), 587–619.
43 H.-S. Hou, E. M. Bonku, R. Zhai, R. Zeng, Y.-L. Hou, Z.-H. Yang, *et al.*, Extraction of essential oil from Citrus reticulate Blanco peel and its antibacterial activity against Cutibacterium acnes (formerly Propionibacterium acnes), *Heliyon*, 2019, **5**(12), e02947.
44 M. H. Alu'datt, T. Rababah, M. N. Alhamad, M. A. Al-Mahasneh, A. Almajwal, S. Gammoh, *et al.*, A review of phenolic compounds in oil-bearing plants: Distribution, identification and occurrence of phenolic compounds, *Food Chem.*, 2017, **218**, 99–106, DOI: **10.1016/j.foodchem.2016.09.057**.
45 X. Cong-Cong, W. Bing, P. Yi-Qiong, T. Jian-Sheng and T. Zhang, Advances in extraction and analysis of phenolic compounds from plant materials, *Chin. J. Nat. Med.*, 2017, **15**(10), 721–731, DOI: **10.1016/s1875-5364(17)30103-6**.
46 S. Kaur, P. S. Panesar, H. K. Chopra and N. Dilbaghi, Encapsulation of citrus polyphenols in multi-phase nano-emulsion: Preservative potential, bio-accessibility and cytotoxicity studies, *Food Biosci.*, 2024, **59**, 103911.
47 X. Zhang, J. Gao, T. Wei, D. Wu, J. Shen, Y. Wei, *et al.*, Polymer brush grafted immobilized metal ion affinity adsorbent based on polydopamine/polyethyleneimine-coated magnetic graphene oxide for selective enrichment of cytokinins in plants, *Microchim. Acta*, 2023, **190**(5), 191, DOI: **10.1007/s00604-023-05776-1**.

48 B. Nayak, F. Dahmoune, K. Moussi, H. Remini, S. Dairi, O. Aoun, *et al.*, Comparison of microwave, ultrasound and accelerated-assisted solvent extraction for recovery of polyphenols from Citrus sinensis peels, *Food Chem.*, 2015, **187**, 507–516, DOI: 10.1016/j.foodchem.2015.04.081.

49 W. Li, Z. Wang, Y.-p Wang, C. Jiang, Q. Liu, Y.-s Sun, *et al.*, Pressurised liquid extraction combining LC–DAD–ESI/MS analysis as an alternative method to extract three major flavones in Citrus reticulata 'Chachi'(Guangchenpi), *Food Chem.*, 2012, **130**(4), 1044–1049.

50 D.-S. Kim and S.-B. Lim, Kinetic study of subcritical water extraction of flavonoids from citrus unshiu peel, *Sep. Purif. Technol.*, 2020, **250**, 117259, DOI: 10.1016/j.seppur.2020.117259.

51 M. Kumar, A. Dahuja, S. Tiwari, S. Punia, Y. Tak, R. Amarowicz, *et al.*, Recent trends in extraction of plant bioactives using green technologies: A review, *Food Chem.*, 2021, **353**, 129431.

52 A. S. Ravipati, L. Zhang, S. R. Koyyalamudi, S. C. Jeong, N. Reddy, J. Bartlett, *et al.*, Antioxidant and anti-inflammatory activities of selected Chinese medicinal plants and their relation with antioxidant content, *BMC Complementary Altern. Med.*, 2012, **12**, 1–14.

53 B. Li, B. Smith and M. M. Hossain, Extraction of phenolics from citrus peels: II. Enzyme-assisted extraction method, *Sep. Purif. Technol.*, 2006, **48**(2), 189–196.

54 K. A. Sir Elkhatim, R. A. Elagib and A. B. Hassan, Content of phenolic compounds and vitamin C and antioxidant activity in wasted parts of Sudanese citrus fruits, *Food Sci. Nutr.*, 2018, **6**(5), 1214–1219.

55 S. M. Mandal, D. Chakraborty and S. Dey, Phenolic acids act as signaling molecules in plant-microbe symbioses, *Plant Signaling Behav.*, 2010, **5**(4), 359–368.

56 K. M. De Araújo, A. De Lima, JdN. Silva, L. L. Rodrigues, A. G. Amorim, P. V. Quelemes, *et al.*, Identification of phenolic compounds and evaluation of antioxidant and antimicrobial properties of Euphorbia tirucalli L, *Antioxidants*, 2014, **3**(1), 159–175.

57 H. Peleg, M. Naim, R. L. Rouseff and U. Zehavi, Distribution of bound and free phenolic acids in oranges (Citrus sinensis) and Grapefruits (Citrus paradisi), *J. Sci. Food Agric.*, 1991, **57**(3), 417–426, DOI: 10.1002/jsfa.2740570312.

58 N. Kumar and N. Goel, Phenolic acids: Natural versatile molecules with promising therapeutic applications, *Biotechnol. Rep.*, 2019, **24**, e00370, DOI: 10.1016/j.btre.2019.e00370.

59 A. Fejzić and S. Ćavar, Phenolic compounds and antioxidant activity of some citruses, *Bull. Chem. Technol. Bosnia Herzegovina*, 2014, **42**, 1–4.

60 H. Munir, S. Yaqoob, K. A. Awan, A. Imtiaz, H. Naveed, N. Ahmad, *et al.*, Unveiling the Chemistry of Citrus Peel: Insights into Nutraceutical Potential and Therapeutic Applications, *Foods*, 2024, **13**(11), 1681.

61 P. C. H. Hollman and M. B. Katan, Dietary flavonoids: intake, health effects and bioavailability, *Food Chem. Toxicol.*, 1999, **37**(9–10), 937–942.

62 C.-S. Lai, S. Li, C.-Y. Chai, C.-Y. Lo, C.-T. Ho, Y.-J. Wang, *et al.*, Inhibitory effect of citrus 5-hydroxy-3,6,7,8,3′,4′-hexamethoxyflavone on 12-O-tetradecanoylphorbol 13-acetate-induced skin inflammation and tumor promotion in mice, *Carcinogenesis*, 2007, **28**(12), 2581–2588.

63 Y.-Q. Ma, X.-Q. Ye, Z.-X. Fang, J.-C. Chen, G.-H. Xu and D.-H. Liu, Phenolic Compounds and Antioxidant Activity of Extracts from Ultrasonic Treatment of Satsuma Mandarin (Citrus unshiu Marc.) Peels, *J. Agric. Food Chem.*, 2008, **56**(14), 5682–5690, DOI: 10.1021/jf072474o.

64 M. Bartnik, and P. Facey, *Glycosides. Pharmacognosy*, Elsevier, 2024, pp. 103–165.

65 M. K. Khan, M. Abert-Vian, A.-S. Fabiano-Tixier, O. Dangles and F. Chemat, Ultrasound-assisted extraction of polyphenols (flavanone glycosides) from orange (Citrus sinensis L.) peel, *Food Chem.*, 2010, **119**(2), 851–858, DOI: 10.1016/j.foodchem.2009.08.046.

66 K.-i Minato, Y. Miyake, S. Fukumoto, K. Yamamoto, Y. Kato, Y. Shimomura, *et al.*, Lemon flavonoid, eriocitrin, suppresses exercise-induced oxidative damage in rat liver, *Life Sci.*, 2003, **72**(14), 1609–1616.

67 J. A. Manthey and K. Grohmann, Phenols in citrus peel byproducts. Concentrations of hydroxycinnamates and polymethoxylated flavones in citrus peel molasses, *J. Agric. Food Chem.*, 2001, **49**(7), 3268–3273.

68 L. Wang, J. Wang, L. Fang, Z. Zheng, D. Zhi, S. Wang, *et al.*, Anticancer activities of citrus peel polymethoxyflavones related to angiogenesis and others, *BioMed Res. Int.*, 2014, **2014**, 453972.

69 M. N. Sarian, Q. U. Ahmed, S. Z. Mat So'ad, A. M. Alhassan, S. Murugesu, V. Perumal, *et al.*, Antioxidant and antidiabetic effects of flavonoids: A structure-activity relationship based study, *BioMed Res. Int.*, 2017, **2017**, 8386065.

70 Y. Jia, Y. Ma, G. Cheng, Y. Zhang and S. Cai, Comparative study of dietary flavonoids with different structures as α-glucosidase inhibitors and insulin sensitizers, *J. Agric. Food Chem.*, 2019, **67**(37), 10521–10533.

71 M. G. Shehata, T. S. Awad, D. Asker, S. A. El Sohaimy, N. M. Abd El-Aziz and M. M. Youssef, Antioxidant and antimicrobial activities and UPLC-ESI-MS/MS polyphenolic profile of sweet orange peel extracts, *Curr. Res. Food Sci.*, 2021, **4**, 326–335.

72 G. Flamini, M. Tebano and P. L. Cioni, Volatiles emission patterns of different plant organs and pollen of Citrus limon, *Anal. Chim. Acta*, 2007, **589**(1), 120–124.

73 C. M. Ambrosio, N. Y. Ikeda, A. C. Miano, E. Saldaña, A. M. Moreno, E. Stashenko, *et al.*, Unraveling the selective antibacterial activity and chemical composition of citrus essential oils, *Sci. Rep.*, 2019, **9**(1), 17719, DOI: 10.1038/s41598-019-54084-3.

74 P. Weimer, J. G. L. Moura, V. Mossmann, M. L. Immig, J. de Castilhos and R. C. Rossi, Citrus aurantiifolia (Christm) Swingle: Biological potential and safety profile of essential oils from leaves and fruit peels, *Food Biosci.*, 2021, **40**, 100905.

75 L. Espina, M. Somolinos, S. Lorán, P. Conchello, D. García and R. Pagán, Chemical composition of commercial citrus fruit essential oils and evaluation of their antimicrobial activity acting alone or in combined processes, *Food Control*, 2011, **22**(6), 896–902, DOI: 10.1016/j.foodcont.2010.11.021.

76 N. Mahato, K. Sharma, R. Koteswararao, M. Sinha, E. Baral and M. H. Cho, Citrus essential oils: Extraction, authentication and application in food preservation, *Crit. Rev. Food Sci. Nutr.*, 2019, **59**(4), 611–625.

77 M. A. Castro, M. A. Llanos, B. E. Rodenak-Kladniew, L. Gavernet, M. E. Galle and R. Crespo, Citrus reticulata peel oil as an antiatherogenic agent: Hypolipogenic effect in hepatic cells, lipid storage decrease in foam cells, and prevention of LDL oxidation, *Nutr., Metab. Cardiovasc. Dis.*, 2020, **30**(9), 1590–1599.

78 E. Marchese, N. D'onofrio, M. L. Balestrieri, D. Castaldo, G. Ferrari and F. Donsì, Bergamot essential oil nanoemulsions: antimicrobial and cytotoxic activity, *Z. Naturforsch. C Biosci.*, 2020, **75**(7–8), 279–290.

79 I. Leherbauer and I. Stappen, Selected essential oils and their mechanisms for therapeutic use against public health disorders. An overview, *Z. Naturforsch. C Biosci.*, 2020, **75**(7–8), 205–223, DOI: 10.1515/znc-2020-0007.

80 L. R. Lizarraga-Valderrama, Effects of essential oils on central nervous system: Focus on mental health, *Phytother. Res.*, 2021, **35**(2), 657–679.

81 K. N. C. Murthy, G. K. Jayaprakasha and B. S. Patil, D-limonene rich volatile oil from blood oranges inhibits angiogenesis, metastasis and cell death in human colon cancer cells, *Life Sci.*, 2012, **91**(11–12), 429–439, DOI: 10.1016/j.lfs.2012.08.016.

82 M. Navarra, C. Mannucci, M. Delbò and G. Calapai, Citrus bergamia essential oil: from basic research to clinical application, *Front. Pharmacol.*, 2015, **6**, 36.

83 I. Oprea, A. C. Fărcaș, L. F. Leopold, Z. Diaconeasa, C. Coman and S. A. Socaci, Nano-Encapsulation of Citrus Essential Oils: Methods and Applications of Interest for the Food Sector, *Polymers*, 2022, **14**(21), 4505, DOI: 10.3390/polym14214505.

84 K. Z. Heydari, K. G. Jahromi, G. Kavoosi and S. Babaei, Citrus peel waste essential oil: Chemical composition along with anti-amylase and anti-glucosidase potential, *Int. J. Food Sci. Technol.*, 2022, **57**(10), 6795–6804.

85 S. Ghasemi, E. Assadpour, M. S. Kharazmi, S. Jafarzadeh, M. Zargar and S. M. Jafari, Encapsulation of orange peel oil in biopolymeric nanocomposites to control its release under different conditions, *Foods*, 2023, **12**(4), 831.

86 H. A. Ahmed, A. A. Nassrallah, M. Abdel-Raheem and H. H. Elbehery, Lemon peel essential oil and its nano-formulation to control Agrotis ipsilon (Lepidoptera: Noctuidae), *Sci. Rep.*, 2023, **13**(1), 17922, DOI: 10.1038/s41598-023-44670-x.

87 B. D. da Silva, P. C. Bernardes, P. F. Pinheiro, E. Fantuzzi and C. D. Roberto, Chemical composition, extraction sources and action mechanisms of essential oils: Natural preservative and limitations of use in meat products, *Meat Sci.*, 2021, **176**, 108463, DOI: 10.1016/j.meatsci.2021.108463.

88 C. Chen, Y. Zeng, J. Xu, H. Zheng, J. Liu, R. Fan, *et al.*, Therapeutic effects of soluble dietary fiber consumption on type 2 diabetes mellitus, *Exp. Ther. Med.*, 2016, **12**(2), 1232–1242.

89 S. K. Gill, M. Rossi, B. Bajka and K. Whelan, Dietary fibre in gastrointestinal health and disease, *Nat. Rev. Gastroenterol. Hepatol.*, 2021, **18**(2), 101–116.

90 S. Fuller, L. C. Tapsell and E. J. Beck, Creation of a fibre categories database to quantify different dietary fibres, *J. Food Compos. Anal.*, 2018, **71**, 36–43.

91 F.-J. Dai and C.-F. Chau, Classification and regulatory perspectives of dietary fiber, *J. Food Drug Anal.*, 2017, **25**(1), 37–42.

92 J. R. Whitaker, Pectic substances, pectic enzymes and haze formation in fruit juices, *Enzyme Microb. Technol.*, 1984, **6**(8), 341–349, DOI: 10.1016/0141-0229(84)90046-2.

93 W. G. Willats, J. P. Knox and J. D. Mikkelsen, Pectin: new insights into an old polymer are starting to gel, *Trends Food Sci. Technol.*, 2006, **17**(3), 97–104, DOI: 10.1016/j.tifs.2005.10.008.

94 L.-F. Wen, K. Chang, G. Brown and D. Gallaher, Isolation and characterization of hemicellulose and cellulose from sugar beet pulp, *J. Food Sci.*, 1988, **53**(3), 826–829, DOI: 10.1111/j.1365-2621.1988.tb08963.x.

95 M. Fu, X. Gao, Z. Xie, C. Xia, Q. Gu and P. Li, Soluble Dietary Fiber from Citrus unshiu Peel Promotes Antioxidant Activity in Oxidative Stress Mice and Regulates Intestinal Microecology, *Foods*, 2024, **13**(10), 1539.

96 Q. Gu, X. Gao, Q. Zhou, Y. Li, G. Li and P. Li, Characterization of soluble dietary fiber from citrus peels (Citrus unshiu), and its antioxidant capacity and beneficial regulating effect on gut microbiota, *Int. J. Biol. Macromol.*, 2023, **246**, 125715, DOI: 10.1016/j.ijbiomac.2023.125715.

97 K. Ishisono, T. Mano, T. Yabe and K. Kitaguchi, Dietary fiber pectin ameliorates experimental colitis in a neutral sugar side chain-dependent manner, *Front. Immunol.*, 2019, **10**, 2979.

98 A. Pattarapisitporn, S. Noma, W. Klangpetch, M. Demura and N. Hayashi, Extraction of citrus pectin using pressurized carbon dioxide and production of its oligosaccharides, *Food Biosci.*, 2024, **57**, 103584, DOI: 10.1016/j.fbio.2024.103584.

99 R. Ciriminna, L. Albanese, F. Meneguzzo and M. Pagliaro, IntegroPectin: A New Citrus Pectin with Uniquely High Biological Activity, *Biol. Life Sci. Forum*, 2021, **6**(1), 76, DOI: 10.3390/Foods2021-11199.

100 V. Butera, R. Ciriminna, C. Valenza, G. L. Petri, G. Angellotti, G. Barone, *et al.*, Citrus IntegroPectin: a computational insight, *Discover Molecules*, 2025, **2**(1), 6, DOI: 10.1007/s44345-025-00013-z.

101 D. Nuzzo, M. Scordino, A. Scurria, C. Giardina, F. Giordano, F. Meneguzzo, *et al.*, Protective, Antioxidant and Antiproliferative Activity of Grapefruit IntegroPectin on

SH-SY5Y Cells, *Int. J. Mol. Sci.*, 2021, **22**(17), 9368, DOI: 10.3390/ijms22179368.

102 P. O. Njoku, J. N. Edokpayi and J. O. Odiyo, Health and environmental risks of residents living close to a landfill: A case study of Thohoyandou Landfill, Limpopo Province, South Africa, *Int. J. Environ. Res. Public Health*, 2019, **16**(12), 2125.

103 R. Sharma, M. Sharma, R. Sharma and V. Sharma, The impact of incinerators on human health and environment, *Rev. Environ. Health*, 2013, **28**(1), 67–72.

104 H. Valdés Morales, A. D. Savariraj, M. Selvaraj, M. Kandasamy, R. Mangalaraja, N. Pugazhenthiran, *et al.*, Biocidal activity of citrus limetta peel extract mediated green synthesized silver quantum dots against MCF-7 cancer cells and pathogenic bacteria, *J. Environ. Chem. Eng.*, 2021, **9**(2), 105089, DOI: 10.1016/j.jece.2021.105089.

105 A. R. Malik, M. H. Aziz, M. Atif, M. S. Irshad, H. Ullah, T. N. Gia, *et al.*, Lime peel extract induced NiFe2O4 NPs: Synthesis to applications and oxidative stress mechanism for anticancer, antibiotic activity, *J. Saudi Chem. Soc.*, 2022, **26**(2), 101422, DOI: 10.1016/j.jscs.2022.101422.

106 K. Pagar, K. Chavan, S. Kasav, P. Basnet, A. Rahdar, N. Kataria, *et al.*, Bio-inspired synthesis of CdO nanoparticles using Citrus limetta peel extract and their diverse biomedical applications, *J. Drug Delivery Sci. Technol.*, 2023, **82**, 104373, DOI: 10.1016/j.jddst.2023.104373.

107 A. Tyagi, K. M. Tripathi, N. Singh, S. Choudhary and R. K. Gupta, Green synthesis of carbon quantum dots from lemon peel waste: applications in sensing and photocatalysis, *RSC Adv.*, 2016, **6**(76), 72423–72432, DOI: 10.1039/C6RA10488F.

108 M. F. W. Baig, S. F. Hasany and M. F. Shirazi, Green Synthesis of Nano Graphite Materials from Lemon and Orange Peel: A Sustainable Approach for Carbon-Based Materials, *Eng. Proc.*, 2023, **46**(1), 42, DOI: 10.3390/engproc2023046042.

109 B. T. Hoan, P. D. Tam and V.-H. Pham, Green Synthesis of Highly Luminescent Carbon Quantum Dots from Lemon Juice, *J. Nanotechnol.*, 2019, **2019**(1), 2852816, DOI: 10.1155/2019/2852816.

110 S. Hiasa, S. Iwamoto, T. Endo and Y. Edashige, Isolation of cellulose nanofibrils from mandarin (Citrus unshiu) peel waste, *Ind. Crops Prod.*, 2014, **62**, 280–285, DOI: 10.1016/j.indcrop.2014.08.007.

111 A. Hideno, K. Abe, H. Yano and H. Uchimura, Characterization of Nanofibers from Japanese Orange Inner Peels Prepared Using Pectinase and Diluted Alkali, *J. Jpn. Inst. Energy*, 2019, **98**(5), 85–89, DOI: 10.3775/jie.98.85.

112 J. Deng, Y. You, V. Sahajwalla and R. K. Joshi, Transforming waste into carbon-based nanomaterials, *Carbon*, 2016, **96**, 105–115, DOI: 10.1016/j.carbon.2015.09.033.

113 P. Rani, R. Dahiya, M. Bulla, R. Devi, K. Jeet, A. Jatrana, *et al.*, Hydrothermal-assisted green synthesis of reduced graphene oxide nanosheets (rGO) using lemon (Citrus Limon) peel extract, *Mater. Today: Proc.*, 2023, DOI: 10.1016/j.matpr.2023.04.419.

114 V. Priliana, C. Sucitro, R. Wijaya, V. B. Lunardi, S. P. Santoso, M. Yuliana, *et al.*, Reduction of Graphene Oxide Using Citrus hystrix Peels Extract for Methylene Blue Adsorption, *Sustainability*, 2022, **14**(19), 12172, DOI: 10.3390/su141912172.

115 S. Šafranko, A. Stanković, S. Hajra, H.-J. Kim, I. Strelec, M. Dutour-Sikirić, *et al.*, Preparation of multifunctional N-doped carbon quantum dots from citrus clementina peel: investigating targeted pharmacological activities and the potential application for Fe3+ sensing, *Pharmaceuticals*, 2021, **14**(9), 857.

116 A. Aouadi, D. H. Saoud, A. Bouafia, H. A. Mohammed, H. G. Gamal, A. Achouri, *et al.*, Unveiling the antioxidant power: synthesis and characterization of lemon and orange peel-derived carbon quantum dots with exceptional free radical scavenging activity, *Biomass Convers. Biorefin.*, 2024, 1–14.

117 L. Gao, S. Mei, H. Ma and X. Chen, Ultrasound-assisted green synthesis of gold nanoparticles using citrus peel extract and their enhanced anti-inflammatory activity, *Ultrason. Sonochem.*, 2022, **83**, 105940, DOI: 10.1016/j.ultsonch.2022.105940.

118 M. M. Alkhulaifi, J. H. Alshehri, M. A. Alwehaibi, M. A. Awad, N. M. Al-Enazi, N. S. Aldosari, *et al.*, Green synthesis of silver nanoparticles using Citrus limon peels and evaluation of their antibacterial and cytotoxic properties, *Saudi J. Biol. Sci.*, 2020, **27**(12), 3434–3441, DOI: 10.1016/j.sjbs.2020.09.031.

119 T. T. Y. Nhi, D. T. Thien, T. D. Cong, N. T. Tung, L. T. Thuy, N. T. Thuc, *et al.*, Green synthesis of pectin-silver nanocomposite: Parameter optimization and physico-chemical characterization, *Vietnam J. Chem.*, 2022, **60**, 66–71.

120 P. Rauwel, S. Küünal, S. Ferdov and E. Rauwel, A review on the green synthesis of silver nanoparticles and their morphologies studied via TEM, *Adv. Mater. Sci. Eng.*, 2015, **2015**, 682749.

121 R. Supreetha, S. Bindya, P. Deepika, H. Vinusha and B. Hema, Characterization and biological activities of synthesized citrus pectin-MgO nanocomposite, *Results Chem.*, 2021, **3**, 100156.

122 T. U. D. Thi, T. T. Nguyen, Y. D. Thi, K. H. T. Thi, B. T. Phan and K. N. Pham, Green synthesis of ZnO nanoparticles using orange fruit peel extract for antibacterial activities, *RSC Adv.*, 2020, **10**(40), 23899–23907, DOI: 10.1039/D0RA04926C.

123 S. Baglari, R. R. Wary, P. Kalita and M. B. Baruah, Green synthesis of CuO nanoparticles using citrus maxima peel aqueous extract, *Mater. Today: Proc.*, 2023, **103**, 141–146, DOI: 10.1016/j.matpr.2023.08.223.

124 B. Matsedisho, B. Otieno, J. Kabuba, T. Leswifi and A. Ochieng, Removal of Ni (II) from aqueous solution using chemically modified cellulose nanofibers derived from orange peels, *Int. J. Environ. Sci. Technol.*, 2024, 1–12.

125 B. Yu, X. Zeng, L. Wang and J. M. Regenstein, Preparation of nanofibrillated cellulose from grapefruit peel and its application as fat substitute in ice cream, *Carbohydr. Polym.*, 2021, **254**, 117415, DOI: 10.1016/j.carbpol.2020.117415.

126 A. Kundu, S. Basu and B. Maity, Upcycling Waste: Citrus limon Peel-Derived Carbon Quantum Dots for Sensitive Detection of Tetracycline in the Nanomolar Range, *ACS Omega*, 2023, **8**(39), 36449–36459, DOI: 10.1021/acsomega.3c05424.

127 O. Adedokun, A. Roy, A. O. Awodugba and P. S. Devi, Fluorescent carbon nanoparticles from Citrus sinensis as efficient sorbents for pollutant dyes, *Luminescence*, 2017, **32**(1), 62–70.

128 S. Alancherry, K. Bazaka, I. Levchenko, A. Al-Jumaili, B. Kandel, A. Alex, *et al.*, Fabrication of nano-onion-structured graphene films from citrus sinensis extract and their wetting and sensing characteristics, *ACS Appl. Mater. Interfaces*, 2020, **12**(26), 29594–29604.

129 C. Karaman, Orange peel derived-nitrogen and sulfur Co-doped carbon dots: a nano-booster for enhancing ORR electrocatalytic performance of 3D graphene networks, *Electroanalysis*, 2021, **33**(5), 1356–1369.

130 N. R. Kim, Y. S. Yun, M. Y. Song, S. J. Hong, M. Kang, C. Leal, *et al.*, Citrus-Peel-Derived, Nanoporous Carbon Nanosheets Containing Redox-Active Heteroatoms for Sodium-Ion Storage, *ACS Appl. Mater. Interfaces*, 2016, **8**(5), 3175–3181, DOI: 10.1021/acsami.5b10657.

131 D. Iannazzo, C. Celesti, C. Espro, A. Ferlazzo, S. V. Giofrè, M. Scuderi, *et al.*, Orange-peel-derived nanobiochar for targeted cancer therapy, *Pharmaceutics*, 2022, **14**(10), 2249.

132 K.-l Hong, L. Qie, R. Zeng, Z.-q Yi, W. Zhang, D. Wang, *et al.*, Biomass derived hard carbon used as a high performance anode material for sodium ion batteries, *J. Mater. Chem. A*, 2014, **2**(32), 12733–12738, DOI: 10.1039/C4TA02068E.

133 W. P. Wicaksono, G. T. Kadja, D. Amalia, L. Uyun, W. P. Rini, A. Hidayat, *et al.*, A green synthesis of gold–palladium core–shell nanoparticles using orange peel extract through two-step reduction method and its formaldehyde colorimetric sensing performance, *Nano-Struct. Nano-Objects*, 2020, **24**, 100535.

134 J. A. Sierra, C. R. Vanoni, M. A. Tumelero, C. C. P. Cid, R. Faccio, D. F. Franceschini, *et al.*, Biogenic approaches using citrus extracts for the synthesis of metal nanoparticles: the role of flavonoids in gold reduction and stabilization, *New J. Chem.*, 2016, **40**(2), 1420–1429.

135 T. Dang-Bao, T. G.-T. Ho, B. L. Do, N. Phung Anh, T. D. T. Phan, T. B. Y. Tran, *et al.*, Green Orange Peel-Mediated Bioinspired Synthesis of Nanoselenium and Its Antibacterial Activity against Methicillin-Resistant Staphylococcus aureus, *ACS Omega*, 2022, **7**(40), 36037–36046, DOI: 10.1021/acsomega.2c05469.

136 S. Jaast and A. Grewal, Green synthesis of silver nanoparticles, characterization and evaluation of their photocatalytic dye degradation activity, *Curr. Res. Green Sustainable Chem.*, 2021, **4**, 100195, DOI: 10.1016/j.crgsc.2021.100195.

137 C. G. Yuan, C. Huo, B. Gui and W. P. Cao, Green synthesis of gold nanoparticles using Citrus maxima peel extract and their catalytic/antibacterial activities, *IET Nanobiotechnol.*, 2017, **11**(5), 523–530.

138 E. Ituen, E. Ekemini, L. Yuanhua and A. Singh, Green synthesis of Citrus reticulata peels extract silver nanoparticles and characterization of structural, biocide and anticorrosion properties, *J. Mol. Struct.*, 2020, **1207**, 127819, DOI: 10.1016/j.molstruc.2020.127819.

139 S. N. Shareef, K. S. Bhavani, T. Anusha, P. Priyanka and M. S. Rao, Eco-friendly green synthesis of Ag@ Cu bimetallic nanoparticles: Evaluation of their structural, morphological and electrochemical characterizations, *Vietnam J. Chem.*, 2023, **61**(2), 220–226.

140 A. S. Abdelsattar, A. G. Kamel and A. El-Shibiny, The green production of eco-friendly silver with cobalt ferrite nanocomposite using Citrus limon extract, *Results Chem.*, 2023, **5**, 100687.

141 C. Huo, M. Khoshnamvand, P. Liu, C.-G. Yuan and W. Cao, Eco-friendly approach for biosynthesis of silver nanoparticles using Citrus maxima peel extract and their characterization, catalytic, antioxidant and antimicrobial characteristics, *Mater. Res. Express*, 2018, **6**(1), 015010.

142 R. Srivastava, S. Bhardwaj, A. Kumar, R. Singhal, J. Scanley, C. C. Broadbridge, *et al.*, Waste Citrus reticulata assisted preparation of cobalt oxide nanoparticles for supercapacitors, *Nanomaterials*, 2022, **12**(23), 4119.

143 P. Tshireletso, C. N. Ateba and O. E. Fayemi, Spectroscopic and antibacterial properties of CuONPs from orange, lemon and tangerine peel extracts: Potential for combating bacterial resistance, *Molecules*, 2021, **26**(3), 586.

144 A. Hashem, H. Abuzeid, M. Kaus, S. Indris, H. Ehrenberg, A. Mauger, *et al.*, Green synthesis of nanosized manganese dioxide as positive electrode for lithium-ion batteries using lemon juice and citrus peel, *Electrochim. Acta*, 2018, **262**, 74–81.

145 M. M. Abomughaid, Bio-Fabrication of Bio-Inspired Silica Nanomaterials from Orange Peels in Combating Oxidative Stress, *Nanomaterials*, 2022, **12**(18), 3236, DOI: 10.3390/nano12183236.

146 S. Vijayakumar, V. Punitha and N. Parameswari, Phytonanosynthesis of MgO nanoparticles: green synthesis, characterization and antimicrobial evaluation, *Arabian J. Sci. Eng.*, 2022, **47**(6), 6729–6734.

147 O. Ouerghi, M. H. Geesi, Y. Riadi and E. O. Ibnouf, Limon-citrus extract as a capping/reducing agent for the synthesis of titanium dioxide nanoparticles: Characterization and antibacterial activity, *Green Chem. Lett. Rev.*, 2022, **15**(3), 483–490.

148 D. Eissa, R. H. Hegab, A. Abou-Shady and Y. H. Kotp, Green synthesis of ZnO, MgO and SiO2 nanoparticles and its effect on irrigation water, soil properties, and Origanum majorana productivity, *Sci. Rep.*, 2022, **12**(1), 5780.

149 F. Bigi, E. Maurizzi, H. Haghighi, H. W. Siesler, F. Licciardello and A. Pulvirenti, Waste orange peels as a source of cellulose nanocrystals and their use for the

development of nanocomposite films, *Foods*, 2023, **12**(5), 960.

150 M. Mariño, L. Lopes da Silva, N. Durán and L. Tasic, Enhanced materials from nature: nanocellulose from citrus waste, *Molecules*, 2015, **20**(4), 5908–5923.

151 E. M. Jacob, A. Borah, A. Jindal, S. C. Pillai, Y. Yamamoto, T. Maekawa, *et al.*, Synthesis and characterization of citrus-derived pectin nanoparticles based on their degree of esterification, *J. Mater. Res.*, 2020, **35**(12), 1514–1522.

152 I. Liakos, L. Rizzello, H. Hajiali, V. Brunetti, R. Carzino, P. Pompa, *et al.*, Fibrous wound dressings encapsulating essential oils as natural antimicrobial agents, *J. Mater. Chem. B*, 2015, **3**(8), 1583–1589.

153 D. Stanisic, L. H. Liu, R. V. Dos Santos, A. F. Costa, N. Durán and L. Tasic, New sustainable process for hesperidin isolation and anti-ageing effects of hesperidin nanocrystals, *Molecules*, 2020, **25**(19), 4534.

154 H. Joshi, A. R. Hegde, P. K. Shetty, H. Gollavilli, R. S. Managuli, G. Kalthur, *et al.*, Sunscreen creams containing naringenin nanoparticles: Formulation development and in vitro and in vivo evaluations, *Photodermatol., Photoimmunol. Photomed.*, 2018, **34**(1), 69–81.

155 S. Onoue, A. Uchida, H. Takahashi, Y. Seto, Y. Kawabata, K. Ogawa, *et al.*, Development of High-Energy Amorphous Solid Dispersion of Nanosized Nobiletin, a Citrus Polymethoxylated Flavone, with Improved Oral Bioavailability, *J. Pharm. Sci.*, 2011, **100**(9), 3793–3801, DOI: **10.1002/jps.22585**.

156 F. M. Ibrahim, R. S. Mohammed, E. Abdelsalam, W. E.-S. Ashour, D. Magalhães, M. Pintado, *et al.*, Egyptian Citrus Essential Oils Recovered from Lemon, Orange, and Mandarin Peels: Phytochemical and Biological Value, *Horticulturae*, 2024, **10**(2), 180, DOI: **10.3390/horticulturae10020180**.

157 D. Yun, Z. Wang, C. Li, D. Chen and J. Liu, Antioxidant and antimicrobial packaging films developed based on the peel powder of different citrus fruits: A comparative study, *Food Biosci.*, 2023, **51**, 102319, DOI: **10.1016/j.fbio.2022.102319**.

158 S. Dev, A. Khamkhash, T. Ghosh and S. Aggarwal, Adsorptive removal of Se (IV) by Citrus peels: Effect of adsorbent entrapment in calcium alginate beads, *ACS Omega*, 2020, **5**(28), 17215–17222.

159 S. Dahmani, R. Chabir, F. Errachidi, W. Berrada, H. Lansari, M. Benidir, *et al.*, Evaluation of in vivo wound healing activity of Moroccan Citrus reticulata peel extract, *Clin. Phytosci.*, 2020, **6**, 1–9.

160 M. Sumathra, D. Govindaraj, M. Jeyaraj, A. Al Arfaj, M. A. Munusamy, S. S. Kumar, *et al.*, Sustainable pectin fascinating hydroxyapatite nanocomposite scaffolds to enhance tissue regeneration, *Sustainable Chem. Pharm.*, 2017, **5**, 46–53.

161 H. V. Palacin Baldeón, *Encapsulation of Bioactive Compounds for Food and Agricultural Applications*, 2022.

162 S. Boostani, and S. M. Jafari, Controlled release of nanoencapsulated food ingredients, *Release and Bioavailability of Nanoencapsulated Food Ingredients*, Elsevier, 2020, pp. 27–78, DOI: **10.1016/B978-0-12-815665-0.00002-3**.

163 S. Ghasemi, S. M. Jafari, E. Assadpour and M. Khomeiri, Nanoencapsulation of d-limonene within nanocarriers produced by pectin-whey protein complexes, *Food Hydrocolloids*, 2018, **77**, 152–162, DOI: **10.1016/j.foodhyd.2017.09.030**.

164 J. S. Santos, J. G. Galvão, M. R. Mendonça, A. M. Costa, A. R. Silva, D. S. Oliveira, *et al.*, Encapsulation of Citrus sinensis essential oil and R-limonene in lipid nanocarriers: A potential strategy for the treatment of leishmaniasis, *Int. J. Pharm.*, 2024, 124464.

165 A. G. Luque-Alcaraz, M. Velazquez-Antillón, C. N. Hernández-Téllez, A. Z. Graciano-Verdugo, N. García-Flores, J. L. Iriqui-Razcón, *et al.*, Antioxidant Effect of Nanoparticles Composed of Zein and Orange (Citrus sinensis) Extract Obtained by Ultrasound-Assisted Extraction, *Materials*, 2022, **15**(14), 4838.

166 M. H. Farzaei, P. Derayat, Z. Pourmanouchehri, M. Kahrarian, Z. Samimi, M. Hajialyani, *et al.*, Characterization and evaluation of antibacterial and wound healing activity of naringenin-loaded polyethylene glycol/polycaprolactone electrospun nanofibers, *J. Drug Delivery Sci. Technol.*, 2023, **81**, 104182, DOI: **10.1016/j.jddst.2023.104182**.

167 Y. Hu, W. Zhang, Z. Ke, Y. Li and Z. Zhou, In vitro release and antioxidant activity of Satsuma mandarin (Citrus reticulata Blanco cv. unshiu) peel flavonoids encapsulated by pectin nanoparticles, *Int. J. Food Sci. Technol.*, 2017, **52**(11), 2362–2373.

168 H. Jin, Z. Zhao, Q. Lan, W. Zhang, J. Pi and C. E. Evans, Nasal delivery of hesperidin/chitosan nanoparticles suppresses cytokine storm syndrome in a mouse model of acute lung injury, *Front. Pharmacol*, 2021, **11**, 592238.

169 S. Maity, P. Mukhopadhyay, P. P. Kundu and A. S. Chakraborti, Alginate coated chitosan core-shell nanoparticles for efficient oral delivery of naringenin in diabetic animals—An in vitro and in vivo approach, *Carbohydr. Polym.*, 2017, **170**, 124–132.

170 S. P. Pradhan, S. Sahoo, A. Behera, R. Sahoo and P. K. Sahu, Memory amelioration by hesperidin conjugated gold nanoparticles in diabetes induced cognitive impaired rats, *J. Drug Delivery Sci. Technol.*, 2022, **69**, 103145, DOI: **10.1016/j.jddst.2022.103145**.

171 D. George, P. U. Maheswari and K. M. S. Begum, Cysteine conjugated chitosan based green nanohybrid hydrogel embedded with zinc oxide nanoparticles towards enhanced therapeutic potential of naringenin, *React. Funct. Polym.*, 2020, **148**, 104480.

172 S. Hasani, S. M. Ojagh and M. Ghorbani, Nanoencapsulation of lemon essential oil in Chitosan-Hicap system. Part 1: Study on its physical and structural characteristics, *Int. J. Biol. Macromol.*, 2018, **115**, 143–151, DOI: **10.1016/j.ijbiomac.2018.04.038**.

173 E. Tavassoli-Kafrani, S. A. H. Goli and M. Fathi, Encapsulation of orange essential oil using cross-linked

electrospun gelatin nanofibers, *Food Bioprocess Technol.*, 2018, **11**, 427–434.

174 F. A. M. Moghadam, A. Khoshkalampour, F. A. M. Moghadam, S. PourvatanDoust, F. Naeijian and M. Ghorbani, Preparation and physicochemical evaluation of casein/basil seed gum film integrated with guar gum/gelatin based nanogel containing lemon peel essential oil for active food packaging application, *Int. J. Biol. Macromol.*, 2023, **224**, 786–796, DOI: **10.1016/j.ijbiomac.2022.10.166**.

175 X. Song, L. Wang, T. Liu, Y. Liu, X. Wu and L. Liu, Mandarin (Citrus reticulata L.) essential oil incorporated into chitosan nanoparticles: Characterization, anti-biofilm properties and application in pork preservation, *Int. J. Biol. Macromol.*, 2021, **185**, 620–628.

176 R. Karimirad, M. Behnamian and S. Dezhsetan, Bitter orange oil incorporated into chitosan nanoparticles: Preparation, characterization and their potential application on antioxidant and antimicrobial characteristics of white button mushroom, *Food Hydrocolloids*, 2020, **100**, 105387, DOI: **10.1016/j.foodhyd.2019.105387**.

177 E. B. Souto, A. Zielinska, S. B. Souto, A. Durazzo, M. Lucarini, A. Santini, *et al.*, (+)-Limonene 1, 2-epoxide-loaded slns: Evaluation of drug release, antioxidant activity, and cytotoxicity in an HaCaT cell line, *Int. J. Mol. Sci.*, 2020, **21**(4), 1449.

178 I. Hira, A. Kumar, R. Kumari, A. K. Saini and R. V. Saini, Pectin-guar gum-zinc oxide nanocomposite enhances human lymphocytes cytotoxicity towards lung and breast carcinomas, *Mater. Sci. Eng., C*, 2018, **90**, 494–503, DOI: **10.1016/j.msec.2018.04.085**.